SAPIENZA

Università di Roma

Facoltà di Scienze Matematiche Fisiche e Naturali

DOTTORATO DI RICERCA
IN BIOLOGIA CELLULARE E DELLO SVILUPPO

XXIX Ciclo
(A.A. 2015/2016)

Fate of antigens encoded by Self-amplifying mRNA vaccines

Dottorando

Lucia Eleonora Fontana

Docente guida

Prof. Benedetta Mattei

Tutore

Dr. Nathalie Norais

Coordinatore

Prof. Rosa Sorrentino

TABLE OF CONTENTS

GLOSSARY

β2-m, Light Chain β2-microglobulin

Ab, Antibody

ABC, Ammonium Bicarbonate

Ag, Antigen

APC, Antigen Presenting Cells

Arg, Arginine

BCA, Bicinchoninic Acid Assay

BHK, Baby Hamster Kidney

BM-DCs, Bone Marrow-Dendritic Cells

BSA, Bovine Serum Albumin

CAN, Acetonitrile

CD80, Cluster of differentiation 80

CD86, Cluster of differentiation 86

CE, Collision Energie

CTL, Cytotoxic T Lymphocyte

Da, Dalton

DC, Dendritic Cell

DDA, Data Dependent Acquisition

DLinDMA, 1,2-dilinoleyloxy-N,N-dimethyl-3-aminopropane

DMP, Dimethyl pimelimidate

DMEM, Dulbecco's Modified Eagle's Medium

DOC, Sodium Deoxycholate

DSPC, 1,2-Diasteroyl-sn-glycero-3-phosphocholine

dsRNA, double strand RNA

DTT, Dithiothreitol

ELISA, Enzyme Linked Immunosorbent Assay

ER, Endoplasmic Reticulum

EU/ml, ELISA Units per ml

FA, Formic Acid

FASP, Filter Assisted Sample Preparation

FBS, Fetal Bovine Serum

FITC, Fluorescent Isothiocyanate

GOI, Gene of Interest

H, Hour

HCD, Higher energy Collision induced Dissociation

HCV, Hepatitis C Virus

HIV, Human Immunodeficiency Virus

HLA, Human Leucocyte Antigen

Hpi, Hours post infection

HRP Ab, Horseradish Peroxidase conjugated Antibody

IAA, Iodoacetamide

ICS, Intracellular Staining

IFNs, Interferons

IgG, Immunoglobulin G

Ile, Isoleucine

I.m., Intra muscular

IS, Internal Standard

IS-PRM, Internal Standard-Parallel Reaction Monitoring

IU, Infection Unit

K, Lysine

KHL, Keyhole Limpet Hemocyanin

LC, Liquid Chromatography

LiCl, Lithium Chloride

LLOQ, Low Limit Of Quantification

LNP, Lipid Nano Particle

Lys, Lysine

mAb, Monoclonal Antibody

MHC, Major Histocompatibility Complex system

MHC I, Major Histocompatibility Complex Class I molecule

MHC II, Major Histocompatibility Complex Class II molecule

MRM, Multiple Reaction Monitoring

mRNA, Messenger RNA

MS, Mass Spectrometry

NK, Natural Killer

NP, Nucleoprotein

Ns P (1-4), Nonstructural Protein (1-4)

OD, Optical Density

ORF, Open Reading Frame

PBS, Phosphate Buffer Saline

PDI, Protein Disulfide Isomerase

p-DNA, Plasmid-DNA

Pen/Strep/Glu, Penicillin/Strepmicyn/Glutamine

PRM, Parallel Reaction Monitoring

PS, Packaging Signal

PTPs, Proteotypic Peptides

PYG, Glycogen Phosphorylase

PVDF Membrane, Polyvinylidene Difluoride Membrane

Q1, First quadrupole

Q2, Second quadrupole

Q3, Third quadrupole

q-TOF, Quadrupole-Time Of Flight mass spectrometer

q-OT, Quadrupole-Orbitrap mass spectrometer

QQQ, Triple Quadrupole

R, Arginine

RDRP, RNA-dependent RNA polymerase

RT, Room Temperature

SAM, Self-amplifying mRNA vaccine

SEAP, Secrete Alkaline Phosphatase

SID, Stable Isotope Dilution method

SISCAPA, Stable Isotope Standards and Capture by Anti-Peptide Antibodies

SMCC, Succinimidyl trans-4-(Maleimidylmethyl)Cyclohexane-1-Carboxylate

SRM, Selected Reaction Monitoring

SV, Sindbis Virus

$\boldsymbol{T_H}$, T helper

$\boldsymbol{T_C}$, T cytotoxic

TBS, Tris Buffer Saline

TBST, Tris Buffer Saline plus Tween 20

TAP, Transporter Associated with antigen Processing

TCA, 2,2,2-trichloroacetic acid

TCR, T Cell Receptor

TIC, Total Ion Current

UA, Urea

UTR, Untranslated Region

VCR, Chimeric Replicon Vector

VEEV, Venezuelan Equine Encephalitis Virus

VRP, Viral Replicon Particle

V/V, Volume/Volume

W/V, Weight/Volume

SUMMARY

Nucleic acid-based vaccines such as viral vectors, plasmid DNA and mRNA have been developed as a means to address limitations of both live attenuated and subunit vaccines. Among them, Self Amplifying mRNA vaccine (SAM) has been widely evaluated in different animal models and has been confirmed to be well tolerated and able to drive *in vitro* antigen expression. However, the molecular mechanism of action of SAM approach has not been fully elucidated. To address this gap, we employed a quantitative mass spectrometry (MS) approach to investigate the molecular fate of vaccine antigens encoded by SAM, from RNA delivery, until MHC-peptide presentation.

In this work, we investigated the quantitative correlation between the antigen expression and epitope presentation on MHC class I molecules in a dose-range and time-lapse assay using myoblast cell cultures. Two delivery systems were compared, viral replicon particles (VRPs) and lipid nanoparticle, both already successfully tested *in vivo* with many different vaccine candidates.

The data obtained show that the rate of intracellular antigen expression driven by VRPs is faster compared to the expression driven by SAM encapsulated in LNPs. Moreover we observed a tight correlation between the onset of protein expression and MHC class I epitope presentation for both delivery systems, providing strong evidence that epitope presentation is temporally linked to antigen translation. Furthermore, after detection, no evident differences in the intracellular amount of protein antigen and in the level of epitope peptide were observed, assuming that the main difference between VRPs and LNPs is only related to the mechanism of cellular uptake.

Then we applied this technology to quantify the SAM encoded antigen in the muscle and lymph nodes of vaccinated mice at the site of injection, where this new type of vaccine are able to generate amount of antigen lower compare to the standard dose given by classical vaccines.

Moreover, we move to an *in vitro* model of co-culture dendritic cells through, we were able to definitively confirm that this cells are not directly transfected by SAM but are able to up take antigen encoded by transfected myoblast cells.

In this study we demonstrated the powerful use of Mass Spectrometry to better understand the mechanism of action of new kind of vaccines during the immune response.

INTRODUCTION

1.1 History of nucleic acid vaccines

Vaccination is one of the greatest historical medical successes, resulting in widespread prevention of morbidity and mortality of many infectious diseases across large human populations.

In particular, since the beginning of the vaccine era, with the introduction of the smallpox vaccine more than two centuries ago, live-attenuated vaccines, have been effectively used in preventing infectious diseases and represent some of the safest and most effective vaccines in use today.

By directly mimicking natural infection without causing disease, the attenuated virus vaccine strategy is attractive. They elicit a robust, broad and long-lived immune response without an *a priori* knowledge of the protective antigens of the pathogen. Moreover the attenuation of the pathogen often can be achieved empirically.

The most recent versions of smallpox vaccines are based on a live, replicating bovine pathogen (Vaccinia virus) that confers protective immunity against disease caused by the human pathogen (Variola virus), and is safe for use in humans. The basis of protective immunity from live attenuated viral vaccines is now believed to be an induction of cross reactive antigen-specific antibody and T cell responses [1] as a result of limited viral infection launched by the delivery of an intact viral genome.

Today, there are several licensed live attenuated vaccines, including those that protect against bacterial and viral diseases (polio, measles, mumps, rubella, influenza, yellow fever, rotavirus, chicken pox).

However, the development of a live attenuated vaccine can become problematic when the organism does not replicate efficiently in cell culture (*e.g.*, HCV) or when there is the potential reversion to a virulent strain (e.g., HIV, rabies). In addition, focus the immune system on certain immunogenic antigens of a given pathogen (e.g., hepatitis B surface antigen) might be a better choice. For this reason, subunit or recombinant protein-based vaccines are typically used but often require the co-administration of adjuvants or carriers to achieve a protective and long-lasting efficacy due to the poor immunogenicity of protein antigens alone.

Nucleic acid-based vaccines have been developed as a means to combine the positive attributes of both live-attenuated and subunit vaccines. These include viral vectors such as those derived from adenoviruses or pox viruses, recombinant bacteria, plasmid DNA and RNA-based vaccines [2].

Bacterial and viral vectors can efficiently deliver nucleic acids into cells, similar to live attenuated organisms [2]. Vector genomes are engineered to express the antigen target(s) and in some cases, the vector may also be engineered to render the construct unable of replicating in the immunized host and to remove virulence factors responsible for pathogenicity. Vector-based vaccines are effective thanks to the efficient delivery of nucleic acid payload using pathways of cellular entry employed by the pathogen. In this way vectors mimic a live viral or bacterial infection, while reducing safety risks associated with live organisms.

The two most common vector platforms, vaccinia [3] and adenovirus [4], have been shown in many human clinical trials to elicit antigen-specific antibody and T cell responses. However, a limitation of this approach resides in the anti-vector immunity, the neutralizing antibody responses directed toward viral proteins present on the surface of the vector or T cell responses against proteins expressed by the vector, reducing the effectiveness of the vaccine [5].

From this, nucleic acid-based vaccines have emerged as attractive alternative as they have the potential to combine the benefits of *in situ* expression of antigens with the safety of inactivated and subunit vaccines. Upon their discovery, more than 20 years ago, nucleic acid vaccines promised to be a safe and effective means to mimic immunization with a live organism vaccine [6]. They involve direct immunization with DNA or RNA encoding the antigen *in situ*, mimicking a true infection and inducing a specific immune response, only directed toward the antigen of interest. Both DNA and RNA-based vaccines do not generate anti-vector immunity, can be used for multiple doses, and are easy to produce, offering the potential to reducing manufacturing cost and to address newly emerging pathogens in a short time [7, 8].

1.1.1 DNA vaccines

To date, the majority of preclinical and clinical studies using nucleic acid-based vaccines have been conducted with plasmid DNA (p-DNA) [9] and DNA-based viral vectors [10].

p-DNA vaccines are bacterial plasmid synthetized to express the encoded antigen following *in vivo* administration. The construction of bacterial plasmids with inserts encoding for vaccine is

based on the recombinant DNA technology. Once constructed, the vaccine-encoding plasmid is transformed into bacteria, for multiple plasmid copies replication. The plasmid DNA is then purified from the bacteria, by separating the circular plasmid from the much larger bacterial DNA and other bacterial impurities [9].

More than two decades of research and development have demonstrated the general utility of p-DNA vaccines to elicit antibody and T cell-mediated protection in animal models of infectious and non-infectious diseases. However, despite intense development efforts, DNA-based vaccines still have some limitations due to the weak immunogenicity in humans compared to small animal models [9, 11] and for the potential risk of DNA integration into the host genome. For these reasons, RNA-based vaccines are considered a safer and more potent alternative to DNA vaccines.

1.1.2 RNA vaccines

Over the past decade, RNA-based vaccines are becoming a safer and more potent alternative to DNA for gene vaccination. RNA vaccines have some advantages compared to DNA-based vaccines. First, DNA needs to be delivered into the nucleus of host cells to induce the expression of the vaccine antigen, while RNA can be directly transcribed and translated into the target protein antigen into the cytoplasm, avoiding the limiting step of crossing the nuclear membrane and the potential risk of genome integration.

Moreover, RNA is produced using a cell-free enzymatic transcription reaction, increasing production yields and avoiding safety concerns associated with the use of living organisms, as in the case of DNA vaccines [12].

Proof of concept for the utility of RNA in vaccination was demonstrated when intramuscular injection of mRNA in mice resulted in local production of the encoded protein and induction of a specific immune response against the encoded antigen [13]. Furthermore, mRNA vaccines can act as “self-adjuvant” by activating the RNA sensing machinery that usually provides the first barrier of defense against viral infections. Members of the Toll-Like Receptor family can sense exogenous RNA and activate innate immune responses involving mainly type I interferons (IFNs) [14].

RNA vaccines are effective in eliciting both antigen-specific humoral and cellular responses in animal models of infectious and non-infectious diseases. Moreover, pre-clinical data have

demonstrated the safety profile of mRNA-based cancer vaccines and their capability to induce tumor antigen-specific immune responses [12].

Currently, there are two major types of mRNA vaccines, distinguished by the translational capacity of the RNA: conventional non-amplifying mRNA molecules and self-amplifying mRNA.

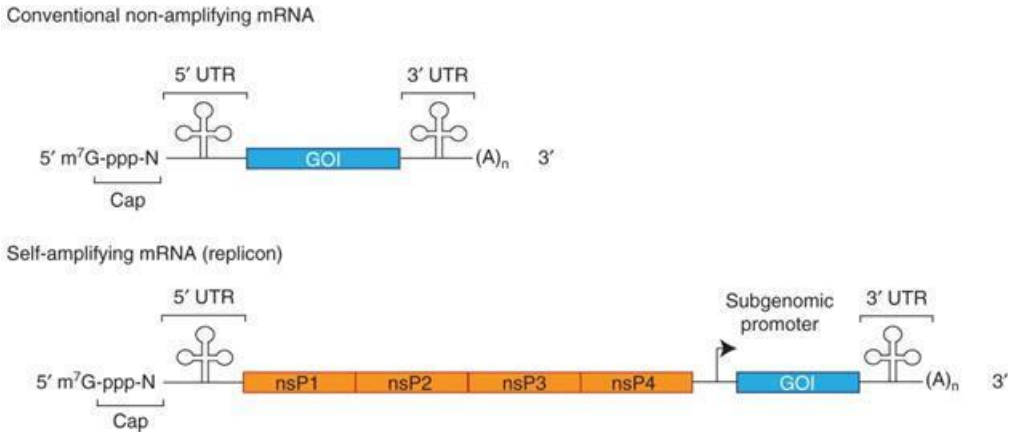

Fig. 1. ***Structural elements of RNA-based vaccines.*** Schematic illustration of a conventional non-amplifying mRNA containing the cap structure, the 5' UTR region, an open reading frame encoding the gene of interest (GOI), 3' UTR and a poly(A) tail, and of a self-amplifying mRNA derived from an alphavirus genome, containing the basic elements described above, an ORF encoding four non-structural proteins (nsP1-4), and a sub-genomic promoter upstream to the GOI [15]. (*Adapted from Nucleic acid vaccines: prospects for non-viral of m-RNA vaccines delivery Expert Opin. Drug Deliv., 2014, Deering R.P.)*

Non-amplifying mRNA molecules consist of five key elements critical in the life cycle and expression of mRNA: a cap structure (m7Gp3N (N: any nucleotide)), a 5' untranslated region (5' UTR) situated immediately upstream of the translation initiation codon; an open reading frame (ORF) that encodes a gene of interest (GOI), a 3' untranslated region (3' UTR), and the tail of 100–250 adenosine residues (poly (A) tail). All five elements in the mRNA construct control the synthesis of proteins by influencing mRNA stability, accessibility to ribosomes, and circularization and interaction with the translation machinery [12].

However, non-amplifying mRNAs are poorly immunogenic *in vivo* [16], probably because of their short half-life resulting in brief time of antigen expression. To extend the duration and the magnitude of antigen expression, self-amplifying mRNAs were developed.

Self-amplifying mRNAs, are derived from positive or negative-stranded RNA viruses like alphaviruses (Sindibis, Semliki Forest, and Venezuelan equine encephalitis viruses) or flaviviruses [17-19]. They contain a large ORF encoding four nonstructural viral proteins (nsP1-4) and a sub-genomic promoter upstream of the genes encoding for the proteins of interest that replaces the genes encoding the viral structural proteins required to make an infectious virus particle (**Figure 1**). Self-amplifying mRNAs derived from different RNA viruses differ with regard to levels and duration of heterologous gene expression, allowing generation of a versatile toolbox for vaccine applications [57].

After delivery into the cytosol of a cell, the released mRNA is translationally competent, and the engagement with the host cell ribosome produces the four functional components of RNA-dependent RNA polymerase (RDRP) or viral genome replication apparatus: nsP1, nsP2, nsP3, and nsp4. Translated nsPs form replication factories on the surface of intracellular membranes and transcribe full-length negative-strand copies from the input mRNA. This negative-strand copy then serves as a template for two positive-strand RNA molecules: the genomic mRNA and a shorter, co-linear sub-genomic mRNA.

This sub-genomic mRNA (also known as the 26S RNA), is transcribed at extremely high levels, permitting the amplification of mRNA encoding the vaccine antigen.

Self-amplifying mRNA vaccines have attractive features that are lacking in non-amplifying mRNA vaccines, such as the auto replicative ability resulting in high levels of expression of the encoded vaccine antigen in host cells, regardless of cell division. In addition, dsRNA molecules that are produced during RNA replication are known to be potent stimulators of innate immunity, resulting in the induction of enhanced immune response [20, 21].

RNA replicons are effective in eliciting humoral and cell-mediated immune responses in different animal models, including mice [16], non-human primates [22], and humans [23], and against several target diseases. One potential disadvantage of RNA-based vaccines is their instability that could be improved by appropriate delivery systems. In fact, high doses of naked RNAs are necessary for eliciting an immunological response *in vivo*. Therefore, one of the most important challenges for RNA-based vaccines is finding effective delivery methods able to prevent RNA enzymatic degradation and to facilitate the transfection of host cells.

A recent advancement in self-amplifying RNA vaccines is the use of a synthetic delivery system including inorganic particles, polymeric-based, cationic lipid-based vectors, and physical methods such as electroporation and gene gun delivery [24].

1.2 Delivery of Self-amplifying mRNA vaccines

1.2.1 Viral delivery system

RNA replicons can be packaged into virus-like particles derived from Alphaviruses, by supplying the structural proteins *in trans* in cell culture.

Alphaviruses are positive-sense RNA viruses that belong to the largest genus of the Togaviridae family.

The alphavirus particle is a 70 nm diameter icosahedron, containing a single-strand, positive-sense RNA genome that is capped and polyadenylated. The genome is approximately 11.5 kilobases and is associated to the capsid protein (C), producing a nucleocapsid core that is enveloped in a cell-derived lipid bilayer embedded with E1 and E2 glycoproteins that provide cell targeting and endosomal escape functions to the virus.

To date is known that alphaviruses enter into cells by receptor-mediated endocytosis, followed by the fusion of the viral membrane to the cell membrane in the endolysosomes. This process allows the release of RNA and nucleocapsid into the host cell cytosol.

However, recent works demonstrate that alphavirus entry is independent to endocytosis, suggesting that viral may entry directly through plasma membrane (reviewed in [25]).

In several studies alphaviruses have been adapted as vaccine vectors [26], in the simplest case, this is accomplished by replacing the structural alphavirus protein genes with a heterologous gene of interest (GOI). The resulting mRNA, called replicon, is capable, when introduced into the cytoplasm of host cells, to replicate and to express the heterologous gene; however, since it does not encode the alphavirus capsid or glycoprotein genes, it is unable of forming effective viral particles or spreading to adjacent cells.

Moreover, if these replicons are introduced into a cell in which the capsid and glycoprotein genes are expressed *in trans*, virus replicon particles (VRPs) with identical protein and lipid structure to wild-type alphaviruses and that encapsulate replicon RNA in place of a normal alphavirus genome are produced. VRPs are capable of infecting cultured cells and cells in inoculated animals allow the expression of GOI, also in this case they are incapable of producing a viral particle and spreading cell-to-cell due to the lack of structural protein genes. VRP-based vaccine candidates have been extensively tested against bacterial and viral infections, in a variety of small animal and primate models [27].

Although both preclinical and clinical data for viral delivery of self-amplifying mRNA are encouraging, this technology requires the electroporation and the use of large-volume of formulations containing the genetic elements into cells in culture, clearly not applicable to industrial-scale production. In addition, during the production of VRPs in cells containing both replicon and helper RNAs, there is the possibility that recombination or co-packaging of replicons and helper RNAs could bring to the assembling of infective virions.

If on one side, viral particle delivery of replicons is the most efficient means to deliver nucleic acids into cells, on the other side, it is limited by complicated manufacturing, safety concern and anti-vector immunity [28]. To avoid these limitations and to provide protection from RNA degradation, non-viral delivery of replicons has been explored in order to develop an effective and safer vaccine.

1.2.2 Non-viral delivery system: SAM vaccines

Recently, Geall *et al.* [29] described the non-viral delivery of self-amplifying mRNAs. The SAM vaccine platform is based on a synthetic, self-amplifying RNA derived from an engineered alphavirus genome containing the alphavirus replication machinery, but lacking the viral structural genes required to produce infectious alphavirus particles. To be commercially competitive as a technology platform, mRNA based vaccines must induce the same immunogenicity of viral vector-based vaccines, at doses of RNA that are not cost prohibitive. For this purpose, Geall and colleagues took advantage of the recent innovations in systemic delivery of short interfering RNA [30] to develop a synthetic lipid nanoparticle (LNP) formulation for SAM replicons [29]. Cationic lipids and mRNA are mixed together to obtain stable particles that prevent RNA enzymatic degradation and deliver the mRNA into host cells by interacting with the negatively charged cell membrane. Once in the cytoplasm, the RNA polymerase, encoded by the non-structural genes of the viral replicon, is expressed and it produces a negative-sense copy of the genome that is used as template for the amplification of the genome, as well as for the transcription of the sub-genomic mRNA encoding the vaccine antigen [31] (**Figure 2**).

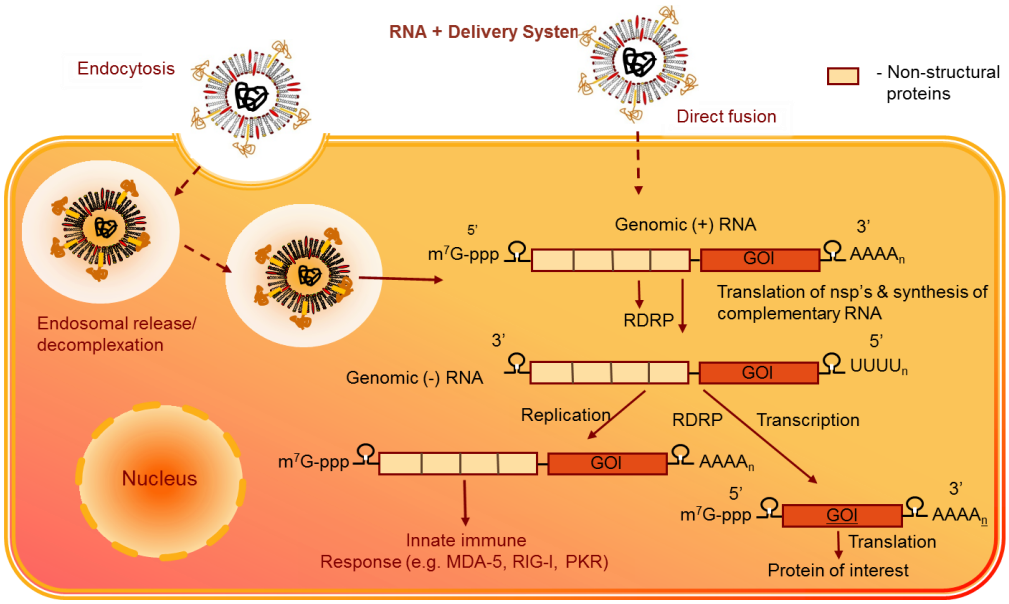

Fig. 2. Schematic illustration of the replication and expression steps of self-amplifying RNA after delivery to a mammalian host cell.
The RNA encapsulated by lipid nanoparticles is delivered in the cytoplasm of a host cell where the RNA polymerase encoded by the non-structural genes is expressed and drives the amplification of the RNA as well as the transcription of the sub-genomic mRNA encoding the vaccine antigens (*Adapted from: A cationic Nanoemulsion for the delivery of next generation RNA vaccines. Mol Ther, 2014*).

The LNP formulation enhances the potency of the self-amplifying RNA, eliciting potent and protective immune responses in preclinical models of infection that are comparable to a viral delivery system, but without the inherent limitations of viral vectors [29]. Preclinical proof of concept for SAM vaccines has been achieved so far in different animal models (mouse, cotton rats, ferrets, rabbits, non-human primates), and against several pathogens like respiratory syncytial virus, influenza virus, human immunodeficiency virus, cytomegalovirus, Ebola and *Plasmodium* [8, 24, 29, 32]. Moreover, the SAM vaccine platform shows several important advantages: synthetic and highly scalable production process; robust, generic means to manufacture vaccines against many pathogen targets; avoidance of anti-vector immunity and safety issues associated with genome integration; high immunogenicity (both humoral and cellular) with low RNA doses [33].

1.3 The immune system

The immune system is a remarkably versatile defense system that has evolved to protect animals from invading pathogenic microorganisms and cancer.

It is able to generate an enormous variety of cells and molecules capable of specifically recognize and eliminate an apparently limitless variety of foreign invaders.

Functionally, an immune response can be divided into two related activities: recognition and response [30].

Immune recognition is remarkable for its specificity. The immune system is able to recognize subtle chemical differences that distinguish one foreign pathogen from another. Furthermore, the system is able to discriminate between foreign molecules and self-cells and proteins. Once a foreign organism has been recognized, the immune system recruits cells and molecules to mount an appropriate response, called effector response, to eliminate or neutralize the foreign organism. In this way, the system is able to convert the initial recognition event into a variety of effector responses, each uniquely suited for eliminating a particular type of pathogen.

Immunity, the state of protection from infectious disease, has both a less specific and more specific component. The less specific component, innate immunity, provides the first line of defense against infection. Most components of innate immunity are present before the onset of infection and constitute a set of disease-resistance mechanisms that are not specific to a particular pathogen but that include cellular and molecular components that recognize classes of molecules peculiar to frequently encountered pathogens.

The principal components of innate immunity are physical and chemical barriers, such as epithelia, phagocytic cells (neutrophils, monocytes and macrophages), dendritic cells (DCs), natural killer (NK) cells, and blood proteins, including members of the complement system and other mediators of inflammation, such as chemokines and cytokines that regulate and coordinate many of the activities of the cells of the immune system. All these mechanisms of innate immunity cooperate to recognize and react against pathogens [34].

In contrast to the broad reactivity of the innate immune, which is uniform in all members of a species, the adaptive immunity (the specific one), is not activated as long as the antigenic challenge penetrate into the organism and was recognized.

An adaptive immune response involves two major groups of cells: lymphocytes and antigen-presenting cells (APC). Lymphocytes belong to the white blood cells produced in the bone marrow by the process of hematopoiesis. Lymphocytes leave the bone marrow, circulate in the blood and lymphatic system, and reside in various lymphoid organs. Because they produce and display antigen binding cell-surface receptors, lymphocytes mediate the defining immunologic attributes of specificity, diversity, memory, and self/non-self-recognition. The two major populations of lymphocytes and are T cells and B cells (**Figure 3**).

T lymphocytes arise in the bone marrow and migrate to the thymus gland to mature. During their maturation T cells became able to express a unique antigen-binding molecule, called the T-cell receptor, on its membrane that can recognize only one fragment (peptides) of protein or glycoprotein called antigenic determinant or epitopes that is bound to cell-membrane proteins called major histocompatibility complex (MHC) molecules. There are two subpopulations of T cells: T helper (T_H) and T cytotoxic (T_C).

When a naïve T_H cell recognizes and interacts with an antigen-MHC molecule complex, the cell is activated and becomes an effector that secretes various growth factors and cytokines. These cytokines play an important role on the activating of B cells, T_C cells, macrophages, and various other cells that participate in the immune response. Under the influence of T_H-derived cytokines, a T_C cell that recognizes an antigen-MHC molecule complex proliferates and differentiates into an effector cell called a Cytotoxic T lymphocyte (CTL). In contrast to the T_C cell, the CTL generally does not secrete many cytokines but exhibits cell-killing or cytotoxic activity. The CTL has a vital function in monitoring the cells of the body and eliminating any that display antigen, such as virus-infected cells, tumor cells, and cells of a foreign tissue graft.

B lymphocytes mature into the bone marrow and express a unique antigen-binding receptor that is a membrane-bound antibody molecule. When a naïve B cell first encounters the antigen that matches its membrane bound antibody, the binding of the antigen to the antibody causes the cell to divide rapidly; its progeny differentiates into memory B cells and effector B cells called plasma cells. Memory B cells have a longer life than naïve cells, and they express the same membrane-bound antibody as their parent B cell. Plasma cells produce the antibody in a form that can be secreted that act as major effector molecules of humoral immunity.

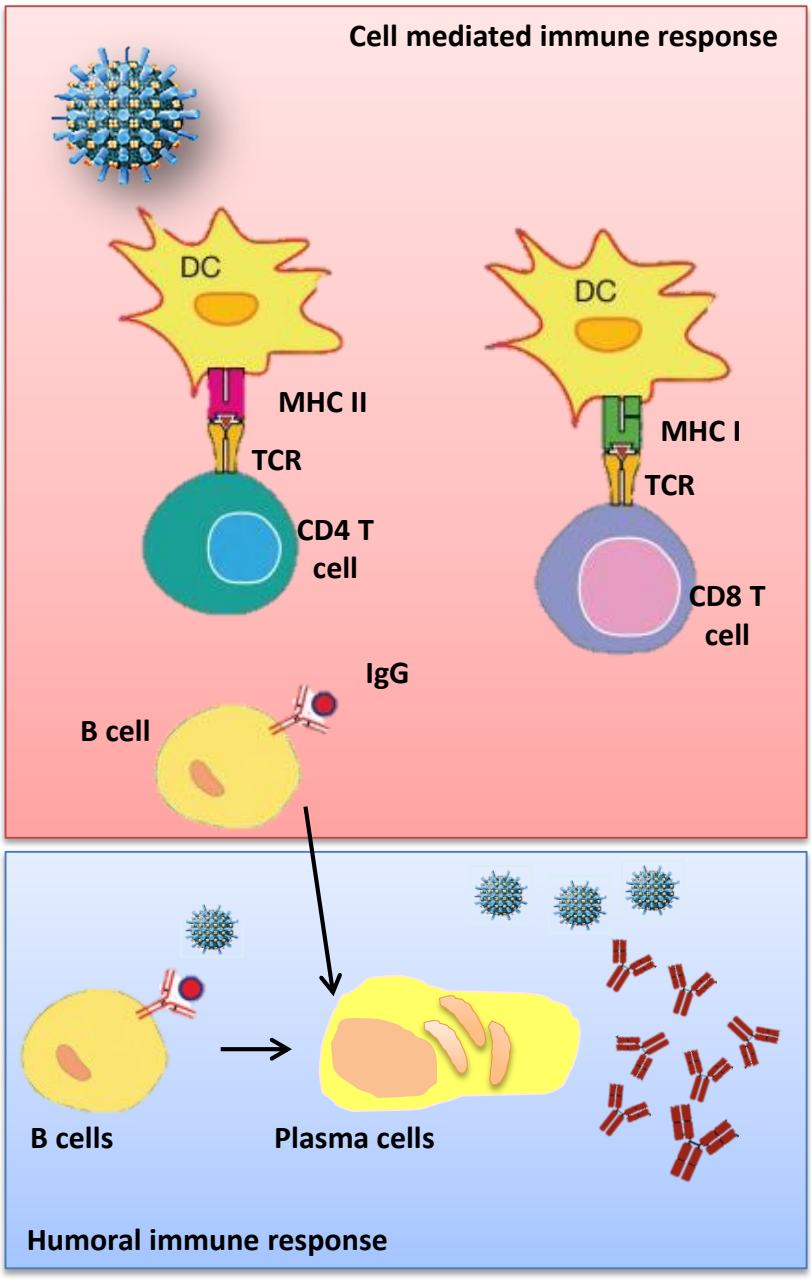

Fig. 3. Humoral and cell mediated branches of the immune system.
In the humoral response, B cells interact with antigen and then differentiate into antibody-secreting plasma cells. The secreted antibodies bind to the antigen and facilitate its clearance from the body. In the cell-mediated response, various sub-populations of T cells recognize antigen presented on self-cells. T_H cells respond to antigen by producing cytokines. T_C cells respond to antigen by developing into cytotoxic T lymphocytes (CTLs), which mediate killing of altered self-cells (virus-infected cells). *(Adapted from Fundamental Immunology, Vaccines (Chapter 43), William E. Paul).*

1.3.1 Antigen presenting cells (APCs)

Activation of both the humoral and cell-mediated branches of the immune system requires cytokines produced by T_H cells. To carefully ensure regulated activation of T_H cells, they can recognize only antigens that are displayed with the MHC molecules on the surface of antigen-presenting cells (APCs).

These specialized cells, which include macrophages, B lymphocytes, and dendritic cells, are distinguished by the expression of MHC molecules on their membranes and for the ability to deliver a stimulatory signal necessary for T_H-cell activation.

1.3.2 The Major Histocompatibility Molecules and Antigenic Peptide Epitopes

Major histocompatibility (MHC) molecules are a large genetic complex with multiple loci that encode for two major classes of membrane-bound glycoproteins: class I and II.

MHC class I and class II molecules are similar in function: they present peptides to the surface of $CD8^+$ and $CD4^+$ T cell respectively, the choice between the two mechanisms appears to be determined by the entry route of the antigen into a cell.

Endogenous antigens, also produce within the host cell as viral proteins synthesized in virus-infected host cells or unique proteins synthesized by cancerous cells, are processed by MHC class I molecules, while exogenous antigens are captured by endocytosis and processed by MHC class II molecules.

Endogenous, normal and abnormal proteins were degraded by the proteasome into peptide fragments. These fragments are translocated to the endoplasmic reticulum (ER) through a peptide transporter called Transporter Associated with antigen Processing (TAP) that is embedded in the ER membrane and allows the access to MHC class I molecules.

In the ER, MHC class I molecules presents a heterodimer form, constituted by a polymorphic heavy chain and a light chain called β2-microglobulin (β2-m) in which the peptide is the third component required for the stability. Without peptides, MHC class I molecules are stabilized by ER chaperone as Calreticulin, ERp57, protein disulfide isomerase (PDI) and Tapasin. TAP forms the peptide-loading complex in the ER, interacting with Tapasin and promotes MHC I binding of peptides with a slow off rate, thereby helping to shape the repertoire of presented peptides.

These are peptides of a very specific length of eight to ten amino acids with appropriate anchor residues. Peptides that are too long can be trimmed by an ER-resident aminopeptidase, ERAP1, before consideration by MHC I molecules that are either in the peptide-loading complex or associating with another Tapasin look-like chaperone in the ER called TAPBPR.

TAPBPR binds peptides longer than eight or nine residues, but not shorter ones, triggers a conformational change in ERAP1 that activates its hydrolysis. Through this mechanism, ERAP1 trims most peptides down to eight or nine residues, corresponding to the size needed for optimal binding to MHC I molecules.

Peptides that are unable to bind an MHC I molecule are ultimately translocated back into the cytosol for degradation.

Peptides should be considered the third subunit of MHC I molecules, required to stabilize the complex, MHC class I molecules fully assembled, leave the ER for presentation at the cell surface of all nucleated cells to $CD8^+$ T cells. These cytotoxic T cells attack and kill cells displaying the antigen MHC class I complexes for which their receptors are specific. MHC class I molecules that never bind proper peptides were finally degraded by a ER-associated protein degradation system (ERAD) [34].

While MHC class I molecules are ubiquitously expressed, MHC class II molecules are primarily expressed by professional APCs, such as DCs, macrophages and B cells. MHC class II presents peptide fragments that are generally larger than those presented by MHC class I, because the peptide-binding groove of MHC class II is open, allowing peptides to extend out of this site. The MHC class II-associated peptides are derived from extracellular proteins and from self-proteins that are degraded in the endosomal pathway (**Figure 4**) [35]. During their assembly in the ER, MHC class II molecules are associated with an invariant chain Ii, which acts as a pseudo-peptide by filling the MHC class II peptide-binding groove and targets MHC II molecules into the endosomal pathway [36-38].

The resulting Ii-MHC class II complex is transported to a late endosomal compartment termed MHC class II compartment (MIIC), where Ii is digested, leaving a fragment of invariant chain (called CLIP) in the peptide-binding groove [39]. CLIP fragment has to be exchanged for higher-affinity peptides, derived from protein degradation in the endosomal pathway, with the help of a dedicated MHC class II-like chaperone called H2-DM [40]. The structure of H2-DM in

association with MHC II reveals that this chaperone locally opens the groove to release CLIP leaving the proper peptide fragments in the MHC class II peptide-binding groove [41].

After some period of residence in MIIC, MHC II molecules move to the plasma membrane either via vesicular transport or in the form of tubules [42-44]. Since the targeting information in the invariant chain has been removed after its degradation in MIIC, MHC II molecules can stably reside on the plasma membrane.

MHC II molecules on dendritic cells present antigen to naïve CD4+ T cell to activate them; later they participate in the interaction of B cells and macrophages with these specific CD4 effector T cells.

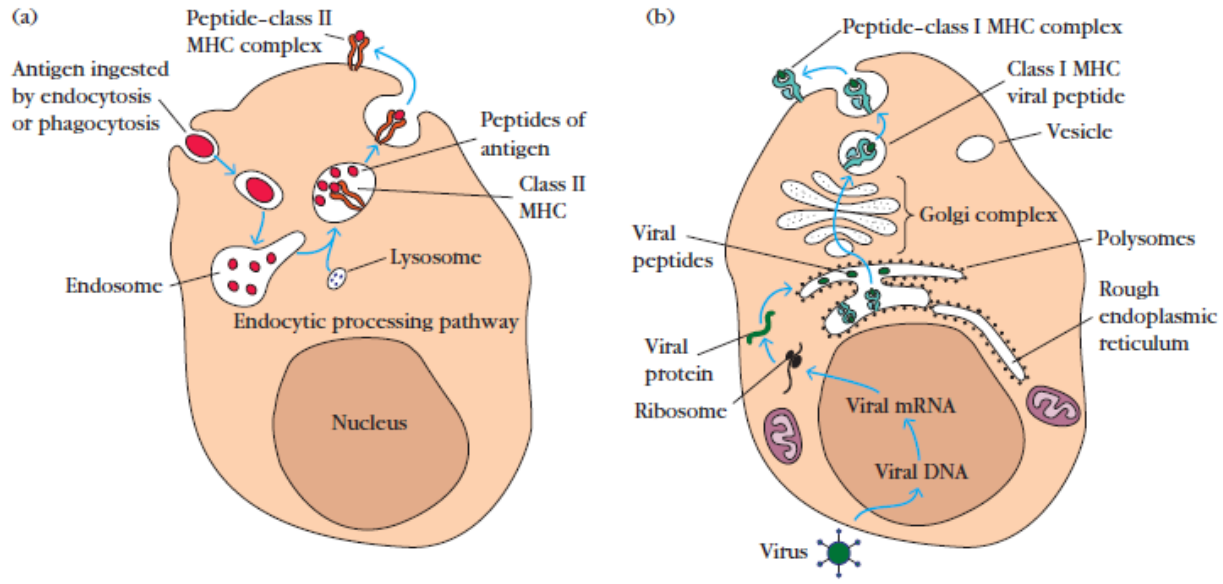

Fig. 4. Processing and presentation of exogenous and endogenous antigens by MHC Complexes.
(A) Exogenous antigen is ingested by endocytosis or phagocytosis and then enters the endosomal processing pathway. Here, within an acidic environment, the antigen is degraded into small peptides, which then are presented with class II MHC molecules on the membrane of the antigen-presenting cell. (B) Endogenous antigen, which is produced within the cell itself (*e.g.*, in a virus infected cell), is degraded within the cytoplasm into peptides, which move into the endoplasmic reticulum, where they bind to MHC class I molecules. The peptide–class I MHC complexes then move through the Golgi complex to the cell surface *(Adapted from Immunology 5e, Golsby 2012).*

1.4 Quantitation of antigen presentation

Cellular immunity is driven by the interaction of T cell receptors (TCRs) on T cells recognizing peptides, presented on the surface of cells in complex with molecules encoded by the major histocompatibility complex (MHC). The total array of MHC-bound peptides (p-MHC), presented at the surface of cells (the immune-peptidome) for recognition by T cells, is likely in the order of tens to hundreds of thousands of complexes.

While the precise relationship between the abundance of a given T cell ligand, its half-life on the cell surface and immune outcome remain to be fully elucidated, simple models suggest that such factors define the magnitude of the immune response to a given T cell epitope. The ability to accurately, rapidly and comprehensively quantify antigen presentation is therefore crucial to develop new models to predict immunogenicity and immune outcomes.

Traditionally, immunologists have measured immune out-puts such as antibody titers and cytokine levels using techniques such as ELISpot and ELISA assays, however despite technological advancements in this field, systematic and accurate epitope identification and quantitation on the surface of cells has remain a challenge in quantitative system immunology.

To date, the use of T cell lines, clones and hybridomas to study antigen presentation has been widely reported in the literature [45]. These biological reagents can be generated or isolated from immune hosts and expanded *in vitro* for semi-quantitative assays of antigen presentation. In this way many T cell hybridomas can recognize their pMHC in a co-stimulation assay, making them a useful tool to study antigen processing and presentation without such signals that can influence the responsiveness of primary T cells.

Moreover the use of antibodies to quantitate T cell epitopes has also been widespread by the pioneering studies of Unanue and colleagues that developed and use of ELISA with anti-peptide antibodies to estimate the lysozyme peptide contents extracted from I-A^k MHC II molecules. Alternatively, m-Abs generated with TCR-like reactivity specific for particular pMHCs are a more attractive option. However all these approaches remain time consuming to generate and their sensitivity and specificity cannot be determined with accuracy [46].

1.5 Contribution of Mass Spectrometry-based proteomics in immunopeptidome.

Over the past few decades, Mass Spectrometry became the core technology for the analysis of MHC ligandome.

After immunoaffinity purification of detergent-solubilized peptides-MHC complexes, followed by acid elution of peptides, liquid chromatography-mass spectrometry could be apply to gain qualitative and quantitative insight into the MHC-presented peptide repertoire. In fact, with this approach, both the intact peptide (precursor ion) and its fragmentation spectra (product ions) can be determined with high accuracy providing unambiguous identification of epitope sequences. This approach has been used to quantitate peptides associated with MHC class I [47] and II molecules [48], overcoming the greater complexity and heterogeneity of class II bound species.

In a recent study conducted by Ternette *et al.*, quantitative mass spectrometry approach was used to monitor the abundance of several immunogenic peptide epitopes, examining in detail the kinetics of the HLA Class I associated immunopeptidome of APCs after infection with a viral vector encoding a HIV vaccine construct. [47].

This study demonstrated the power of quantitative MS for the identification and quantitation of HLA class I-associated peptides for T-cell epitope discovery and its use to optimize and inform vaccine design [47].

Moreover, while the above technique can provide relative quantitation and estimates of epitope copy number in cell surface, the inclusion of stable isotope labeled peptide standards provides an absolute quantitation [49, 50]. In this case the quantitation is achieved through the parallel detection of the light (native) and isotopically labeled (heavy) peptides, both having matching liquid chromatographic separation due to identical sequence, followed by a comparison of their intensity profiles.

The method, known as Selected Reaction Monitoring (SRM) or Multiple Reaction Monitoring (MRM), is employed worldwide as the benchmark technique for highly sensitive quantitation of peptides isolated from biological samples and is based upon the precise knowledge of a peptide mass coupled to its unique fragmentation spectra.

SRM has been used to quantitate selected MHC class I [51-53] and class II-bound peptides [54]. In particular, in a study by Croft *et al.*, SRM was used to perform MHC class I epitope quantitation *in vitro* and *in vivo* utilizing the H-2K^{b}-SIINFEKL model system to detect and

quantitate SIINFEKL presentation. This was achieved for cell lines expressing the intact parental ovalbumin antigen [53], on cells infected with recombinant viruses expressing ovalbumin as a surrogate of viral antigen [51] and during presentation of ovalbumin *in vivo* [53]. In these studies SIINFEKL was detected in as low as just a few copies per cell *in vivo*, to several hundred copies on APCs transfected with ovalbumin-expressing constructs through to tens of thousands of copies when recombinant vaccinia virus encoding ovalbumin was used to infect APC.

SRM was also considered the tool of choice to investigate the endogenous MHC class II peptides presentation. In work by Bozzacco *et al*., SRM analysis was used to perform a qualitative and quantitative profile of the endogenous MHC class II peptides presented *in vivo* by mouse spleen dendritic cells, and B cells allowing a direct comparison between to these two types of immune cells. In this study is shown as the endogenous source proteins for the MHC II bound peptides identified on DCs and B cells are localized among different cellular compartments and reflects the distinct immune functions of the two cell types [54].

In particular, for DCs, epitope peptides derive from proteins involved in antigen presentation [55, 56], in contrast to B cells where peptides derive from proteins involved in cell to cell signaling and DNA recombination and repair, required during antibody production and immunoglobulin class switching [57-59].

Moreover, the simultaneous quantitation of the source protein antigen and the peptides bound on MHC molecules facilitates understanding the relationship between the presence of antigen and the following generation of the specific peptide epitopes. Also in this case, mass spectrometry plays a key role being used to identify and quantify simultaneously both proteins and epitope peptides. In fact mass spectrometry has the capability to delve deep into cellular proteome, obtaining information related to proteins expressed across large dynamic ranges where highly sensitive technique for their detection and quantification are required.

In this contest a work by Purcell *et al.*, defines the powerful use of SRM to simultaneously quantify the presentation of eight Vaccinia virus peptide-MHC class I complexes on infected cells and the amount of their source antigen at multiple time point after infection, in order to dissect anti-viral immunity. This study showed the tight correlation between onset of protein expression and epitope display for most antigens provides the strongest support that antigen presentation is largely linked to protein translation and not to later degradation of antigens during virus infection.

1.5.1 Targeted proteomics technique: Selected reaction monitoring-and Parallel reaction monitoring

The ability to detect and quantify proteins with high precision across multiple samples is an essential task in biological and biomedical research. In this field, SRM has emerged as a promising technique for such precise quantification of targeted proteins [60-62]. Originally applied to the measurement of small molecules (such as metabolites or drugs [63]), SRM is a mass spectrometry technique involved in the detection and quantification of specific, predetermined analytes with known fragmentation pattern in complex backgrounds. Whit this purpose, SRM exploits the unique capability of triple quadrupole (QQQ) mass spectrometers [64], to act as mass filters and to selectively monitor a specific analyte molecular ion and one or several fragment ions generated from the analyte by collisional dissociation [64].

The number of such fragment ions that reach the detector is counted over time **Figure 5**, resulting in a chromatographic trace with retention time and signal intensity as coordinates. Several such precursor–fragment ion pairs, termed SRM transitions, can be sequentially and repeatedly measured at a periodicity that is fast compared to the analyte chromatographic elution, yielding chromatographic peaks for each transition that allow for the concurrent quantification of multiple analytes. When applied to proteomics, SRM measures peptides produced by the enzymatic digestion of a proteome as surrogates of the corresponding proteins. Molecular ions within a mass range centered around the mass of the targeted peptide are selected in the first mass analyzer (Q1), fragmented at the peptide bonds by collision-activated dissociation (in Q2) and one or several of the fragment ions uniquely derived from the targeted peptide are measured by the second analyzer (Q3) [60, 65].

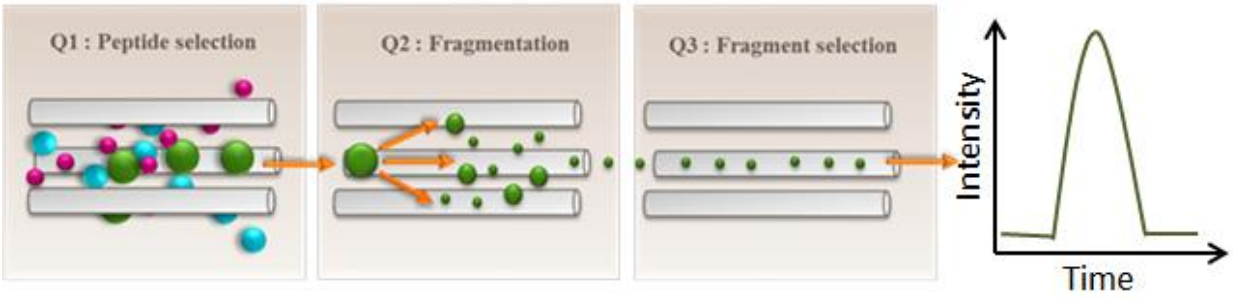

Fig.5. Selected Reaction Monitoring technique. Molecular ions of a specific analyte are selected in Q1 and fragmented in Q2. A specific fragment ion from the targeted analyte is selected in Q3 and guided to the detector.

In contrast to conventional shotgun proteomic studies, SRM requires a more complex workflow. An SRM-based proteomic experiment starts with the identification of a list of target proteins, followed by the selection of peptides, called proteotypic peptides, which are uniquely associated to the protein of interest [66, 67]. Then, for each proteotypic peptide, a set of suitable SRM transitions were identified and validated (described in 3.1.4.1 Results section). Finally, the assay was applied for the detection and quantification of the specific proteins (**Figure 6**).

First desirable target peptide, uniquely associated to target protein and easily detectable by mass spectrometry have to be selected. The selection of peptides with favorable mass spectrometry features is crucial and determines the sensitivity of the assay. In an ideal case, the target proteins are available as purified products, and the mass spectrometry signal-response of all their tryptic peptides can be directly tested via LC-MS/MS. In general, short hydrophilic and long hydrophobic peptides should be avoided, whereas fully tryptic peptides with an average length of ten amino acids, devoid of residues prone to artefactual or post-translational modifications should be targeted [65].

Moreover the fragmentation patterns (fragment ions) for each peptides (precursor ions), that provide the highest signal intensity and lowest level of interfering signal were selected to define the specific SRM transition. In fact for the quantification of a protein in SRM experiment using a QQQ instrument, it is essential to select the specific *m/z* value for the first (Q1) and third quadrupole (Q3) in order to identify the peptide parent ions and the daughter ions.

The collision energy (CE) value associated for the ion fragmentation in Q2 is then another fundamental value that has also been optimized individually for each peptide in order to provide the best signal intensity. This is obtained using a CE step variations analysis, monitoring the corresponding obtained peak area intensity [65, 68].

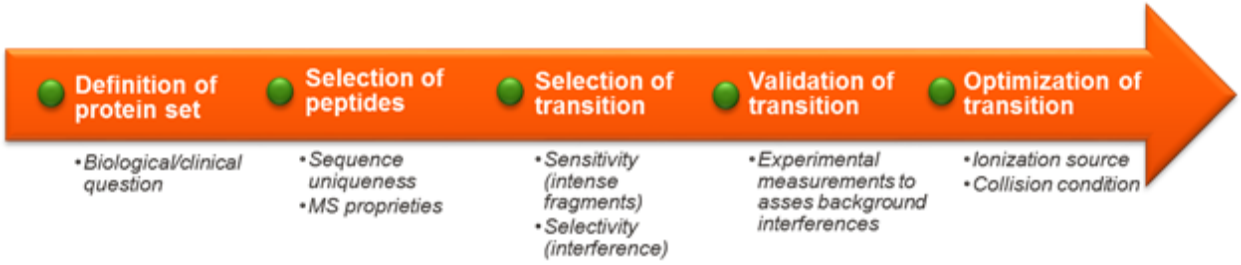

Fig. 6. Workflow of a SRM-based proteomic experiments

Finally the precise and absolute quantitation of the target proteins is achieved through the parallel detection and comparison of the intensity of native peptides and the isotopically labeled (heavy) ones, both having identical liquid chromatographic separation due to same sequence.

Thus, the success of SRM is dependent on the transitions of the target peptides that are pre-selected and used for monitoring during data acquisition: selecting the best possible transitions for the target proteins results in reliable quantification.

For this reason, SRM requires significant effort in building a data acquisition method for a set of candidate proteins and, in order to select the best set of peptides and transitions, multiple iterations and optimizations may be required

Recent studies have shown that a same targeted experiments known as Parallel Reaction Monitoring (PRM) can also be performed on hybrid quadrupole-Orbitrap (q-OT) or quadrupole time-of-flight (q-TOF) mass spectrometers.[69-72] The Orbitrap in a q-OT replaces the third quadrupole (Q3) mass analyzer of a QQQ instrument. Studies using SRM and PRM have shown that both these targeted methods have comparable sensitivity with similar linearity, dynamic range, precision, and repeatability for quantification of proteins.[73] However, PRM has certain advantages over SRM, such as it is relatively easier to build the data acquisition method because a priori selection of target transitions is not required. Furthermore, PRM provides high specificity because the MS/MS data is acquired in high resolution mode that can separate co-isolated background ions from the target peptide ions. In SRM, only three to five transitions are monitored, whereas in PRM a full MS/MS spectra is acquired that contains all the potential product ions and confirms identity of the target peptide.

The development and implementation of higher energy collision-induced dissociation (HCD) fragmentation enabled MS/MS spectra to be acquired in the Orbitrap analyzer with high resolution and high mass accuracy. HCD is a beam-type collisional dissociation similar to the dissociation achieved in triple quadrupole mass spectrometers, as well as in quadrupole time-of-flight (QTOF) mass spectrometers.

An advantage of the q-OT mass spectrometer is that both discovery and targeted experiments can be performed on the same instrument. This makes it easier to transfer instrumental parameters (e.g., collision energy, quadrupole isolation window, automatic gain control, retention time etc.) between the two data acquisition methods.

In PRM, when performed in q-OT, a predefined precursor ion is selected in the quadrupole and transferred via the C-trap to the HCD cell for fragmentation. The C-trap can fill with ions for longer times, increasing signal-to-noise ratio of the ions measured in the Orbitrap. [70, 74]

From the HCD cell, fragment ions are transferred back to the C-trap and eventually injected and analyzed in the Orbitrap mass analyzer (**Figure 7**). Since full MS/MS spectra of the targeted peptides are acquired with high resolution and high mass accuracy, a PRM-based targeted method of protein quantification is highly selective and specific.[69, 70] Moreover to further improve data acquisition efficiency, also in this type of analysis, isotopically-labeled internal standards can be used to drive PRM acquisitions of the endogenous peptides (IS-PRM) and perform the absolute quantitation.[75]

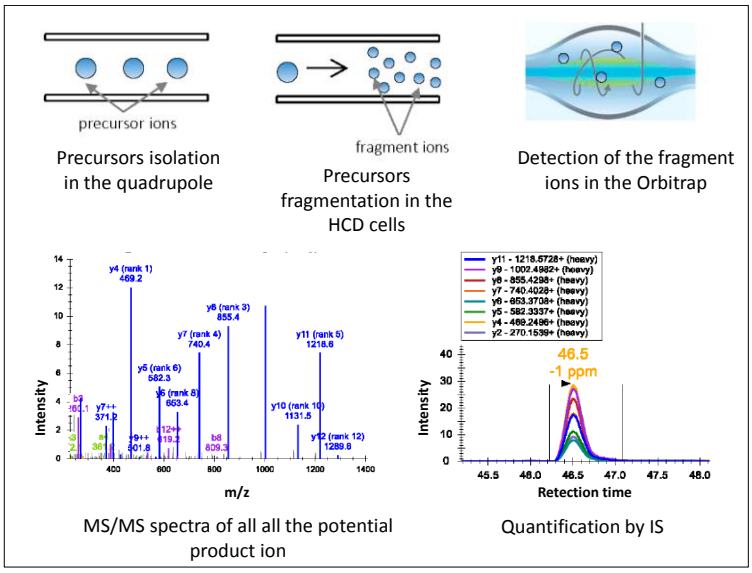

Fig.7. Parallel reaction monitoring technique. PRM workflow.
In PRM, a target precursor ion is isolated in the quadrupole analyzer and fragmented in the HCD cell; the fragment ions are then detected in the Orbitrap mass analyzer. PRM generates high resolution, full MS/MS data. During data processing, the MS/MS spectrum is used for the identification of the peptide and a subsets of fragment ions with highest intensities in the MS/MS spectrum are used for quantification using the internal standard (IS) approach *(Adapted from Parallel Reaction Monitoring: A Targeted Experiment Performed Using High Resolution and High Mass Accuracy Mass Spectrometry, International journal of molecular science, 2015).*

For its features, SRM and PRM are similar to Western blotting analysis; used for the identification and quantification of specific known set of proteins in a complex background. However, the methods differ substantially in their implementation, the reliability of the resulting assays, and the quality of results they produce [76].

A Western blotting assay essentially depends on the specificity of the antibody used [77, 78], in contrast to an SRM or PRM assays that depends on multiple parameters, such as the retention time, the mass-to-charge ratio of the parent ions and daughter fragment ions of the targeted peptide, and the relative signal intensities of the detected fragment signals [68].

Moreover the quality of quantitative data obtained is very different, quantification by Western blotting is based on the intensity of a band obtain by the reaction of specific antibody that may be poorly characterized, moreover a reference sample is not always available to test the performance of the assay. In contrast, mass spectrometry targeted assays depend on isotopically labeled reference peptides, the quality of which can be always verified in a fragment ion spectrum. Moreover, multiple independent peptides are monitored simultaneously to quantify a specific protein, which signals are integrated into a composite score indicating the protein quantity.

SRM and PRM are then consider to date the key technologies to delve deep into a proteome, obtained a precise and absolute quantitative information related to protein or more proteins expressed across large dynamic range and applied to obtain sensitive data from different and very complex biological background as cellular lysate and tissue in different filed as biology, clinical and to study protein interaction and modification.

RATIONALE AND AIM

Nucleic acid-based vaccines such as viral vector, plasmid DNA and mRNA are being developed as a means to overcome the limitations of both live-attenuated and subunit vaccines. However, viral vectors and DNA vaccines still have some constriction. Efficiency of recombinant viral vector technologies is hampered by anti-vector immunity, complex production, and safety concerns, whereas DNA-based vaccines require multiple administrations and high doses to overcome the low immunogenicity in humans. Despite significant advancements, none of these vaccines has been licensed to date. Among them, Self-amplifying mRNA vaccines are emerging as a novel class of nucleic acid. They preclude safety concerns about DNA integration into the host genome and can be directly translated in the host cell cytoplasm, circumventing the complications associated with nuclear transport. Moreover, the simple cell-free, *in vitro* synthesis of RNA avoids the manufacturing issues associated with viral vectors.

In particular, non-viral delivery of self-amplifying mRNAs (SAM platform), derived from a modified alphavirus genome, was successfully applied to different pathogens, in different animal models and was confirmed to be able to elicit a very potent immune response due to broad antigen expression and to their intrinsic adjuvant activity [24, 29, 79].

To date, most of the analysis of SAM vaccines encoded antigen expression and localization, in an *in vivo* model system based on reporter genes as Firefly Luciferase or Secrete Alkaline Phosphatase (SEAP), where bioluminescence or chemoluminescence were the monitored parameters [24]. In that assay bioluminescence intensity induced by LNP/RNA, was comparable to the bioluminescence induced by a viral delivery system. In particular mice injected with LNP/RNA showed measurable bioluminescence that was already detected on day 3, peak on day 7 and decrease to background by day 63 post immunizations. This kinetic contrasted with those observed by the same RNA but delivered by VRPs where bioluminescence was observed at day 3 compared to LNP/RNA, but with a much more rapid decay that reached background level already by day 28.

Moreover little has been described about the mechanism of action of these vaccines. Nevertheless it seems that myocyte cells and not immune cells (antigen presenting cells) are the predominant cell type transfected within the injection site at time of vaccination [24]. Recent studies demonstrate that *in vivo* priming of MHC class-I restricted $CD8^+$ T cells following SAM

immunization involves bone marrow-derived professional APCs. Therefore, myocytes can only provide an antigen source for the induction of a MHC class-I restricted $CD8^+$ T cell response by APCs [80].

The aim of this study is to provide a better understanding of the molecular mechanism involved in the antigen expression step and in the endogenous intracellular processing on MHC class I molecule during SAM vaccination.

Quantitative mass spectrometry (MS) approach based on Selected Reaction Monitoring (SRM) is used, rapid advances in MS instrumentation enabled both the relative and absolute quantification of specific set of proteins. For these reasons, we focused our attention to the expression of antigenically conserved protein Nucleoprotein (NP) from Influenza virus setting up an *in vitro* cellular model based on myoblast cell line C2C12, where SRM was applied to investigate the quantitative correlation between antigen expression and epitope presentation on MHC class I molecules, using the two delivery systems: Viral Replicon Particles (VRPs) and the synthetic Lipid Nanoparticles (LNPs). Moreover, we moved toward an *in vivo* model investigating the antigen expression in muscles and the draining lymph nodes at the site of injection. With this data we would improve the tracking of antigen following SAM vaccination, understanding the main differences between LNPs and VRPs mechanism that might involve cellular internalization, antigen expression or peptide presentation.

RESULTS AND DISCUSSION

Part I

3.1 Experimental strategies set up.

3.1.1 Generation and characterization of Influenza replicon for proteomic studies

SAM vectors encoding full-length Nucleoprotein (NP) gene from Influenza virus *A/Puerto Rico/8/1934 (H1N1)* pandemic strain was generated as a monocistronic SAM (NP) vector (**Figure 7**, A). The NP gene was amplified from the reverse-transcribed RNA genome of the virus, and then cloned into the DNA plasmid backbone containing the specific promoter for the T7 bacteriophage RNA polymerase [29]. The plasmid was transformed in *Escherichia coli* and purified by alkaline cell lysis and DNA anion exchange chromatography. Plasmid DNA was then linearized by PmeI endonuclease digestion using a unique restriction site downstream the 3' end of transcription cassette and isolated by phenol/chloroform extraction and ethanol precipitation. Linear plasmid DNA was transcribed into RNA through the *in vitro* transcription reaction and purified by LiCl precipitation. Finally, to increase RNA stability, a poly (A) tail was added to RNA by enzymatic post transcription reaction and further purified by LiCl precipitation. The quality and the integrity of purified nucleic acids, both DNA and RNA were assessed by agarose gel electrophoresis: expected molecular weights and no products of degradation were observed (**Figure 8**, B**).**

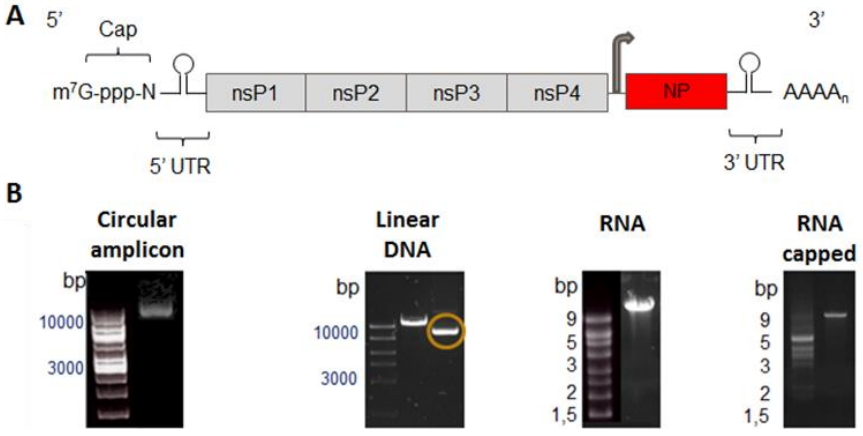

Fig. 8. Schematic representation of SAM (NP) generation
(A) Schematic representation of SAM (NP) construct. SAM derived from alphavirus genome, contains a 5' cap, four nonstructural genes (nsp1-4), a 26S sub-genomic promoter (grey arrow), the vaccine gene antigen (NP in this study) and 3' polyadenylated tail. **(B)** Analysis on agarose gel electrophoresis of the DNA or RNA obtained in each of four steps: circular amplicon, linearized DNA and RNA before and after the capping reaction.

The functionality of the replicons was evaluated by their self-amplification ability in Baby Hamster Kidney cells (BHK), a cell line usually used in molecular biology as a host for nucleic acid transfection. In details, BHK cells were transiently transfected through electroporation with an increasing amount (from 200 to 800 ng) of NP encoding mRNA. Amplification and antigen expression were evaluated by intracellular staining (ICS) and flow cytometry using two monoclonal antibodies selected for ds RNA and NP antigen **(Figure 9).**

From this analysis the percentages of NP and dsRNA positive cells matched and were correlated to the RNA amount used, indicating the production of functional RNA with replication capability.

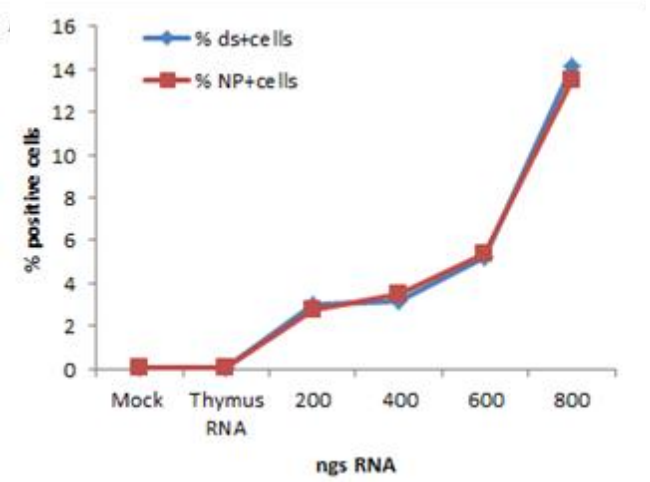

Fig. 9. Characterization of SAM (NP) vector:
NP vector was characterized analyzing RNA amplification capability by intracellular antigen expression after transfection in BHK cells with 200-400-600-800 ng of RNA. Thymus RNA and mock were used as negative control. The graph shows the percentage of cells containing replicating SAM vectors ($dsRNA^+$) that correlates with the frequency of antigen expressing cells ($NP\ antigen^+$).

3.1.2 Production and purification of Viral Replicon Particles (VRPs) encoding NP

There are limited published data on the *in vivo* delivery of self-amplifying RNA using non-viral delivery strategies; instead there have been extensive works on the viral delivery of RNA molecules using Viral Replicon Particles (VRPs) that are potent vaccines in mice, non-human primates and humans. These single-cycle alphavirus vectors are considered the most efficient tools to deliver nucleic acids into cells and for this reason, they were selected in this present study as nucleic acid delivery benchmark.

VRPs were produced into a susceptible cell line usually, BHK cells, as previously described [62]. In this system, the NP expressing replicons were packaged into VRPs by co-electroporation in BHK cells along with defective helper RNAs encoding the Sindbis virus capsid and glycoprotein. In detail, capsid and envelope glycoproteins genes were amplified from the reverse-transcribed RNA genome of Sindbis virus and then cloned into DNA plasmid backbone under the transcriptional control of bacteriophage SP6 promoter. The plasmid was transformed in *Escherichia coli* and purified by cell alkaline lysis and anion exchange chromatography. Plasmid DNA was then linearized by PmeI endonuclease digestion and isolated by phenol/chloroform extraction and ethanol precipitation. Finally, to increase RNA stability, a poly (A) tail was added to RNA by enzymatic post-transcription reaction further purified by LiCl precipitation.

At 24 and 48 hours post co-electroporation, VRPs (NP) were released to BHK media **(Figure 10).** Finally, highly purified VRPs were obtained from the harvested supernatants through "sucrose cushion" by sucrose gradient zonal ultracentrifugation.

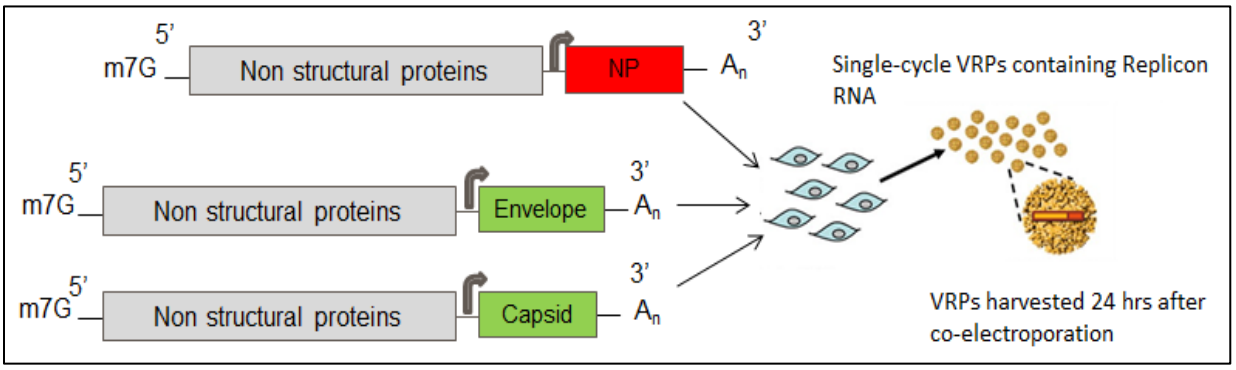

Fig. 10. Schematic representation of VRPs production.
VRPs were produced by co-electroporation of BHK cells with replicon RNA, encoding the NP gene, along with defecting helper replicon encoding glycoproteins and capsid genes.

Viral replicon particles titers were determined by intracellular staining of expressed NP protein antigen follow by an overnight infection of BHK cells with three serial dilutions of particles. By flow cytometry analysis, the percentage of positive NP cells was determine and used to calculate the titer. In previous work by Balsitis et al., calculation has been found to be consistently linear when cells are 2-60% positive post infection. In the table below, (**Table 1**) our result are summarized. The two dilutions allowed determining a titer of $5.7x10^8$ infection unit per ml.

	Diluition factor	% positive cells	Infected cells	VRPs Titer (IU/mL)	Average (IU/mL)
NP-VRPs	250	43,2	$3,22x10^5$	$4,03x10^8$	$5,7x10^8$
	1250	18,7	$1,18x10^5$	$7,38x10^8$	

Table 1. Evaluation of VRPs titer (Infection unit per mL) by flow cytometry data.
The calculation of VRPs titer was performed based on the percentage of positive cells to infection. The calculation has been found to be consistently linear when cells are 2-60% positive.

3.1.3 Non-viral delivery system for SAM vaccines, Lipid Nano Particle (LNPs)/RNA formulation

RNA molecules were encapsulated in a non-viral delivery system based on lipid nanoparticle as previously described [29].

Briefly, the lipids 1,2-Diasteroyl-sn-glycero-3-phosphocholine (DSPC), 1,2-dilinoleyloxy-N,N-dimethyl-3-aminopropane (DLinDMA), Cholesterol, 1,2-dimyristoyl-sn-glycero-3-phospethanolamine-N-[methoxy(polyethylene glycol)-2000] (ammonium salt) (PEG DMG 2000) and cholesterol, were combined at molar ratio of 40:10:2:48 (DLinDMA:DSPC:PEG-DMG 2000:cholesterol) by an ethanol dilution to produce the LNP (**Figure 11**) .

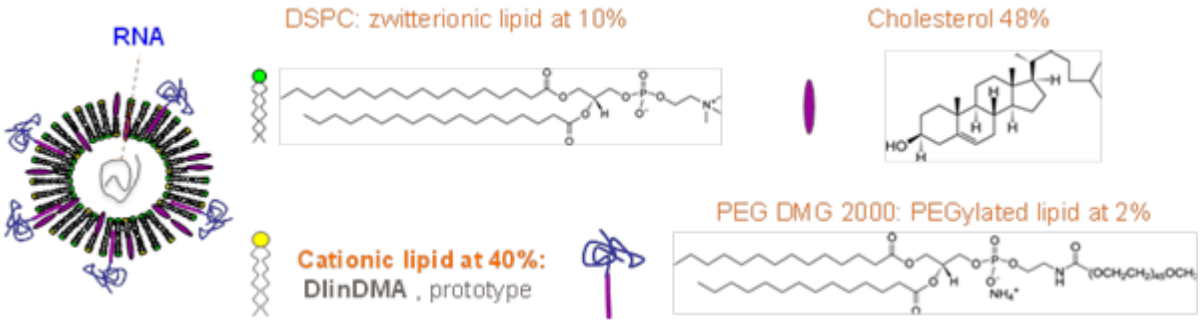

Fig. 11. Schematic illustration of Lipid nanoparticle (LNP) structure.
This system is composed of zwitterionic lipid, cationic lipid, cholesterol, and PEGylated lipid, formulated with self-amplifying mRNA *(Adapted from Self-amplifying mRNA vaccines. Adv Genet, 2015)*

LNPs were produced mixing through a T-Junction, with a syringe pump system, equal volumes of lipid in ethanol and RNA in 100 mM citrate buffer at molar ratio 8:1 N:P (Nitrogen from DLinDMA: phosphate on RNA). The resulting LNPs were dialyzed overnight at 4°C against PBS and then characterized for particle size, RNA encapsulation efficiency and RNA integrity as previously described [29].

The formulated LNPs were characterized by dynamic light scattering (DLS) evaluating the mean particle size and polydispersity index. The Z-average diameters ranged from 160 to 170 nm with a low polydispersity index ranging from 0.09 to 0.14, indicating the formation of small and uniform lipid particles. The percentage of RNA entrapment was evaluated from the difference of "unencapsulated amount" of RNA measured before and after LNPs Triton treatment. The data showed that lipid particles are able to encapsulate more than 90% of mRNA (data not shown).

Moreover the RNA integrity was evaluated by agarose gel electrophoresis after RNA extraction from LNPs and comparison with NP-RNA prior the formulation in the LNPs (**Figure 12**).

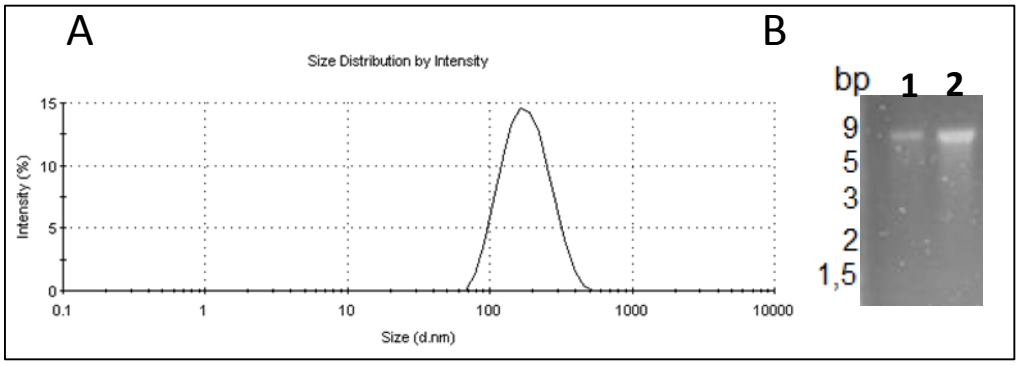

Fig. 12. Characterization of NP SAM-LNPs.
(A) Size distribution of standard LNPs formulated with T-Junction were provided by DLS. The size distributions were characterized by a single peak with a low polydispersity index, indicating a relatively monodisperse size distribution**.** (**B**) Evaluation of NP-RNA integrity on agarose gel electrophoresis. Comparison between NP-RNA extracted from LNPs (line 1) and NP-RNA prior the formulation in the LNPs (line 2).

3.1.4 Absolute quantification of Nucleoprotein antigen by Selected Reaction Monitoring (SRM) mass spectrometry

With the purpose to specifically quantify the NP expression from a complex biological background, such as mammalian cell lysate, we employed Selected Reaction Monitoring (SRM), a quantitative mass spectrometry technique for the detection and quantification of specific, predetermined analytes with known fragmentation pattern [68].

In this assay, isotopically labeled peptides identical to those deriving from the tryptic digestion of the NP protein (proteotypic peptides, PTPs), were used as surrogates for the final protein quantification.

In particular, we developed an experimental approach in which isotopically forms of PTPs of known amount were spiked in the biological sample before trypsin digestion to increase the accuracy of the antigen quantitation.

3.1.4.1 Selection of proteotypic peptides (PTPs) for NP quantification

The PTPs were experimentally selected from the tryptic digestion of commercially available recombinant form of Nucleoprotein and the generated peptides were analyzed by nano LC-MS/MS in an ESI-Q-TOF instrument in data dependent acquisition mode. The spectra obtained by MS/MS were processed using MASCOT search engine program against a database containing the Nucleoprotein protein sequence deduced from the pandemic strain A/Puerto Rico/8/34/H1N1 genome. This search provided a list of 29 peptides that covered the 56% of NP amino acid sequence (**Table 2).**

Peptide	Observed (m/z)	Mascot Score	Key selection criteria	% NP coverage
K.RSYEQMETDGER.Q	506,2178	32	Oxidation (M)	
R.SYEQMETDGER.Q	673,2819	29	Deamidated (NQ) & Oxidation (M)	
R.SYEQMETDGERQNATEIR.A	724,9937	72	Oxidation (M)	
R.QNATEIR.A	417,2212	8	Deamidated (NQ)	
K.MIGGIGR.F	360,1988	31	Oxidation (M)	
K.LSDYEGR.L	**420,2016**	**35**		
R.LIQNSLTIER.M	594,3436	72	Deamidated (NQ)	
R.MVLSAFDER.R	542,2623	60	Oxidation (M)	
K.YLEEHPSAGK.D	**565,7797**	**54**		
K.KTGGPIYR.R	446,2588	10	KK-RR	
K.TGGPIYR.R	382,2069	43	RR	
R.QANNGDDATAGLTHMMIWHSNLNDATYQR.-	816,3634	46	Deamidated (NQ) & Oxidation (M)	
R.TGMDPR.M	338,6595	12	Low MASCOT score	
K.GVGTMVMELVR.M	604,3273	56	Oxidation (M)	56%
R.IAYER.M	326,1771	8	Low MASCOT score	
K.AMMDQVR.E	441,7009	45	Oxidation (M)	
R.NPGNAEFEDLTFLAR.S	847,9266	96	Deamidated (NQ)	
R.SALILR.G	**336,7262**	**37**		
R.EGYSLVGIDPFR.L	**676,8499**	**100**		
R.LLQNSQVYSLIRPNENPAHK.S	774,4168	136		
R.VLSFIK.G	353,7304	22	Low MASCOT score	
R.GVQIASNENMETMESSTLELR.S	1170,5493	65	Deamidated (NQ)+ Oxidation (M)	
R.YWAIR.T	354,6956	20		
R.ASAGQISIQPTFSVQR.N +	846,4595	8	2 Deamidated (NQ)	
R.NLPFDR.T	381,705	34	Deamidated (NQ)	
R.TTIMAAFTGNTEGR.T	743,3476	3	Oxidation (M)	
R.MMESARPEDVSFQGR.G	591,2666	60	Deamidated (NQ) & 2 Oxidation (M)	
R.GVFELSDEK.A	**512,2559**	**42**		

Table 2. NP peptides identified by LC-MS/MS analysis.
List of 29 peptides obtained from the MS/MS spectra analysis by MASCOT program. In the table, peptide sequence, *m/z* value, Mascot Score and modified amino acids identified were reported.

From this list, we selected five proteotypic peptide (PTPs) (highlighted in red) that do not displayed amino acids with observed and predicted chemical modifications (glutamine and asparagine deamidation, cysteine and methionine oxidation, N-terminal glutamine for cyclization), and present a specific length from 5 to 20 amino acids. Moreover peptides with low Mascot score and generated form of digestion site characterized by KK, RK, RR, KR consecutive amino acids, which lead of an incomplete tryptic digestion, were neither selected. Furthermore each PTPs were investigated for the uniquely association to the targeted protein in the specific biological background. For this reason the sequence of the selected PTPs were inspected against a database containing sequences deduced from the C3H mouse model genome and no matches were found.

PTPs were then investigated for the quality of MS/MS spectra in Q-TOF and triple quadruple instrument and the three of them that present the most intense fragment ions were finally selected (**Figure 13**). PTPs sequences are: SALILR (residues 262 to 267), EGYSLVGIDPFR (residues 304 to 315) and GVFELSDEK (residues 472 to 480) located in the middle and N terminus of NP sequence.

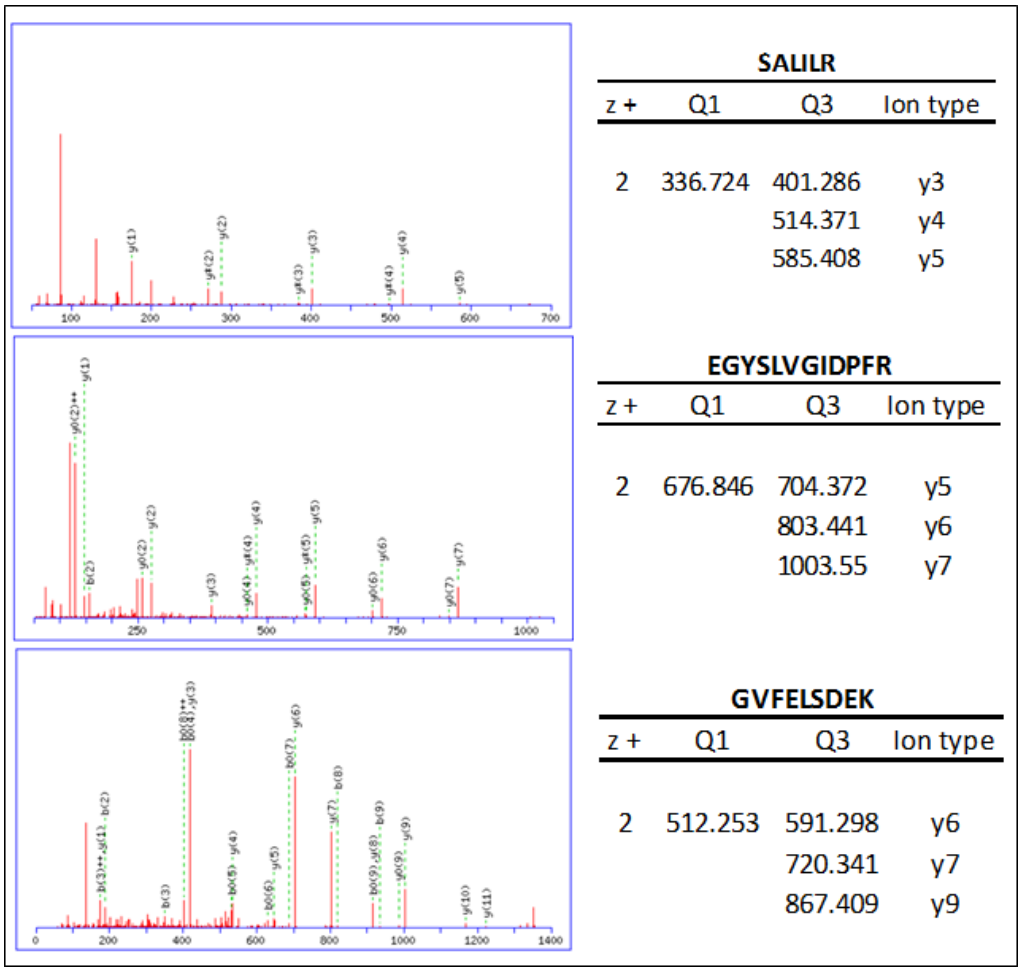

SALILR

z +	Q1	Q3	Ion type
2	336.724	401.286	y3
		514.371	y4
		585.408	y5

EGYSLVGIDPFR

z +	Q1	Q3	Ion type
2	676.846	704.372	y5
		803.441	y6
		1003.55	y7

GVFELSDEK

z +	Q1	Q3	Ion type
2	512.253	591.298	y6
		720.341	y7
		867.409	y9

Fig. 13. MS/MS spectra of selected PTPs.
MS/MS spectrum of the three most intense fragment ions associated to each selected PTPs In the right panel of the figure the specific PTPs properties are summarized: *m/z* of parent ions (Q1) and the selected fragment ions selected (Q3), charge state of the parental ion (z^+), and the ion type of the three selected fragments .

For these three peptides, SRM transitions were selected, representing the precursor ion mass and three different characteristic fragment ions required to reduce the possibility of false positives

during the analysis. This is particularly relevant for the analysis of complex mixture of peptides in which co-eluting isobaric peptides exhibiting similar primary structure.

For an accurate quantification of NP in the biological sample, the stable isotope dilution method (SID) was selected. For this reason the identified PTPs were synthetized either in light- and heavy-labeled forms by incorporating ^{13}C-^{15}N lysine or arginine residues and quantified by the provider according to amino acid composition analysis (JPT Peptide Technologies GmbH). The peptides were used to build up a linearity curve, moreover the heavy-labeled one were also used as a spike of a known amount in the sample to precise protein quantitation.

These synthetic peptides were also used to optimize another fundamental parameter in SRM transition, the collision energy (CE) value associated to fragmentation in the Q2 collision cell.

In order to obtain the higher fragment ion signal intensities, collision energy (CE) optimization was performed in SRM acquisition in which panels of different CE were applied to the parental ions in order to monitor their fragmentation and the correspondently peak area.

The optimized PTPs transitions for NP were reported in the **Table 3**, both for light and heavy labeled PTPs form.

	Light		Heavy		
	Q1	Q3	Q1	Q3	CE
	m/z		m/z		Voltz
SALILR	336,724, $Z^+ = 2$	401,286	341,728	411,295	12
		514,371		524,329	14
		585,408		595,416	16
GVFELSDEK	512,253, $Z^+ = 2$	591,298	516,261	599,312	20
		720,341		728,355	18
		867,409		875,423	16
EGYSLVGIDPFR	676,846, $Z^+ = 2$	704,372	681,85	714,382	23
		803,441		813,499	23
		1003,55		1013,55	23

Table 3. List of optimized SRM transitions for the selected PTPs

This approach was also used to determine the optimal SRM transitions for the detection of NP immunodominant peptide SDYEGRLI (H-2K^{K} haplotype). This peptide is well ionized and results in a MS good signal, moreover is not characterized by amino acids prone to chemical modification. For all this reason is considered as a good candidate for proteomic studies.

Transitions were selected among the most intense fragment ions to maximize the sensitivity (**Table 4**).

	Light		**Heavy**		
	Q1	Q3	Q1	Q3	CE
	m/z		m/z		Voltz
SDYEGRLI	476,74, Z^{+}=2	458,307	480,24	465,324	23
		587,35		594,367	23
		750,413		757,432	23

Table 4. List of optimized SRM transitions of the immunodominant MHC H-2K^{k} class I peptide.

3.1.5 SISCAPA development method for low abundance protein quantitation in complex biological sample by SRM.

In this study, SRM has been applied to protein quantitation in complex biological samples as cell lysate or tissue homogenates characterized by an extreme difference in the range of expression. In particular for low abundance expressed proteins, the decrease of sample complexity and the increase of targeted SRM assay sensitivity are required for the quantitation of those proteins.

For this reason, here we have investigated an approach (summarized in **Figure 14**), that exploited the unparalleled ability of antibodies to specifically extract a target peptide in a complex biological matrix. This method termed Stable Isotope Standards and Capture by Anti-Peptide Antibodies (SISCAPA) have been pioneered by Anderson in 2003 and combines quantitative MS up-stream to immune affinity enrichment of desired peptides in an immune SRM assay [62]. This approach was applied for NP antigen and MHC class I immune-dominant peptide quantitation.

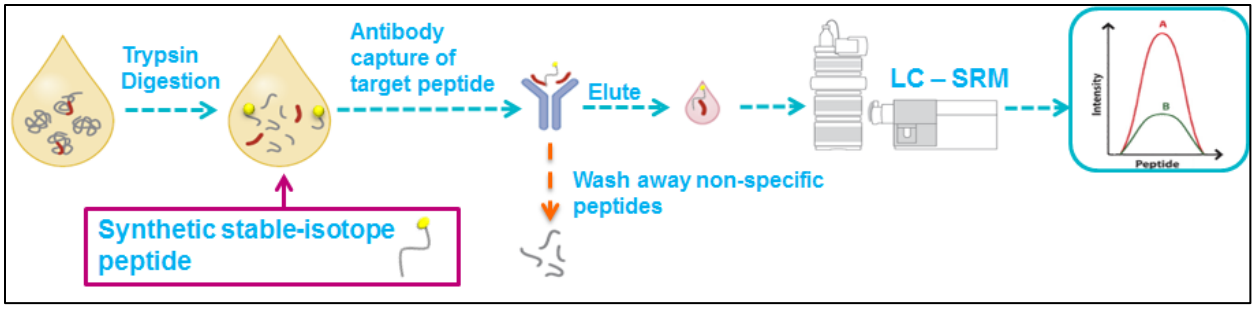

Fig. 14. Schematic diagram of the SISCAPA method for peptide quantitation
SISCAPA approach combines four elements previously described: (1) digestion of a protein sample to peptides; (2) addition of internal standard peptides labeled with stable isotopes; (3) enrichment of low abundance peptides by capture with anti-peptides antibodies; and (4) quantitation by MS. (*Adapted from: Quantitative mass spectrometric multiple reaction monitoring assays for major plasma proteins, Anderson, 2006).*

To obtain immune-dominant sera for the selected PTPs and NP-MHC I peptide, the synthetic form of the peptides were produced, conjugated to Bovine Serum Albumin (BSA) or Keyhole Limpet Hemocyanin (KLH) via N-terminal cysteine (JPT Peptide Technologies GmbH) and used to immunize rabbits.

In details, two New Zealand White rabbits (for each single peptide) were immunized, according to 49-day protocol of 3 injections, three and two weeks apart, with 50 μg of synthetic BSA conjugated peptides in alum adjuvant.

To assess the presence of peptide specific IgG, sera from each rabbit were collected two weeks post third immunization and used to determine antibody titer by indirect ELISA, spotting KLH-conjugated peptides onto microtiter plates. Rabbit sera with the higher titer were chosen as a source of polyclonal antiserum. ELISA titers obtained for MHC Peptide-BSA antibody were reported in **Figure 15** as an example.

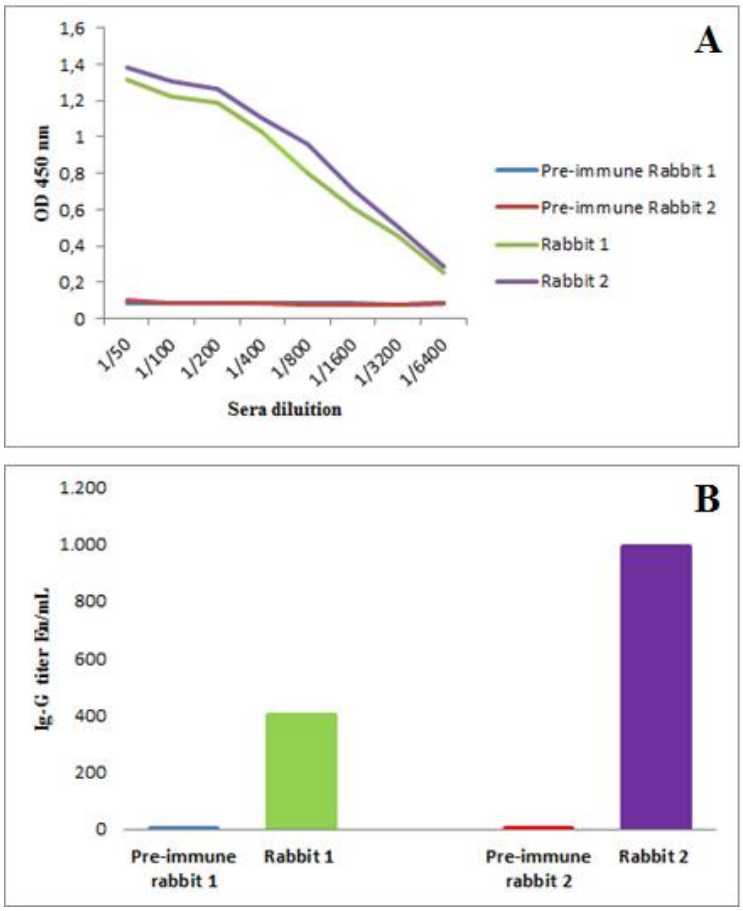

Fig. 15. ELISA titers from sera derived from New Zealand White rabbits immunized with MHC-I peptide conjugated to BSA carrier.

(A) Serum and pre-immune serum samples were 2-fold serially diluted in PBS containing 1% (w/v) BSA 0.05% (v/v) Tween, and transferred into the coated and blocked plates. After 1 h incubation, plates were incubated with alkaline phosphatase-conjugated goat anti-rabbit IgG to detect antigen-specific IgG antibodies. Absorbance was measured at 405 nm after addition of P-nitrophenyl phosphate disodium substrate. **(B)** The titers were normalized respect to the pre-immune serum assayed in parallel, choosing an OD threshold=1, and indicated as ELISA Units/ml (EU/ml). Rabbit number two, (in violet) shows antibody titers significantly higher than those obtained with rabbit number one (in green), for this, the corresponding serum was used as antibody source.

Antibodies were then purified by affinity on Protein G and eluted with glycine-HCl pH 2.5 immediately followed by neutralization to pH 7.0 with Tris-HCl pH 8.0 to preserve antibody activity. IgG concentrations were spectrophotometrically determined evaluating sample absorbance (A) at 280 nm using the specific mass extinction coefficient (ε) established for most of mammalian antibodies. Antibodies purified from the affinity chromatography were checked by SDS-PAGE in reducing conditions. As an example, in **Figure 16 (**A**),** the electrophoresis profile of Ab generated for MHC class I peptide was reported. Dithiothreitol (DTT) reduces the disulfide bridges in the antibody molecule (~150 kDa), releasing light and heavy chains that appear as two distinct bands of 50 and 25 kDa. The protein profile on SDS-PAGE confirmed the purification of the Ab, with an average yield of 20 mg at a concentration of 1 mg/ml, starting from 20 ml of rabbit sera.

Moreover the polyclonal antibody specificity was confirmed by dot blot assay **Figure 16** (B) in which, KHL-conjugated peptides, BSA-conjugated peptides and BSA were spotted in the nitrocellulose membrane and revealed by anti BSA-conjugated peptides antibody. **Figure 16** (B) shows that the purified antibodies present activity against BSA conjugated peptides and BSA alone. Selectivity towards peptides was evaluated identifying reactivity against KHL conjugated peptides.

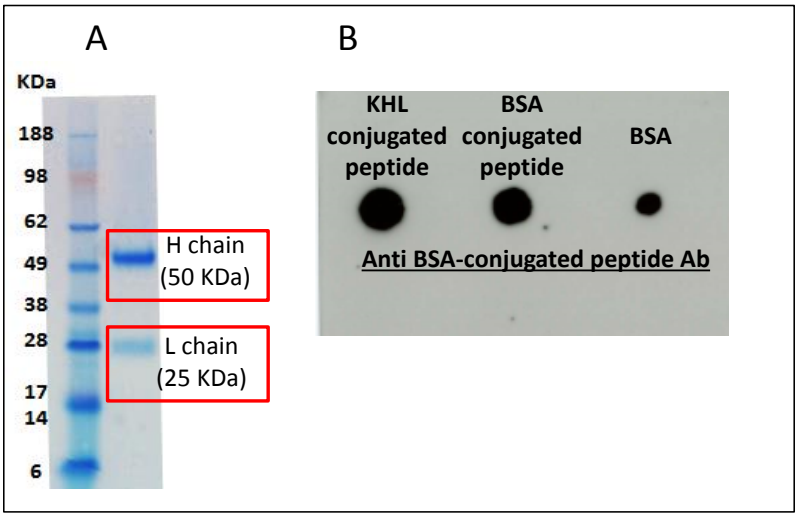

Fig. 16. Characterization of anti-peptide antibodies for SISCAPA method
(A) The protein profile in reducing condition of SDS-PAGE stained with Coomassie Blue confirmed the purification of the Ab from individual rabbit 2. In red light and heavy Ab chain are highlight. **(B)** Dot blot assay confirmed the Ab specificity versus the specific peptides: purified Ab shows specificity not only versus BSA conjugated peptides and BSA but also against KHL conjugated peptide spotted in nitrocellulose membrane.

Antibodies for all the selected PTPs were also produced and purified.

ELISA titers, average amount and specificity for each antibody were summarized in **Table 5**

	SALILR-Ab	GVFELSDEK-Ab	EGYSLVGIDPFR-Ab	MHC I peptide-Ab
Higher Elisa titer	1200 EU/mL	525 EU/mL	1500 EU/mL	989 RU/mL
Average amount (mg)	25	14	32	20
Specificity	+	+	+	+

Table 5. List of antibodies produced and purified for all PTPs and immunodominant MHC class I peptide

Part II

3.2 Characterization of NP expression during SAM vaccination: an *in vitro* model system.

Preliminary data, suggested that muscle cells play an important role during *in vivo* SAM vaccination [24]. Many studies have shown that intramuscular injection of mRNA encoding reporter genes, results in protein expression in myocytes. Also for SAM vaccines, different studies have reported that antigen expression occurred mostly in the muscle fibers after RNA administration with a lipid-based delivery system. To better elucidate the *in vivo* antigen expression during SAM vaccination, we started to set up an *in vitro* cellular model using the myoblast cell line C2C12.

In **Figure 17** a schematic representation of myoblast cell line (C2C12) SAM transfection in a time course experiment is represented. Myoblast cells were collected at different time point after SAM transfection and intracellular Nucleoprotein expression was evaluated trough intracellular staining (ICS), flow cytometry and quantitative mass spectrometry assays.

For the flow cytometry analysis, myoblast cells were intracellular-stained with a fluorescent isothiocyanate (FITC)-labeled anti NP antibody in order to identify the percentage of NP positive cell. On the other hand, NP absolute quantification in total cell lysate was performed by SRM. The results obtained from both techniques allowed measuring the NP molecule number per myoblast cell that we defined as “NP cellular abundance”.

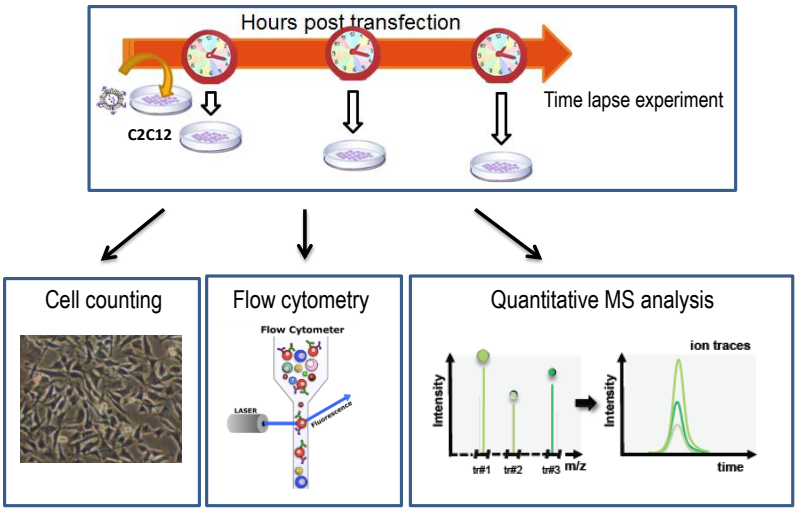

Fig. 17. Schematic workflow of experimental strategy.
Cell line C2C12 was transfected by SAM, and at different time point after transfection cells were collected and counted. NP expression was analyzed using flow cytometry and its absolute abundance in total cell lysate was performed by quantitative mass spectrometry.

3.2.1 Characterization of protein antigen expression in myoblast cells, comparing VRPs infection and SAM transfection.

In order to define the experimental model employed in the characterization of protein antigen expression upon SAM vaccination, cell line C2C12, were treated with NP expressing Viral Replicon Particles NP-(VRPs), taking advantage of their high *in vitro* infection rate. The same approach was then applied to SAM, in which myoblast cells were transfected with LNPs.
In details, C2C12 were treated with two different NP-(VRPs) and NP-(LNPs) amounts to monitor protein antigen expression during 24 hours by ICS and SRM.
Two amount of VRPs (10^5 and 10^6 Infection Unit (IU) were used to infect 200.000 C2C12 cells, grown at confluence. At 2, 4, 12, and 24 hours, the cells were collected and the percentage of NP positive cells were assesses by ICS and flow cytometry. The results were summarized in **Figure 18**. For both amount of VRPs an early antigen expression was observed already at 2 hours post infection (hip). With the lower amount (10^5 U.I., in blue in the graph represented in Figure 11) a maximum of positive cells, corresponding to 60% of the total cells were observed at 4 and 12 hours, at 24 hours NP positive cells was 30%. The diminution of NP positive cells between 12 and 24 hours might reflect the intracellular degradation or loss of functionality of the dsRNA or NP protein. The integrity of the cells at this time point was checked by flow cytometry to

exclude potential cellular lysis. This behavior was not observed for the infection with the higher amount of VRPs (10^6 U.I., in red in the graph represented in **Figure 18**) where almost all myoblast cells were positive to NP expression at all time point, probably reflecting a high amount of dsRNA uptake per cell.

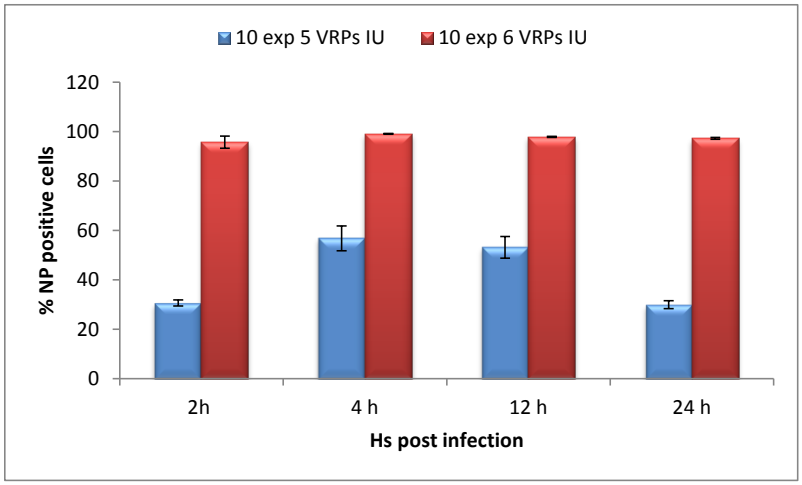

Fig. 18. Intracellular staining and flow cytometry assay to identify the positive percentage of myoblast cells to NP expression during VRPs infection.
Cell line C2C12 was infected with 10^6 VRPs IU (in red) and 10^5 VRPs IU (in blue) and the NP antigen expression were monitoring during 24 hours post infection by ICS and flow cytometry using a NP antibody FITC conjugated. Histograms represent the percentage of NP $^+$ myoblast. Data are representative of three independent experiments.

No quantitative information could be obtained from this type of analysis. For this reason SRM was applied in parallel to determine the absolute quantitation of NP protein antigen. With this purpose, myoblasts cells from each time point, were lysated and subjected to reduction and alkylation. The labeled form of three PTPs were then added and the mixture were subjected to trypsin digestion using the FASP (filter assisted sample preparation) method previously described [81] and detailed in the material and methods section in order to quantify the endogen PTPs as surrogate of NP quantitation.

The amount of endogen PTPs was deduced from a calibration curve established in a matrix that mimics the same "environment" of the sample. To build this curve, a fixed amount of heavy forms of PTPs (25 fmol/µg of ^{13}C-^{15}N-labeled PTPs) and scalar concentration of light PTPs (ranging from 0,2 to 810 fmol/µl) were added to a fix amount of matrix (1 µg of C2C12 total cell lysate). The protein and peptide mixture was digested with trypsin and the peptides were

analyzed by LC-SRM. Each PTPs concentration was plotted against the light and heavy peak area ratio obtained in order to account any variations during LC-MS approach as loading sample step, age of column, perturbations during the LC run etc.).

As an example, the dose range-response curve of the PTP GVFELSDEK is reported in **Figure 19**. The response was linear from 1,6 to 405 fmol/µl and the Lower Limit of Quantitation (LLOQ), defined as the lowest concentration point on the fitted curve with an accuracy deviation ≤ 20%, was established at 3.2 fmol/µl. Considering an average molecular weight of 56,000 Da for NP molecule, a low limit of quantification of 0.6 pg per 1 µg of total cell lysate was calculated.

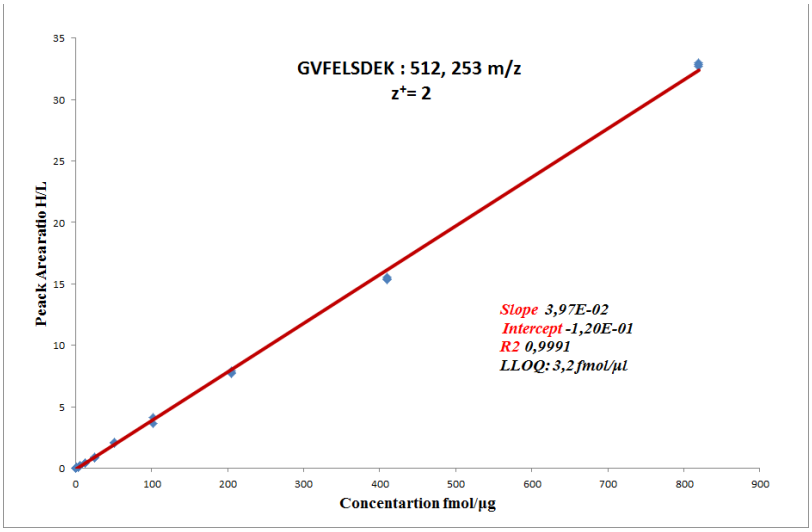

Fig. 19. Dose-response curve of PTP GVFELSDEK.

The lower limit of quantification was simultaneously identified for all PTPs and, the highest value obtained, was used to define the global NP LLOQ. In this case, the value achieved for all PTPs was the same, (0,6 pg per 1 µg of total cell lysate), and was used as standard to the further quantifications.

Moreover to evaluate the interchangeability of three PTPs selected for the analysis; NP protein antigen quantification was performed in each considered time point. The coefficient of variation (% CV) at each PTPs, ranged from 10 to 15%, showing a low overall data variability and indicating the interchangeability of all PTPs (data not shown).

In **Figure 20** the simultaneous PTPs signal detection for both, light and heavy form, performing during LC-SRM approach was shown.

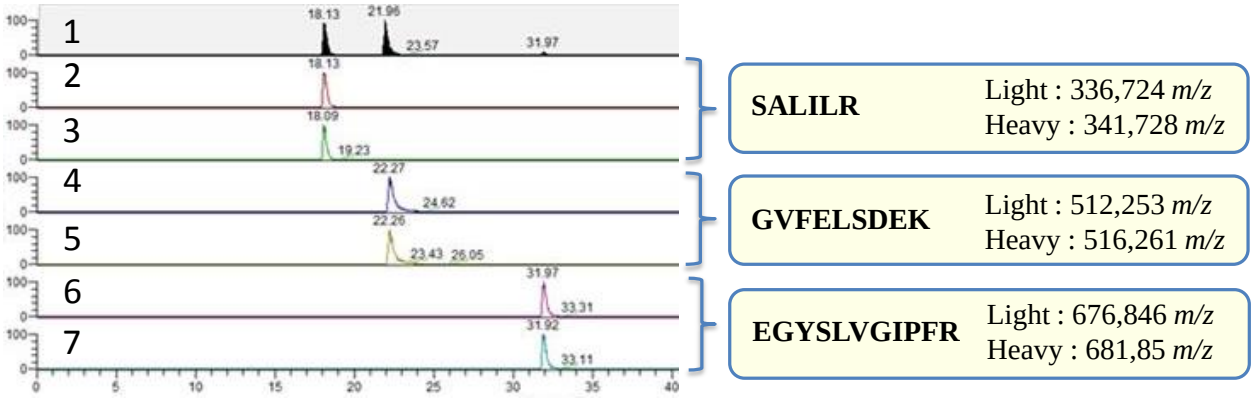

Fig. 20. Simultaneous detection of multiple PTPs by LC-SRM MS.
Multiplexed detection of 3 PTPs. A mixture of each synthetic light and heavy peptide, 800 fmol and 50 fmol respectively, were loaded and analyzed directly by LC-SRM using a method to detect all peptides simultaneously. The mass chromatogram represents mass spectrometry data, where the x-axis represents the time of analysis and the y-axis the signal intensity. Line 1 defines the mass chromatogram derived from the total ion current (TIC) that represents the summed signal intensity across the entire range of the selected masses detected at every point in the analysis. In the other lines, the mass chromatogram derived only from signal intensity associated to each PTPs. Co-elution of light and heavy peptide was observed between line two-three for SALILR peptide, line four-five for GVFELSDEK peptide and line six-seven for EGYSLVGIPFR peptide.

Precise quantitation of NP protein antigen from each time point was measured. NP protein antigen was already detected and quantified at two hours post infection. For the both doses, no increase of NP amount was observed until 4 hours, followed by a substantial increase of expression, peaking around 12 hours post infection. Steady amount was observed until 24 hours post infection (**Figure 21**).

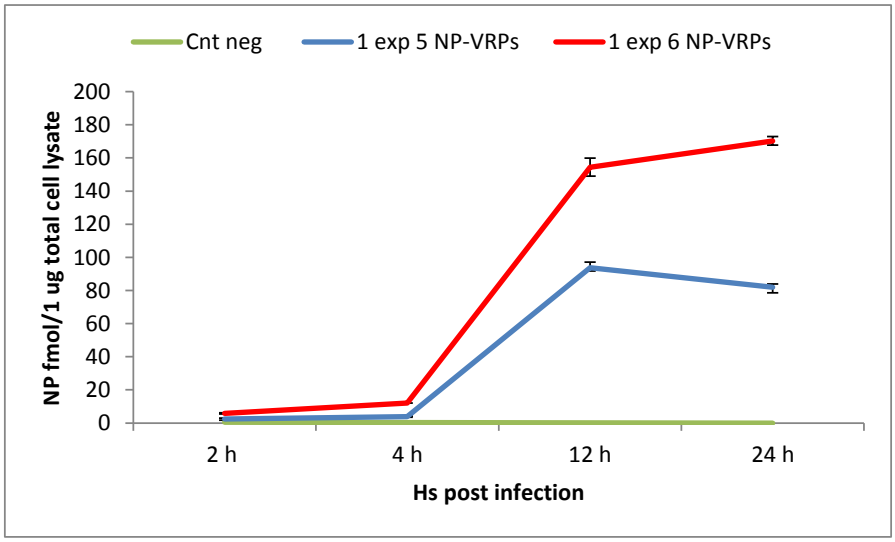

Fig. 21. Absolute quantification NP protein in 1 µg of total cell lysate over the course of VRPs infection.
The red line represents the NP quantitation during the infection with 10^6 VRPs IU instead the blue one represents the NP quantitation after infection with 10^5 VRPs IU. In green the negative control in which cell are infected by empty VRPs.

The early antigen detection and quantitation evaluated with VRPs probably reflecting the high *in vitro* infection capability of alphavirus particle. The time frame required to protein detection in our experiment (2 hours) is consistent with previously published data that have reported how alphavirus infection process occurs. In fact, only when an appropriate interaction between virus and cellular receptors is established, the process of transferring virus genome to the cell interior, mediated by E1 an E2 glycoprotein, can take place allowing the detection of specific RNA virus and proteins. All these events, during alphavirus infection occur in a time frame of 1-2 hours as we observed in our experiment.
Moreover, from results obtained by ICS and SRM, the copies of NP antigen per myoblast cell were estimated (NP cellular abundance) (**Figure 22**).

From this data, an increase of NP protein antigen copies per cells between 4 to 12 hours post infection was observed for both VRPs IU. In particular, for 10^5 VRPs IU, the NP cellular abundance increases from around $4x10^5$ to $9x10^6$, reaching $1.5x10^7$ molecules at 24 hours post infection. For 10^6 VRPs IU, NP protein abundance increases from $7x10^5$ to $8x10^6$, reaching around at $1x10^7$ molecules at 24 hours post infection. From this results we can observe that the NP cellular abundance at 24 hours post infection, obtained from 10^6 VRPs IU is about a third of that observed with 10^5 VRPs IU.

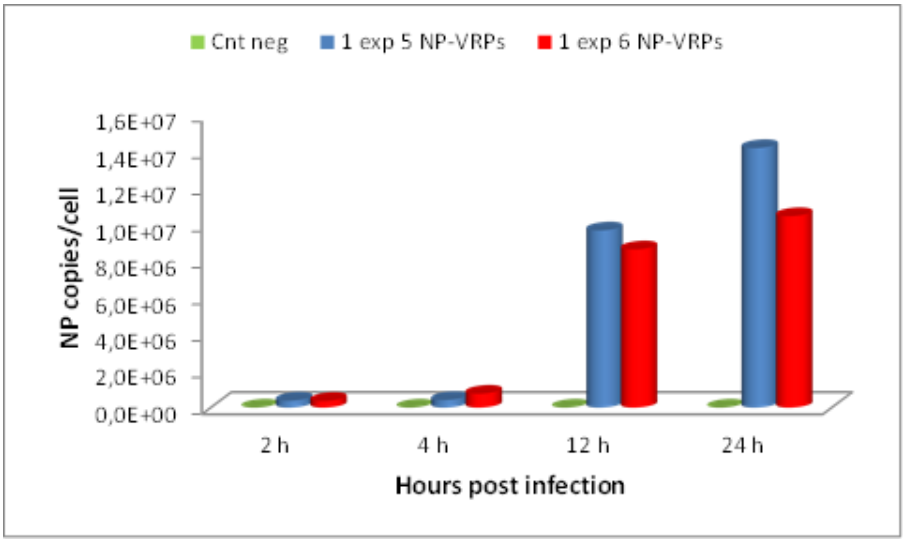

Fig. 22. Absolute quantification of NP protein in myoblast cell over the course of VRPs infection. Histograms represent NP abundance in myoblast cell for each time point. In blue value for 10^6 VRPs IU was represented instead the red one where the value for 10^5 VRPs IU.

This is might be related to a toxic effect associated to high cellular level of NP encoding RNA. The intracellular production of high amount of ds RNA might induce the cellular RNA sensitive machinery that built a first barrier of defense against for example infection, inducing RNA degradation. On the other hand high RNA amount could be interfering with protein antigen expression, synthetizing truncated form of proteins which will degraded subsequently. Other possibilities could be considered and could be interesting to understand all biological processes such a signaling pathway, gene expression, protein-protein interaction and changes induced by this kind of environmental stimuli. SRM also in this case could be used as a key tool, having the capability to delve deep in a cellular proteome with high sensitivity and selectivity.

The same strategy was then applied to monitor NP protein antigen quantitation after in *vitro* SAM transfection using two different mRNA amounts: 250 ng and 2 µg. The percentage of NP positive cells was evaluated by ICS at 4, 12 and 24 hours post transfection (**Figure 23**)

In this case the expression was observed at 12 hours post transfection. Moreover an increase of the percentage of NP positive cells from 3 to 8% was measured with 250 ng of RNA (in red) between 12 to 24 hours post treatment. This was not observed with 2 µg of RNA (in blue), where the NP positive percentage remain almost the same during the two time points.

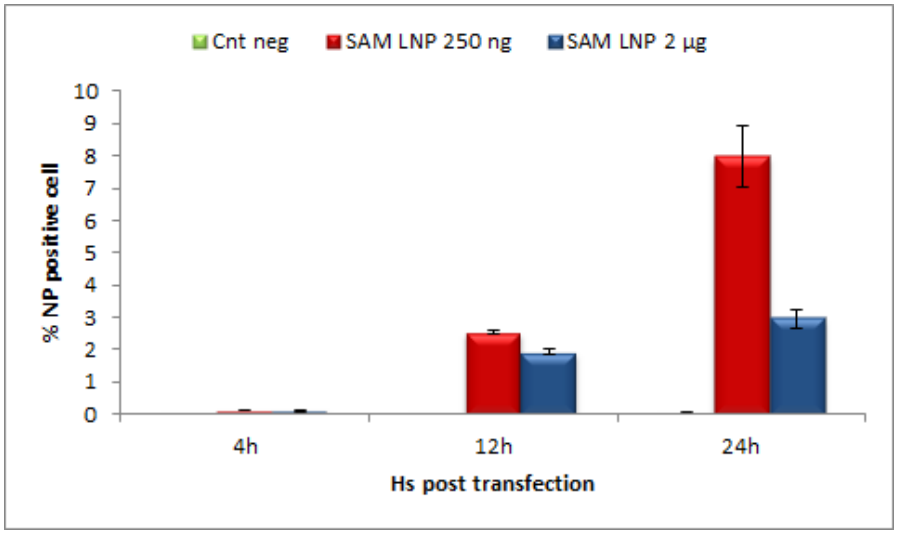

Fig. 23. Intracellular staining and flow cytometry assay to identify the percentage of myoblast cells that express NP protein antigen during SAM transfection.

Cell line C2C12 was transfected with 2 µg (in blue) and 250 ng (in red) amount of LNP-SAM. NP antigen expression were monitoring during 24 hours by intracellular staining using. Histograms represent the percentage of NP^{+} myoblast. Data are representative multiple experiment.

Compering LNPs with VRPs a lower percentage of NP expressing cells was notice. This observation could be explain by low efficiency of LNPs internalization, release of RNA in the cells or moreover for low antigen expression. Quantitative approach was the applied to better elucidate this point. With this kind of analysis we were able to investigate only the NP antigen expression, without acquire more information related to LNPs internalization or the following RNA release.

We then focused in the quantitative data, obtained by SRM, using the three PTPs as surrogates of protein quantitation (**Figure 24**)

NP protein antigen was detected and quantified only at 12 hours post transfection, consistent with what already seen by ICS. Moreover, for 250 ng of mRNA dose (in red), the NP amount substantial increase from 12 to 24 hours post transfection peaking around 35 fmol per 1 µg of total cell lysate. Different behavior was observed with 2 µg of mRNA for which constant low level of expression was observed.

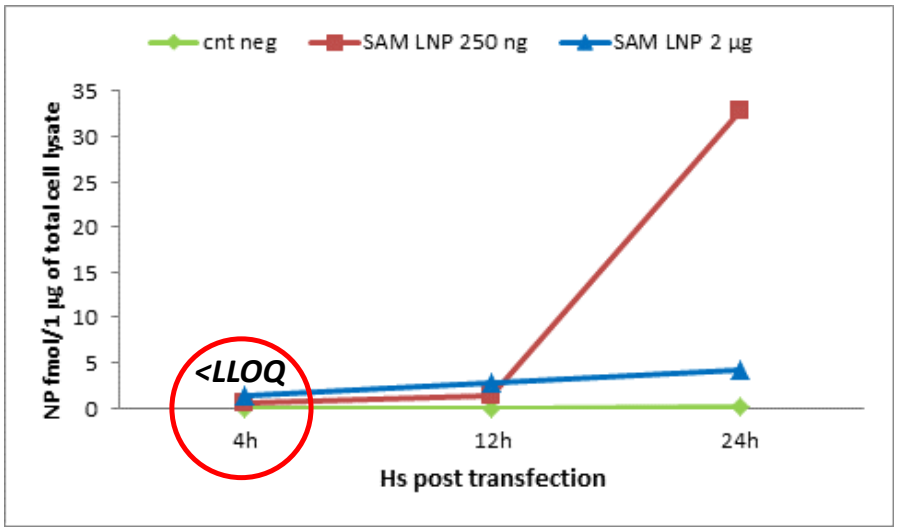

Fig. 24 Absolute quantification NP protein in 1 µg of total cell lysate during SAM immunization.
The red line represents the NP quantitation with 250 ng of LNPs SAM, instead the blue one that represent the NP quantitation with 2 µg of LNPs SAM. In green the negative control in witch cell were not transfected. Value at 4 hours post transfection could not be monitored because < of LLOQ of analysis.

From this data we can suppose that the lower percentage of NP expressing cells towards what observed with VRPs could be related to an inefficient LNPs transfection or RNA release. This is might be associated with the mechanism by which LNPs are internalized in the cellular system not mediated by receptors but probability due to electrostatic interaction between liposome, that hold a positive charge conferred by cationic lipid, and plasma membrane. Moreover low transfection efficiency could be also caused by a PEG-mediate liposome aggregation, not observed after formulation, but which could preventing desirable cell internalization. This phenomenon was amplified with 2 µg RNA dose, where a probable toxic effect due to high amount liposome affected the cell viability.

These results were converted, as done for VRPs, to the number of NP copies per myoblast cell as shown in **Figure 25**.

With 250 ng of mRNA dose, an increase of NP cellular abundance between 12 to 24 hours post transfection was observed from around $5x10^6$ to $4.5\ x10^7$. Otherwise with 2 µg RNA dose, we did not appreciate the same trend, where no NP increase abundance was observed ($3x10^6$ to $3.7x10^6$ at 24 hours post transfection).

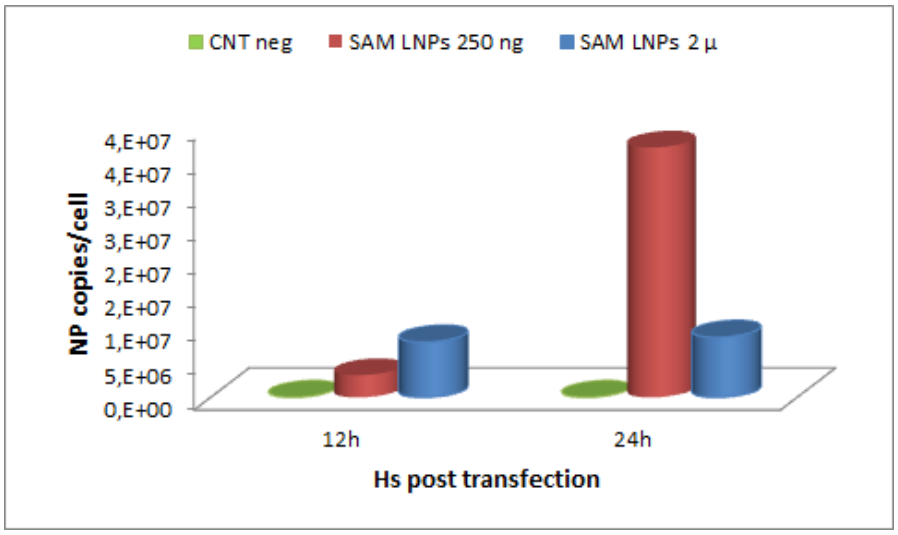

Fig. 25. Absolute quantification of NP protein in myoblast cell after SAM transfection.
Histograms represent NP abundance in myoblast cell for each time point. In blue values for 2 µg LNP SAM were represented, in red one where the values for 250 ng LNP SAM.

To conclude, a different kinetic of NP protein antigen expression from VRPs and LNPs can be observed. In particular, with VRPs, NP was detected and quantified at 2 hours post infection. Otherwise, with LNPs, a different temporal expression was observed where the evaluation of protein amount could be performed at 12 hours post transfection. After detection, no evident differences in the intracellular amount of NP protein antigen were observed. With the experimental evidence that once internalized the step of antigen expression are in the same extent, we can assume that main difference between VRPs and LNPs is related to the mechanism of cellular uptake.

3.3 Characterization of NP endogenous processing and MHC class I peptide presentation in myoblast cells during SAM transfection.

To correlate the intracellular NP protein antigen expression with the subsequent antigen endogenous processing on MHC complex system, SRM was employed to perform the absolute quantitation of MHC class I associated peptide at different time point after SAM transfection.

Myoblast cell line C2C12 and VRPs represented a suitable *in vitro* tool to validate the experimental set-up, in order to characterize the NP protein antigen presentation on MHC class I system upon SAM vaccination.

In detail, 5×10^8 C2C12 cells were treated with NP-(VRPs) or NP-(LNPs), harvested at different time points and lysated in order to monitor peptide epitope presentation. MHC K^k-peptide complexes from lysed cells were captured by immunoaffinity chromatography using a monoclonal anti MHC H-$2K^k$ haplotype antibody bound to protein G-Sepharose. Bound MHC-peptide complexes were dissociated and eluted with 10% acetic acid. Peptides were separated from MHC class I heavy chain β2m and polymers from detergent by filtration through a low protein binding spin filter and then subjected to LC-SRM analysis. The use of immunoaffinity chromatography drastically improves the specificity of the peptide extraction process and provides the most appropriate material to identify individual peptide ligand restricted by a defined MHC allele.

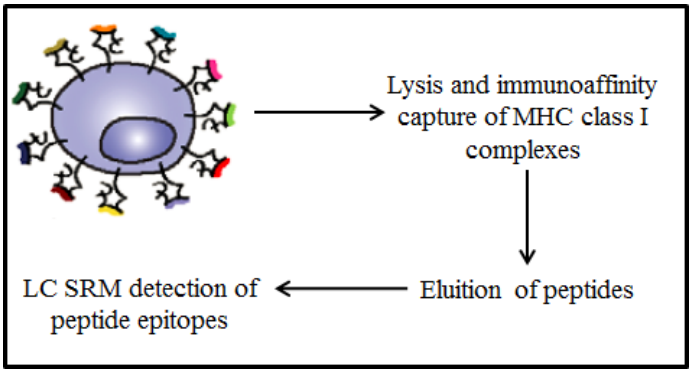

Fig. 26. Representation of approach used to study antigen presentation using mass spectrometry.
In this protocol, cells were treated with VRPs or LNPs. At various time points, cells were harvested and lysated. Mass spectrometry analysis employed the targeted method of LC-SRM, where the known MHC-I peptide is detected and quantified. (*Adapted from Kinetics of antigen expression and epitope presentation during virus infection. PLoS Pathog, 2013*)

During immunological response, $CD8^+$ T cell are often skewed toward a small number of peptides in a phenomenon known as immune-dominance. For this reason, the immunodominant peptide SDYEGRLI predicted and identified as K^k-restricted epitope in Influenza virus Nucleoprotein (residues 50 to 63) [82] was selected to quantitation and synthetized either in light- and heavy-labeled forms by incorporating ^{13}C-^{15}N in the isoleucine residue and quantified by the provider according to amino acid composition analysis (JPT Peptide Technologies GmbH).

To obtain an accurate peptide epitope quantitation the internal standard dilution (ISD) approach was employed and a known amount of stable isotope-labeled version of the immunodominant peptide was spiked into the sample. This heavy labeled peptide was added prior the filtration step to account for losses during sample preparation. The amount of immunodominant peptide was deduced from a calibration curve established in a matrix that mimics the same "environment" of the sample to be analyzed the same amount of no treated myoblast cells immunopurified for cellular MHC complex. To build this curve, a fixed amount of heavy forms of PTPs (25 fmol/µg of ^{13}C-^{15}N-labeled PTPs) and scalar concentration of light PTPs (ranging from 0.2 to 810 fmol/µl) were added to a fix amount of matrix. After LC-SRM assay, SDYEGRLI peptide light and heavy peak area ratio obtained was plotted against concentration. In **Figure 27** calibration curve was reported. The response was linear from 1.6 to 405 fmol/µl and the Lower Limit of Quantitation (LLOQ), was established at 1.6 fmol/µl. Considering an average molecular weight of 952 Da, a low limit of quantification of 0.6 pg per 1 µg of total cell lysate was calculated and used for further quantification.

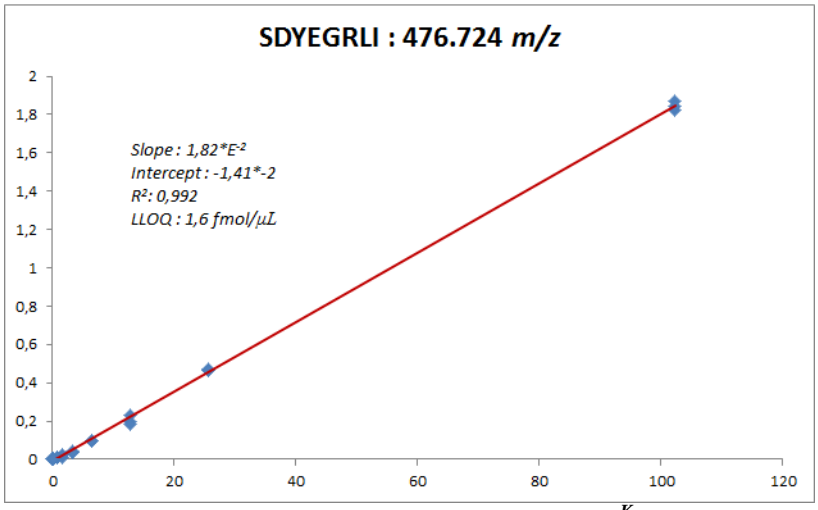

Fig. 27. Dose-response curve of SDYEGRLI immunodominant H-2K^K peptide.
For this PTP the LLOQ is 1.68 fmol/µl.

Absolute quantitation of SDYEGRLI peptide was performed after VRPs infection of 5×10^8 cells at 6 and 24 hours post infection.

The two selected time points were chosen to discriminate the specific phases that describe NP antigen expression after VRPs infection (**Figure 28**). In particular, 6 hours matched with the phase of antigen expression instead to 24 hours that corresponded to last antigen measured amount.

Peptide SDYEGRLI was already detected and quantified already at six hours post infection reaching around 27 pg per 5×10^8 cells and then decreasing until 2 pg (<LLOQ) at 24 hours post infection, from this study is clear that epitope presentation is essentially coincident with neo-synthesis of the source protein antigen. Moreover, even if the source of proteins continued slowly rise after this time point, epitope turnover is rapid and not more detectable in the last time point. The number of copies of peptide SDYEGRLI per myoblast cell was estimated, SDYEGRLI presentation on C2C12 infected cells was calculated to be 343 copies per cell at 6 hours post infection and 20 at 24 hours post infection (**Figure 28**).

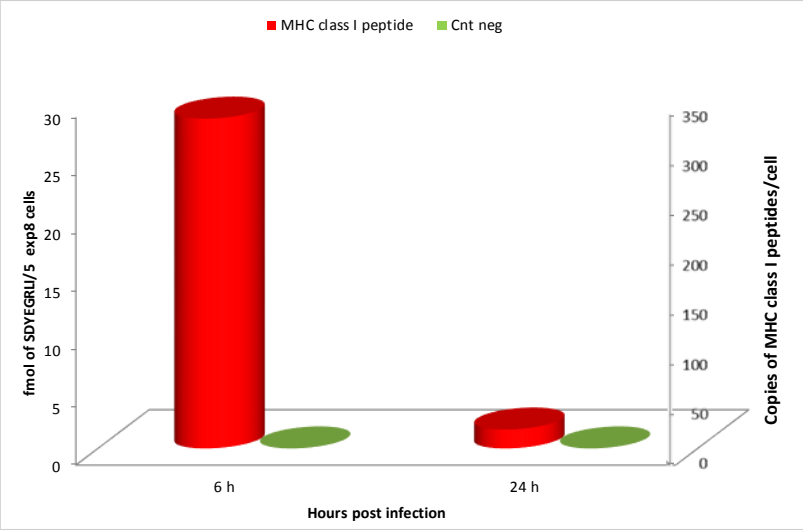

Fig. 28. Kinetic of NP antigen presentation after VRPs infection.
C2C12 cell were infected with VRPs (or mock treated at time 0) and incubated for 6 and 24 hours. MHC peptides were eluted at each time point and epitope level monitored by LC-SRM. Data shows fmol of peptide in $5x10^8$ cells and the peptide copies of per cell, obtained considering the positive percentage of NP expressing cells (data representative of two independent experiments).

The same strategy was applied to evaluate the SDYEGRLI quantitation after *in vitro* SAM transfection of 5×10^8 myoblast cells.

The absolute amount was evaluated at 18 and 24 hours post transfection, where 18 hours matched with the phase of antigen expression instead to 24 hours that corresponded to last antigen measured amount.

In this case the low positive percentage of NP expressing cells after SAM transfection did not allow us to detect and quantify SDYEGRLI. For this reason a SISCAPA approach was applied in order to decrease sample complexity and increase assay sensitivity by the immune affinity enrichment of this peptide MHC K^k-peptide complexes were purified from lysed cells as previously described and the eluted peptides were further enriched by α-peptide antibody obtained from the development of SISCAPA method (detailed in the part one of the result section)The SDYEGRLI peptide, processed at NP protein, was detected and quantified at 18 hours post transfection around 17 pg in of 5×10^8 myoblast cells, tracked closely with the phase of protein antigen expression. A rapid decline in epitope levels at 24 hours post transfection was observed reaching a level below the limit of detection of the developed method. The copies of SDYEGRLI peptide for each myoblast cell was calculated to be 438 copies per cell at 18 hours post transfection and no more detectable at 24 hours post transfection **Figure 29**.

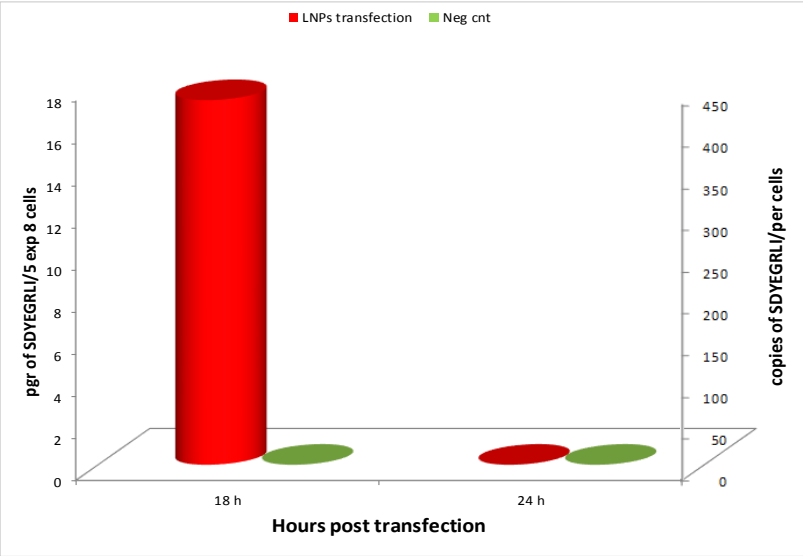

Fig. 29. Kinetic on NP antigen presentation after LNPs transfection.
C2C12 cell were transfected with LNPs (or mock treated at time 0) and incubated for 18 and 24 hours. MHC peptides were eluted at each time point and epitope level monitored by LC-SRM. Data show fmol of peptide in $5x10^8$ cells and the peptide copies of per cell, obtained considering the positive percentage of NP expressing cells. (Data representative of two independent experiments).

To conclude from our result we can observe for both delivery, a lag between peak of protein expression and peak of epitope presentation. In fact from this study is clear that, after NP-VRPs infection and NP-LNPs transfection, the epitope presentation is essentially coincident with neo-synthesis of the source protein.

Moreover, even if the source of proteins continues to slowly rise after the last time point, epitope turnover is rapid and then not more detectable after 24 hours post infection: the abundance of epitope varies massively from high of 400 to low of 20 copies per cells. All these results are consistent with previously published data [51], where the kinetic of multiple Vaccinia virus peptide epitope, and the corresponding viral protein were monitored by SRM. In that work, immunodominant peptide epitope, displayed on surface of antigen presenting cells, was characterized by a similar behavior, providing a strong support that antigen presentation is largely linked to translation and not later degradations of the antigens. Otherwise the epitope abundance measured in our experiment is tenfold lower than thus observed in this paper. In fact, even if muscle cells can acts as APC in the immune system, they do not express the CD80-CD86 costimulatory molecules, needed for efficient presentation.

Moreover, a high dynamic process characterized by multiple epitope simultaneously detected by SRM was described in the same paper. This lead to suppose that SAM presentation could not be described by only peptides and future works will focus to get more insight on peptide presentation during SAM vaccination.

Obtained results, relating to NP protein antigen expression and subsequent intracellular endogenous processing on MHC class I molecules in myoblast cells line by VRPs or LNPs were summarized in the **Table 6**.

Number of copies for myoblast cell

	VRPs infection (10^5 VRPs IU)					LNPs infection			
	2 hours	4 hours	6 hours	12 hours	24 hours	4hours	12 hours	18 hours	24 hours
NP protein antigen	**3,80 E^5**	**4,13 E^5**		**9,69 E^6**	**1,42 E^7**	**<LLOQ**	**3,29 E^6**		**3,70 E^7**
MHC class I peptide			**343**		**20**			**438**	**Not-detected**

Table 6. Kinetic of antigen expression and epitope presentation in in vitro model system with VRPs and LNPs.

Comparison between the number of NP copies (in blue) and peptide epitope presented (in red) between the two delivery systems.

A different kinetic of NP protein antigen expression between VRPs and LNPs can be observed. In particular, with VRPs, NP was detected and quantified already at 2 hours post infection, while with LNPs, a different kinetic of expression was observed, in which the detection of protein amount happened only at 12 hours post transfection. After detection, no evident differences in the intracellular amount of NP protein antigen and in the level of epitope peptide bound on MHC class I molecules were observed.

From this data we can assume that the main difference between VRPs and LNPs is related to the mechanism of cellular uptake: once RNA was internalized, the steps of antigen expression and peptide presentation are comparable.

3.4 Characterization of NP expression in mouse muscles and lymph nodes during SAM immunization.

To better elucidate the antigen expression step upon SAM vaccination, an *in vivo* model system based on NP expressing antigen was employed. In particular, this model allowed investigating antigen expression and following epitope presentation in muscles and draining lymph nodes at the site of injection.

Previous studies [24, 29] have been focused on the analysis of SAM vaccine-encoding antigen expression and localization, in an *in vivo* model based on reporter genes as firefly luciferase or secreted alkaline phosphatase (SEAP), where bioluminescence or chemioluminescence were the monitored outputs. With these assays a strong signal induced by LNP/RNA were observed, compared to those obtained from VRPs, that peaks at 7 days and persist for long time, until 49 days after SAM immunization. These kinds of assays do not allow obtaining precise quantitative information insight the kinetics of protein expression. To overcome these limitations, SRM approach was used in this study. To correlate the *in vitro* result obtained with C2C12 cell line with *in vivo* conditions we used C3H mice as animal model system. This mice present the same H2-K^k haplotype of myoblast cell line C2C12, allowing to use the specific immunodominant epitope peptide SDYEGRLI for the further *in vivo* studies on MHC class I presentation.

C3H mice were intramuscular (i.m.) immunized with 0.1 μg of SAM expressing NP delivered by LNPs, using PBS treated mice as negative control. Muscles at the site of injection and draining lymph node were collected after 6 hours, and one, three, eight and ten days after immunization and subjected to SRM analysis to evaluate NP protein antigen expression (**Figure 30**).

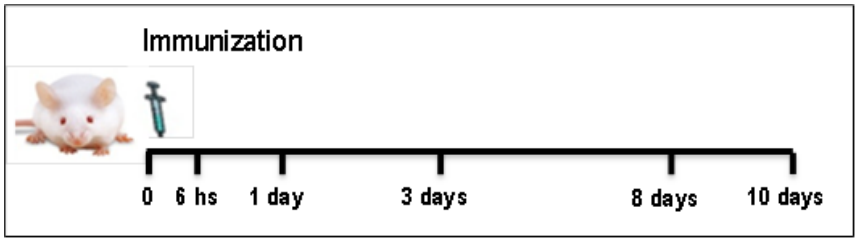

Fig. 30. Schematic representation of immunological scheme for SAM in vivo study.
C3H mice (n=25) were immunized i.m. with 0.1 μg of SAM (NP), five of them with PBS as negative control. Six hours, one, three, eight and ten days after immunization, 5 mice per group were sacrificed, and muscles and distal lymph node, at the side of immunization were collected to evaluate antigen expression at the selected time points.

In details, after collection, tissues were disrupted by mechanical homogenization. From tissue lysated, protein content were isolated by 2,2,2-trichloroacetic acid (TCA) precipitation and subjected to reduction, alkylation and tryptic digestion in order to obtain tissue peptide mixture to be analyzed by SRM for NP precise quantitation. For each time points, the three PTPs already used for the *in vitro* quantification, were monitored in a matrix that mimic the same complex "environment" that characterized muscle samples. This matrix was also used to create calibration curve to identify the linearity correlation between PTPs dose range and the MS signal obtained. As an example, the dose-response curve of the PTP GVFELSDEK in mouse muscle matrix was reported in **Figure 31**. The LLOQ was calculated as 89 pg for 1 µg of total tissue lysate. The same LLOQ was assessed for the two other PTPs and used as a standard value for NP protein antigen quantitation.

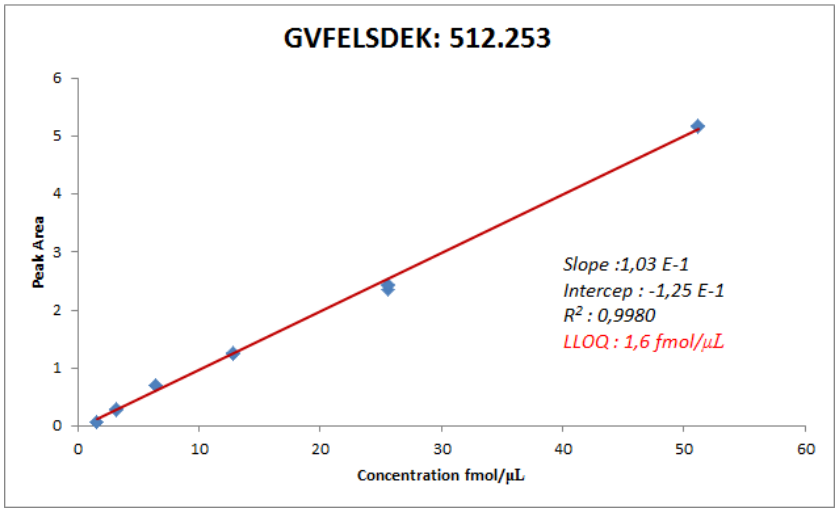

Fig. 31. Dose-response curve of the PTP GVFELSDEK in mouse muscle.
For this PTP the LLOQ is calculated at 1.6 fmol/µl. Considering an average NP molecular weight of 56000 Da, the limit of quantitation is determined as 89 pg per 1 µg of total cell lysate.

The abundance of NP protein antigen was precisely quantified on the treated total muscle, for each time points, in presence of a known amount of heavy spike as internal standard. Quantification was first performed evaluating the NP protein antigen amount in 1 µg of protein tissue lysate (data not shown). These values were then extrapolated to the total mass of mouse muscle tissue. Results are reported in **Figure 32.**

With 0.1 μg of SAM-LNPs dose used in the immunization, 25 ng of NP protein antigen was detected at 6 hours post immunization, no increase was observed until 8 post immunization where the amount was around 56 ng. The amount at 10 days post immunization was around 65 ng.

These results are consistent with published data obtained by luciferase report antigen in which peak of expression was monitored at 7 days post immunization. Further analysis should be performed to evaluate the persistency of NP protein antigen in mouse muscle.

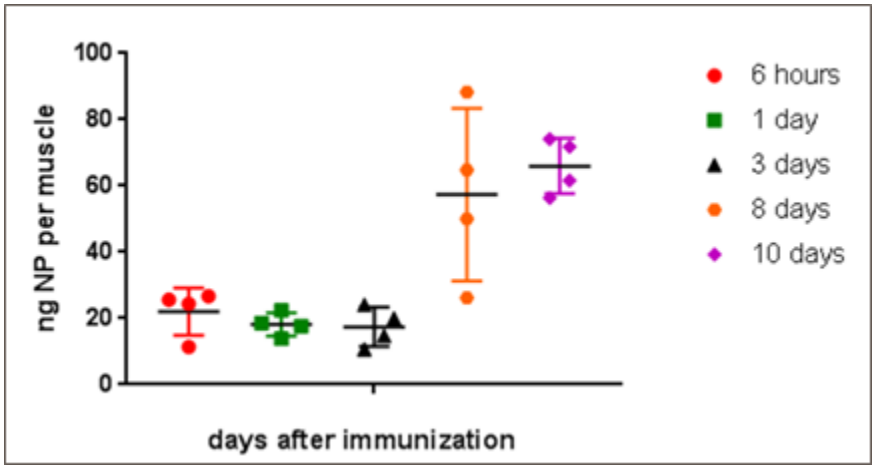

Fig. 32. Absolute quantitation of NP antigen during SAM immunization in total mouse tissue lysate.
The absolute quantification of NP antigen expressed as ng per muscle, was performed at 6 hours (red), 1 day (green) 3 days (black) 8 days (orange) and 10 days after immunization (magenta).

To compare the results obtained *in vivo* with the dynamic range of the muscle proteome the NP amount measured at 10 days after immunization were compared to the amount of specific housekeeping proteins derived from the same muscle. To perform this kind of analysis, mouse muscle homogenate was digested with trypsin and the obtained peptides were measured using MS^E analysis in a data-independent acquisition mode. With this approach all detectable peptide ions were measured, without *a priori* knowledge of them. Quantification of proteins was performed spiking 200 fmol of internal peptide standard (rabbit phosphorylase b) into the sample. Thanks to the observation that the intensity of the three most intense (most efficiently ionized) tryptic peptides are linked to the protein amount, whatever the dynamic range of the

protein (Hi3 method), the amount of all proteins can be inferred by known amount of added standard (**Figure 32**) [83].

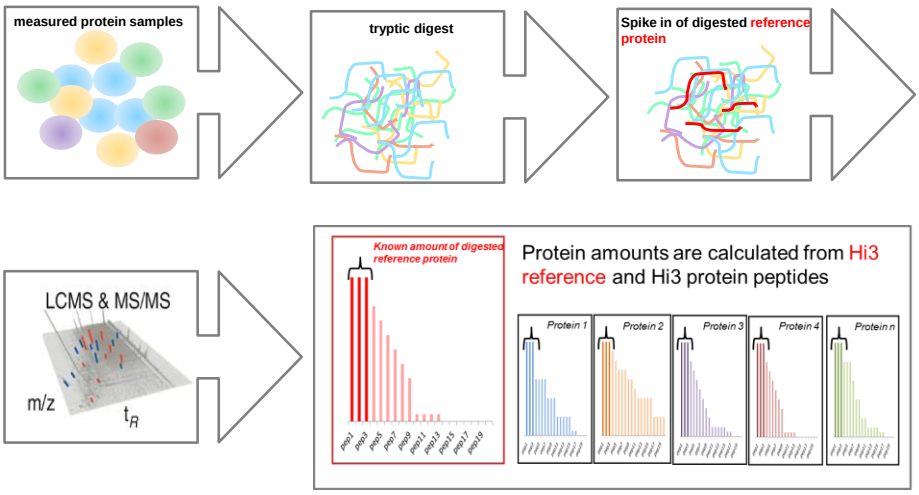

Fig. 33. Schematic representation of the workflow used for sample preparation for total muscle proteins quantitation.
Total muscle protein content were isolated through TCA precipitation and subjected to tryptic digestion. Rabbit Phos B was spiked in the peptides mixture as internal standard and analyzed by nano LC-MS^E. Relative quantitation was performed comparing the three most intense peptide ions of the reference with the those obtained from each detected components.

The obtained results were summarized in **Table 7.**

Motor proteins, such as myosin, actin, troponin and tropomyosin represent the most abundant proteins in total muscle proteome.

In particular, combining the abundance of all identified heavy and light myosin isoforms, they represent the 21% of total mouse muscle weight, positioning myosin as the highest abundance protein in skeletal muscle. In the same way, according to MS measurement, other high abundant proteins were alpha actin, troponin and tropomyosin that constitute the 3%, 4%, 0.2% and 0.17 % of total mouse muscle respectively. Moreover, also protein involved in the skeletal muscle metabolism as glycogen phosphorylase (Pyg) constitutes the 0.5% of total mass muscle. This data are in accordance with the skeletal muscle proteome quantification recently published by Deshmukh et al [84]. NP protein expressed after SAM LNP infection represented the 0.0029‰ of mouse muscle proteome. **Table 7** summarized these results.

	No-labeled quantitative HI3 method					SRM
	H and L myosine form	Alpha actin	Pyg	Troponin	Tropomyosin	NP protein antigen
Amount per muscle	51 mg	8,2 mg	1,3 mg	0,67 mg	0,42 mg	71 ng
% of total muscular mass	21%	3,4%	0,5%	0,20%	0,17%	0,0029‰

Table 7. MS quantification by label-free Hi3 method of the most abundant housekeeping proteins in mouse muscle tissue.
Final protein amounts were calculated and expressed as mg per muscle and as percentage of the total mass muscle proteins.

Moreover, the same approach was used to detect and quantify NP protein antigen in mouse distal lymph node at different time points after immunization.

This information could be particular relevant in the vaccinology field since the lymph node organ promotes the interaction between T lymphocytes, B lymphocytes, APCs acquiring an important role rising both humoral and cell-mediated immune response.

Within this purpose, LC-SRM assay was performed as described above starting prom the proteome of the distal lymph node. A new dose-response curve for NP PTPs were evaluated using lymph node proteome as matrix and the LLOQ for all PTPs was measured as 30 pg for 1 µg of total lymph node lysate. As an example, the dose-response curve of PTP GVFELSDEK in was reported in **Figure 34.**

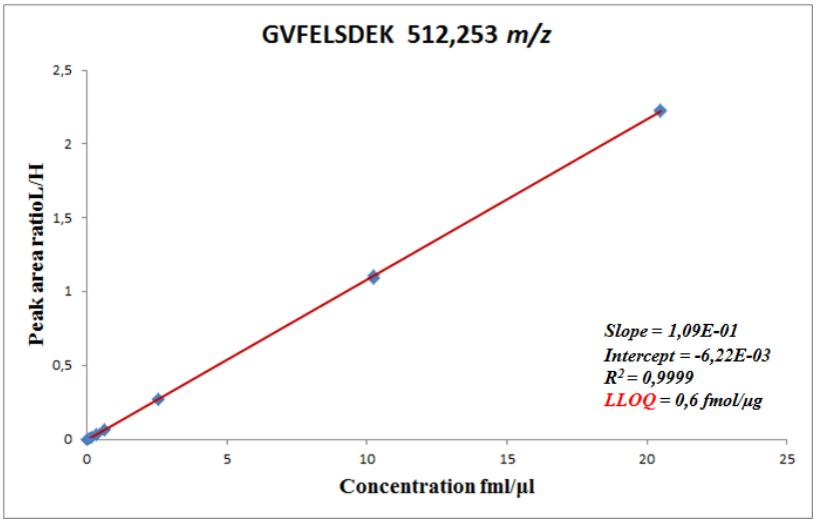

Fig. 34. Dose-response curve of PTP GVFELSDEK in lymph node.
For this PTP the LLOQ was set at 0.6 fmol/µl. Considering an average NP molecular weight of 56000 Da, the limit of quantitation is determined as 30 pg per 1 µg of total cell lysate derived from lymph node.

Then the abundance of NP protein antigen was assessed on the treated total lymph node, for each time points, in presence of a known amount of heavy spike as internal standard.

For each time point we detected a specific signal of NP but below the LLOQ for this experiment (30 pg per 1 µg of total cell lysate), and for this reason not quantifiable. This is a promising preliminary data and SISCAPA approach employed to overcome this limitation in sensitivity.

3.5 BM-DCs are not directly transfected by SAM encoding NP in *in vitro* model system.

Previous studies have demonstrated that the *in vivo* priming of MHC class I restricted $CD8^+$ T cells follow SAM vaccination involved Bone Marrow derived professional APCs, but to date no evidence of *in vivo* or *in vitro* direct transfection, evaluated by ICS and flow cytometry assay, was observed [80].

From these observations we cannot exclude that some APCs can be transfected by SAM but express antigen at low level not detectable by any high sensitivity approach. To address this question, SISCAPA method was applied to increase assay sensitivity and allow detecting low amount of antigen expressed in transfected bone marrow-dendritic cells (BM-DCs) by SRM. SAM-expressing NP antigen was used as tool for our proteomic studies.

In order to investigate if APCs can be transfected by a SAM vector and express the encoded protein antigen, an *in vitro* model system based on BM-DCs was set up. In detail 14 x 10^7 BM-DCs were transfected with SAM (NP/LNP) and harvested and lysate after 18 hours. Lysate was subjected to reduction, alkylation and trypsin digestion using the FASP method in order to obtain a tryptic cellular peptide mixture to be analyzed by SRM for NP precise quantitation. Previously, the immune affinity enrichment of PTPs was performed, using the specific anti-PTP m-Ab previously produced, in order to improve the sensitivity of the assay.

The PTPs signals were monitored in a matrix that mimic the same "environment" that characterized immune-affinity enriched PTPs sample and the calibration curve useful to identify the linearity correlation between PTPs dose range and the MS signal was created. Each point of this curve was measured in a fixed amount of matrix (BM-DCs lysate immunoaffinity purified with anti-PTPs m-Ab) heavy form of PTPs and scalar concentration of light form (ranging from 0.05 to 51 fmol/µl).

The protein mixture was digested with trypsin, immune-affinity purified using αPTPs m-Ab and analyzed by LC-SRM**.** For each PTP, concentration was plotted against the peak area ratio (/Light/Heavy) obtained. As an example the dose-response curve of PTP GVFELSDEK was reported in **Figure 35.** During this step the LLOQ for all PTPs was set as 44 pg for 1 µg of total BM-DC lysate.

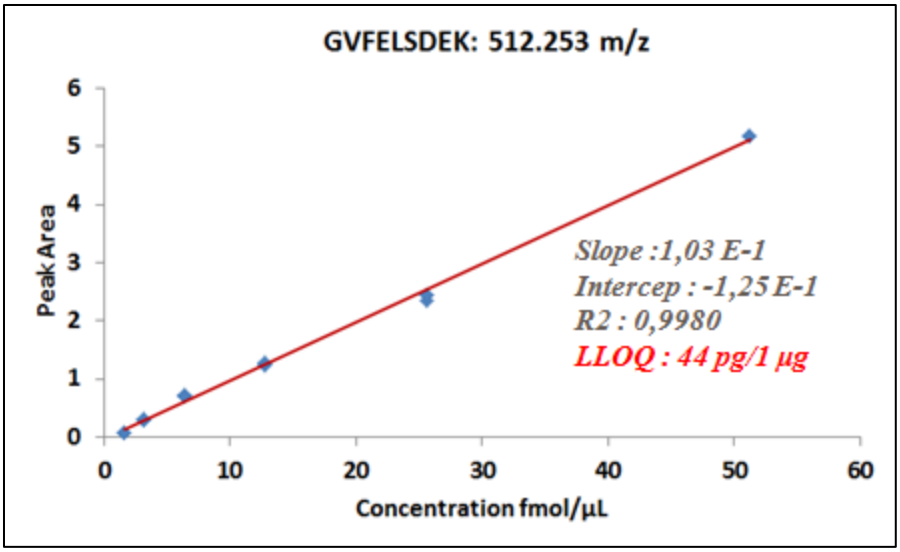

Fig. 35. Dose-response curve of PTP GVFELSDEK in BM-DC.
For this PTP the LLOQ is detected at 0.6 fmol/µl. Considering an average NP molecular weight of 56000 Da, the limit of quantitation is determined as 44 pg per 1 µg of total cell lysate.

Two different analytical sessions were performed starting from two independent biological experiments. No detection of NP was measured in both experiments, suggesting that BM-DCs could not be transfected.

Moreover, this data further indicate that APCs do not directly transfected by SAM.

3.6 BM-DCs are not directly transfected by SAM but can migrate toward transfected myoblasts *in vitro* model and take up exogenous NP expressed antigen.

Previous studies evidenced that the direct expression of antigen in BM-DCs was not necessary to prime CD 8 T cells but APC could acquire antigen and dsRNA from transfected myoblast cells implicating cross-priming mechanism in the activation of $CD8^+$ T cells [80].

To better elucidate the mechanism by which BM-DCs are able to take up endogenous expressed antigen from myoblast cells, BM-DCs were cultured in the upper compartment of a trans-well chamber in which infected C2C12 were transfected with VRP (NP) and placed 12 hours before in the lower compartment. After 2 hours, BM-DCs migrated in the lower compartment of the trans-well chamber. BM-DCs, which are not adherent cells, are easily separated from myoblast cells and collected. C2C12 were also collected and LC- SRM assay was applied to evaluate the NP antigen amount/distribution in the two cellular lines.

Quantification of NP protein antigen was performed, evaluating the precise amount of NP in myoblast cells before and then adding BM-DCs. Moreover the amount of NP protein was measured also in BM-DCs. Results were summarized in the **Figure 36**.

From the obtained results we can observed that the total amount of NP protein antigen in myoblast cells decrease from around 1.22 pmol in the first time point to around 0.6 pmol after two hours. This is concomitant with the new presence on BM-DCs of NP protein antigen with an amount of around 0.7 pmol in total cell lysate.

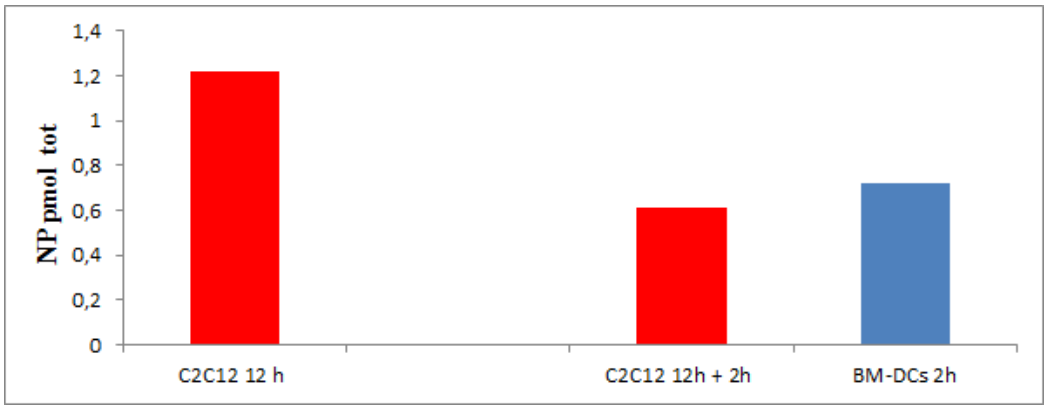

Fig. 36. Absolute quantitation of NP antigen in 1 µg of C2C12 and BM-DCs cells in a co-culture experiment.

The absolute quantification of NP antigen expressed in fmol/µg of total cell lysate was evaluated. In red the total amount of NP in C2C12 cell prior and then the adding of BM-DCs was measured. In blue the quantification on BM-DCs was perform after 2 hours of co-culture.

This concomitance and amount distribution are another demonstration that BM-DCs are able to take up endogenous protein antigens from myoblast cell and denying the possibility that during this short interval NP antigen is directly produced by BC-DCs from the dsRNA [80]. Moreover preliminary results showed a further increase of antigen presence in BM-DCs harvested after 5 hours, higher than the original amount observed in myoblast cells. Possible explanation could be possibility of a direct antigen expression in BM-DCs from the dsRNA up taken from myoblast cells. Furthermore, immunoaffinity purification of MHC class I bound peptides from BM-DCs at 2 hours post co-culture with myoblast cells was performed (as described in 3.3 in results section and 4.11 of material and methods section) to potentially detect and quantify immunodominant MHC class I peptide. No detection of MHC-I peptide was obtained even if the amount of NP antigen quantified in BM-DCs correlates with those in myoblast when antigen presentation occurs. New later time points (3-5 hours) could be useful to deepen this aspect and better understand the molecular mechanism of action of this new kind of vaccines.

CONCLUSION

In the 21st century, vaccines will play a major role in safeguarding the world's health. However, despite advances, many medical needs remain and current new technologies are now able to bring innovations in the vaccine field. Nucleic acid based vaccines have long held the promise to address these needs but despite decades of research and development there is still no licensed vaccine for human use. Among them, RNA vaccines (mRNA or self-amplifying) has emerged during the last decades as good alternative to recombinant viral vector or DNA technology, with a number of high profile reports using RNA for vaccines and gene therapy application.

However even if naked RNA (mRNA or self-amplifying RNA) induces *in vivo* protein expression and generate immune response, they suffer from limited potency in part due to *in vivo* RNA instability, related their intrinsic biochemical nature and to the presence of degradative enzymes in tissues. For these reasons, there has been extensive work on the delivery of self amplifying mRNA using no viral system. The SAM vaccine technology in which the delivery was facilitated by lipid nanoparticles, synthetic vehicles such as liposomes and cationic polymers that bind the RNA, enhances its delivery and increase potency of the vaccines. SAM vaccine has been widely evaluated in different animal model and has been confirmed to be well tolerated and able to drive, for the nature as replicon, high level of antigen expression, showing to elicit broad and potent humoral and cellular immune response against several pathogens comparable with those obtained by viral delivery (VRPs).

However, little has been published on the mechanism of action of these vaccines. To date it is known that myocyte cells and not immune cells (antigen presenting cells) seem to be the predominant cell type transfected within the injection site at time of vaccination [24]. Moreover, recent studies demonstrate that *in vivo* priming of MHC class-I restricted $CD8^+$ T cells following SAM immunization involves bone marrow-derived professional APCs. Therefore, myocytes can only provide an antigen source for the induction of a MHC class-I restricted $CD8^+$ T cell response by APCs [80].

In this scenario, the aim of this study was to provide a better understanding of the in vivo kinetics of antigen expression and its subsequent endogenous processing on MHC class I molecules, during SAM vaccination.

Previous studies were focus on the analysis of SAM vaccines encoded antigen expression and localization, in a in vivo model system based on reporter genes as firefly luciferase or secrete alkaline phosphatase (SEAP), where bioluminescence or chemoluminescence were the parameters monitored. With these assays a strong signal induced by LNP/RNA were observed, comparable to those produced by VRPs, that peaks early and persist for long time after SAM immunization. These kinds of assays don't allow us to obtain precise quantitative information insight the kinetics of protein expression. To overcome all this limitation, a quantitative mass spectrometry (MS) approach was applied In fact rapid advances in MS instrumentation are enabling to perform relative and absolute quantification analysis. The method of choice in this field is the Selected Reaction Monitoring (SRM), a quantitative mass spectrometry approach that allows the precise and absolute quantitation of a specific set of proteins. Thanks to this, we focused our attention to the expression of antigenically conserved protein Nucleoprotein (NP) from Influenza virus. Furthermore, as intracellular encoded protein, NP could be used to build up a unique simple model system to monitor simultaneously intracellular antigen expression and the following endogenous processing and presentation on MHC class I molecules.

Here, we started the study setting up an *in vitro* cellular model using the myoblast cell line C2C12. SRM have been applied to investigate the quantitative correlation between antigen expression and epitope presentation on MHC class I molecules in a time course experiment, using two different delivery systems for RNA, the Viral Replicon Particles (VRPs) and the synthetic Lipid Nanoparticle (LNPs for SAM)), also in order to better to understand the main differences that occur during SAM and VRPs immunization.

RNA encoding NP protein was synthetized by *in vitro* transcription reaction and characterized for its self-amplification capability and expression of NP antigen in BHC cells and then formulated in VRPs and synthetic LNPs, in order to enhance RNA delivery and potency.

From our results, a different temporal expression was observed between the two delivery systems. With VRPs antigen expression was observed at two hours post infection, differently to LNPs where antigen expression was detected at 12 hours post transfection.

The early antigen detection and quantitation evaluated with VRPs are probably related to the high infection capability of alphavirus particle. Moreover the time frame required for protein detection observed in our experiment (2 hours) is consistent with previously published data that report how alphavirus infection process occurs. In fact when virus genome is transferred to host

cell cytoplasm, the detection of viral encoded proteins in infected cells occurs in a time frame of 1-2 hours as observed in our experiment. On the other end, with LNPs, where the cellular-liposome connection is mediated by electrostatic interaction between the cationic lipid and plasma membrane, we observed lower and later antigen expression. This is probably due to a slower LNPs internalization or RNA release in the cells or moreover to PEG-mediate liposome aggregation, which prevents desirable cell internalization.

Then, to identify the kinetic correlation between NP protein antigen build-up and the subsequent endogenous processing on MHC class I peptide epitope, after both VRPs infection and LNPs transfection, SRM approach was applied to perform immunodominant epitope precise quantitation. A dynamic setting in which antigen levels are changing after transfection/infection can provide more insights into the relationship between antigen and epitope level. From our results is clear that, after NP-VRPs infection and NP-LNPs transfection, epitope presentation is essentially coincident with neo-synthesis of the source protein. Moreover, even if the source of protein continues slowly to rise, epitope turnover is rapid and not more detectable after this point. These results are consistent with previously published data [51], where the kinetic of multiple vaccinia virus peptides epitope and corresponding viral protein were monitored by SRM. In that work, immunodominant peptide epitope, displayed on surface of dendritic cells, was characterized by a similar behavior, providing the strong evidence that antigen presentation is temporally linked to translation and not with later degradation of the antigen. The epitope abundance measured in our experiment is ten times lower than the amount observed in the mentioned study. Actually, even if, muscle cells can acts as APC in the immune system, they do not express the CD80-CD86 costimulatory molecules, need for efficient presentation. Moreover, a high dynamic process characterized by multiple epitope simultaneously detected by SRM was described in the same study. In the same way, the analysis of MHC class I presentation of SAM vaccines through the immunodominant peptide, might not reflect the whole complexity and mechanism of presentation. Future works will focus to get more inside this dynamic process. To conclude this part, no evident differences in the intracellular NP expression and peptide epitope presentation was observed after protein detection between the two considered delivery systems. We can assume that the different behavior between VRPs and LNPs is only related to a different mechanism of cellular uptake and internalization.

To better elucidate the antigen expression step upon SAM vaccination, we moved toward an *in vivo* mouse model system where NP antigen was monitored at the site of injection in muscle and lymph node at 6 hours, 1 day, 3 day, 8 day and 10 days post immunization.

The abundance of NP protein antigen was precisely quantified on the treated total muscle, for each time points, showing that with 0.1 μg of SAM-LNPs, 25 ng of NP protein antigen was detected at 6 hours and no increase was observed until 8 days post immunization where amount was measured around 56 ng. Despite the magnitude of elicited immune response between SAM and commercial subunit vaccines is comparable, with this data is clear that this new type of vaccine are able to generate at the side of injection an amount of antigen lower respect to the standard dose given by classical vaccines (20-50 μg).

Then to delve deep into the SAM immune response, we focus on professional antigen presenting cells. Previously studies have been evidenced that DCs are not directly transfected by SAM, but are able to uptake endogenous antigen from transfected myoblast cells. To better elucidate this point, SRM approach was applied to describe antigen amount and its distribution between DCs and myoblast during co-culture experiment. The data obtained showed a decrease of protein amount in myoblast cell concomitant with the presence of antigen in DCs. This could be explained by the possibility that DCs acquired endogenous protein antigen from myoblast cell were expression take place.

Moreover, studies are in place to identify the peptide repertoire presented on the surface of DCs.

In summary we confirmed the pivotal role of muscle cells in antigen expression step during SAM vaccination in both *in vitro* and *in vivo* models, defining the kinetic of antigen expression and the subsequent endogenous processing on MHC class I. Further studies will be performed to better elucidate antigen presentation in DCs, improving, with new methods and technologies, the current knowledge about the mechanism of action of this new kind of vaccines.

Moreover, this study also demonstrated the power of MS for the quantitation and identification of MHC-associated peptides for T-cell epitope discovery and its use to optimize and inform vaccine design [47].

MATERIAL AND METHODS

4.1 RNA synthesis

Influenza NP gene was amplified from the cDNA of the influenza virus A/Puerto Rico/8/34 (H1N1), and then were cloned as a SalI and NotI fragment into an optimized replicon construct [29, 85]. Briefly, DNA plasmids encoding NP (SAM(NP)) replicons were amplified in *Escherichia coli* and purified using Qiagen Plasmid Maxi kits (Qiagen). DNA was linearized after 3' end of the self-amplifying RNA sequence by digestion with PmeI. Linearized DNA templates were transcribed into RNA using the MEGAscript T7 kit (Life Technologies) and purified by LiCl precipitation. RNA was then capped using the ScriptCap™ m7G Capping System (Cell Script) and further purified by LiCl precipitation.

4.2 BHK cell transfection and NP expression evaluation

Baby hamster kidney cells (BHK) were cultured in Dulbecco's modified Eagle's medium (DMEM) (Gibco, Carlsbad, CA) containing 5% (v/v) fetal bovine serum (FBS) (Hyclone) at 37°C at 5% CO_2 incubator, and transfected at 80% confluence.

To determine the efficiency of RNA self-amplification, BHK cells were electroporated (120V, 25ms pulse) with 200 ng of RNA and incubated for 16-18 h at 37°C in a CO_2 incubator. Cells were collected, stained with Live/Dead Aqua (Invitrogen), fixed and permeabilized with Cytofix/Cytoperm (BD Biosciences), and stained with Allophycocyanin (APC)-conjugated anti-dsRNA antibody (J2 monoclonal mAb mouse IgG2a kappa chain, Bioclass). Anti-dsRNA IgG2a was conjugated using the Zenon APC labeling kit (Invitrogen). Frequencies of $dsRNA^+$ cells were measured by flow cytometry on a FACS Canto II flow cytometer (BD Biosciences).

To determine the efficiency of protein expression, BHK cells were transiently transfected in a 6-well plate with 3 µg of each SAM construct and LIPOFECTAMINE 2000^{TM} (Invitrogen) according to manufacturer's instructions. BHK cells were collected 18-20 h after transfection and lysed using RIPA buffer (Sigma) supplemented with complete protease inhibitor cocktail (Roche), and whole cell lysates were separated under reducing conditions on a 4–12% Bis-Tris polyacrylamide gel in MES electrophoresis buffer (Life Technologies) and blotted onto PVDF

membranes (Life Technologies). NP was detected with anti-NP antibody (HB65 purified Hybridoma; ATCC Clone H16-R10-4R5) and reveled using a Goat anti-Mouse IgG HRP secondary antibody (Thermo Fisher).

4.3 Production of viral replicon particles (VRPs)

VRPs were produced in BHK cells as previously described [62]. In this system, the antigen expressing alphavirus chimeric replicon vector (VCR) derived from the genome of Venezuelan equine encephalitis virus (VEEV) engineered to contain the 3′ untranslated region (3′ UTR) and the packaging signal (PS) of Sindbis virus (SV), was electroporated into BHK cells along with defective helper RNAs encoding the Sindbis virus capsid and glycoprotein genes.

4.4 LNP/RNA formulation

RNAs were encapsulated in LNPs as previously described [29, 86].

Briefly, the lipids 1,2–dilinoleyloxy–3–dimethylaminopropane (DLinDMA) [87], 1,2–Diastearoyl–*sn*–glycero–3–phosphocholine (DSPC, Genzyme), 1,2–di-myristoyl–*sn*–glycero–3–phosphoethanolamine–N–[methoxy(polyethylene- glycol)–2000] (ammonium salt) (PEG–DMG 2000; Avanti Polar Lipids) and cholesterol (Sigma–Aldrich) were dissolved in ethanol at a ratio of 40:10:2:48 (v/v/v/v). RNA in 100 mM citrate buffer pH 6.0 (Teknova), was combined with the lipid solution through a T-junction via a KDS-220 syringe pump (KD Scientific) considering a molar ratio of 8:1 between nitrogen (N) from DLinDMA and phosphate (P) from RNA. An additional buffer volume of 100 mM citrate buffer (pH 6.0) was added simultaneously to the RNA/lipid suspension to obtain the final RNA/lipid nanoparticles. The resulting LNPs were dialyzed overnight at 4°C against PBS pH 7.4 (Ambion) using Pierce slide-A-Lyzer® G2 dialysis cassettes (Thermo Scientific) with a 3.5 K membrane molecular weight cut off. Formulations were characterized for particle size, RNA concentration, encapsulation efficiency and antigen expression in transfected cells. Prior to administration, LNPs were diluted in PBS to the desired concentration (1 ng/μl).

4.5 Induction of Bone Marrow-Derived Dendritic Cells (BM-DCs)

BM-DCs were induced from bone marrow (BM) cells obtained from 6-8 weeks-old C3H mice as previously described [88]. Briefly, a single cell suspension was prepared from BM obtained from femurs. After lysing red blood cells, $2x10^6$ BM cells were cultured in RPMI 1640 medium (Gibco) supplemented with 25 mM HEPES (Gibco), 10% heat inactivated FBS (low endotoxin, HyClone), Penicillin/Strepmicyn/Glutamine (Pen/Strep/Glu) antibiotic solution (100x, Gibco), 50 μM β-mercaptoetanol (Sigma) 10 ng/ml mouse GM-CSF (Gentaur) and 5 ng/ml mouse IL-4 (Miltenyi) in 10 cm diameter Petri dishes at 37 °C in 5% CO_2. Supplemented medium was refreshed every three days. On day 8, non-adherent and DCs were collected and analyzed for CD11c expression by flow cytometry using APC-eFluor780-labeled anti-CD11c Ab (eBioscience). All prepared BM-DC population used expressed CD11c on at least 60 % of the cells.

4.6 C2C12 infection

C2C12 (H-2*k* MHC I aplotype) mouse myoblasts cells were obtained from ATCC (Rockville, MD) and maintained in high-glucose Dulbecco's Modified Eagle Medium (DMEM, Gibco) supplemented with 10% (v/v) FBS and Pen/Strep/Glut (Gibco). C2C12 cells were infected using VRPs expressing NP. The day before infection, C2C12 cells were plated in a 24 well plate in culture media without antibiotics. Culture media was then removed and 100 μl of DMEM containing only 1% FBS and 10^6 VRPs (NP) infectious units (IU) were added to the cells. After incubation at 37°C for 1 hours, 400 μl of complete culture media was added to the cells for 2 4 12 and 24 hours incubation. Cells were then washed with PBS, trypsinized and further analyzed by flow cytometry for NP and H-2*k* expression using a FITC-labeled anti-NP (Thermo Fisher). Cells were further pelleted and keep at -80 °C for proteomic analysis.

4.7 LNP/RNA *in vitro* transfection

C2C12 and BM-DCs were transfected in a 24-well plate using serial dilutions of LNP formulated SAM (NP). The formulation stock was diluted until a final concentration of 10 μg/mL in DMEM (Gibco) containing only 1 % (v/v) FBS (EuroClone) for C2C12 cells or RPMI

1640 medium (Gibco) supplemented with 25 mM HEPES (Gibco), 10 % (v/v) heat inactivated FBS (low endotoxin, HyClone), Pen/Strep/Glut (100x, Gibco) and 50 µM β-mercaptoetanol (Sigma) for BM-DCs.

Diluted formulates were then pre-incubated in respectively working medium added with FBS (10% (v/v) final) at 37°C for 15 min and then incubated with cells at desired dilutions in respectively growth media (1% (v/v) FBS final) for 4-12-24 hours.

The media was then removed, and cells were trypsinized and stained with the Live/Dead Fixable Yellow viability marker (Invitrogen). BM-DCs were stained also with APC-eFluor780-labeled anti-CD11c Ab (eBioscience). Cells were fixed and permeabilized with Cytofix/Cytoperm (BD Biosciences), washed with Perm-wash buffer (BD Biosciences) and stained with a FITC-labelled anti-NP antibody (Thermo Fisher) and anti-dsRNA antibody (Bioclass), previously conjugated with Zenon Allophycocyanin Labeling kit (Invitrogen). Stained cells were acquired on LSR II SOS1 flow cytometer (BD Biosciences) and analysed with FlowJo software (TreeStar). For BM-DCs analysis, NP^+ and $dsRNA^+$ DCs were gated on $CD11c^+$ cells. Cells were pelleted and keep at -80 °C for proteomic analysis.

4.8 Filter Assisted Sample Preparation (FASP) method for LC-SRM of total cell lysate

C2C12/BM-DCs cell pellet were lysed in 150 µl of solution containing 4% (v/v) sodium dodecylsulfate (SDS), 100 mM TrisHCl pH 7.6, 0.1 M dithiothreitol (DTT) and incubated 30 min in ice . Obtained lysate was centrifuged at 16,000 x *g* for 10min and from the collected supernatant, total protein content was evaluated by colorimetric techniques as Bicinchoninic acid assay (BCA Assay Kit, Sigma Aldrich). These freshly prepared cell lysates contain contaminants, such as salt, detergents, nucleic acids, and lipids that can interfere with the subsequent analysis, for this, protein extract was subjected to FASP method for MS sample preparation.

20 µg of protein extract was mixed with 400 µl of 8 M urea (Sigma) in 0.1 M Tris-HCl pH 8.5 (UA) in filter unit (Microcon YM-30 Millipore) and incubated at RT for 30 min. Filter was then centrifuged at 14,000 x *g* for 15 min and washed twice with UA. Alkylation of cysteine residue of protein was performed adding to the filter 50 mM iodoacetamide in UA (IAA). The solution was mixed at 600 rpm in a thermo-mixer for 1 min and then incubates in the dark without mixing

for 20 min at 37 °C. After this time frame, filter was centrifuged again at 14,000 x *g* for 20 min and washed twice with UA. pH was then adjusted to 8 by washing filter twice with 50 mM ammonium bicarbonate (ABC). Isotopically labeled peptides (25 fmol for 1µg of total protein content), required for precise quantification by targeted LC-SRM were added at this stage, in order to account losses during sample preparation. Trypsin digestion was performed overnight incubating sample with 1 µg of trypsin (Gold MS Grade Promega) (25:1-sample: trypsin) at 37 °C.

Peptide mixtures were collected to centrifugation at 14,000 x *g* for 10 min and the digestion reaction was stopped with FA at 0.1% (v/v) final concentration, until obtaining acid pH (pH=2). The peptide mixtures were then desalted using OASIS cartridges (Waters), concentrated with a Centrivap Concentrator (Labconco, Kansas City, KS) and suspended in 20 µL of of 98% H_2O, 2% acetonitrile (CAN), 0.05% trifluoroacetic acid (TFA) (all v/v ratio). The SRM analysis was performed on a nanoUPLC Dionex (Thermo Fisher®) coupled with a triple-quadrupole mass spectrometer (TSQ Vantage, Thermo®) equipped with a nanoelectrospray ionization source (nano-ESI, Thermo Fisher). Samples were loaded fist in a trap column PepMap® 100 C18 Columns 100 µm x 2 cm (Thermo Scientific®) at a flow rate of 5 µl/min performed by the loading pump (98% water, 2% acetonitrile and 0.05% trifluoroacetic acid). Peptides were separated using EASY-Spray column PepMap® RSLC C18 50 µm x 150 mm (Thermo Scientific®). A five-step 65 minute gradient with an injection volume of 2 µL was used. Buffer A contained 98% water, 2% acetonitrile and 0.1% formic acid; buffer B contained 98% acetonitrile, 2% water and 0.1% formic acid. PTP were measured by SRM assay in positive mode form 0 to 40 minutes. The following parameters were used: predicted collision energy values, Q1 peak width (FWHM): 0.70 Th, Q3 peak width (FWHM): 0.70 Th, Gas Pressure (mTorr): 1.2 bar, Tuned S-Lens value: Yes, cycle time (s): 1.000 DCV. Io order to optimize the collision energy three transitions per peptide was selected based on their relative intensity; transitions with the highest intensity were preferred. Then the corresponding collision energy was selected.

4.9 Animal studies

C3H mice, 5-weeks old, 4 mice/group were immunized by quadricep intramuscular injection (i.m.) on both hind legs with 25 µl of PBS containing 0,1 µg of SAM (NP/LNP) self-

amplifying mRNA encoding NP antigen encapsulated in LNP. PBS alone was used as negative control. Mouse muscle and distal lymph node at the side of injection were collected at 6 hours, 1 day, 3 days, 8 days and 10 days after immunization. Muscles and lymph nodes were immediately frozen in liquid nitrogen and stored at -80 °C.

All animal studies were carried out in compliance with the arrive guidelines, the current Italian legislation on the care and use of animals in experimentation (Legislative Decree 116/92), and with the GSK Animal Welfare Policy and Standards. Protocols were approved by the Italian Ministry of Health (authorization 249/2011-B).

4.10 Mouse tissue (muscle and lymph node) sample preparation for LC-SRM.

Frozen mouse tissues were weighed, immediately disrupted in small pieces and lysated in a solution (1:10 w:v) containing 4% (v/v) SDS, 100 mM Tris-HCl pH 7.6, 0.1M DTT supplemented with complete protease inhibitor cocktail (Roche).

Mechanical homogenation was performed in Fastprep®24 Homogenator (MP Biomedicals) through the multidirectional, simultaneous beating of specialized Lysing Matrix beads (Lysing matrix D -MP Biomedicals) formed by 1.4 mm ceramic spheres, put inside the sample. Homogenation of tissue suspension was done with 10 short bursts of 10 sec followed by intervals of 30 sec for cooling. Tissue lysate was centrifuged at 10,000 x *g* for 10 min and from the collected supernatant, total protein content was evaluated by BCA assay. These freshly prepared cell lysates contain contaminants, such as salt, detergents, nucleic acids, and lipids that can interfere with the subsequent MS analysis, for this, 2,2,2-trichloroacetic acid (TCA) precipitation method was used to isolate protein component.

50 µg of total tissue lysate were denatured and reduced with 0.1 % (v/v) Rapigest® (Waters) and 5 mm DTT at 100 °C, for 10 min. Alkylation of cysteine residue was performed with 20 mM IAA incubating the solution in the dark without mixing for 20 min at 37 °C. 20 mM DTT was added to stop IAA reaction and after mixing, proteins were precipitated in ice for 2 hours adding 10% (v/v) TCA and 0.1% (v/v) sodium deoxycholate (DOC). The mixed protein-detergent precipitate was collected by centrifugation (10,000 x *g*, 10 minutes 4°C). The supernatant was carefully removed, 400 µl of cold ethanol were added to wash the pellet and vortexing was carried out until the pellet was completely solubilized. Centrifugation was carried out as

described above. The supernatant was removed, pellet was further washed with 400 µl of cold ethanol. Finally, the pellet was dissolved in 50 µl of ABC (with 10 min. of sonication). Denaturation and reduction with 0.1% (v/v in H_2O) Rapigest® (Waters) and 5 mm DTT at 100 °C were performed again and after a cool down at room temperature, isotopically labeled peptides (25 fmol for 1µg of total protein content) and 2 µg of Trypsin (Gold MS Grade Promega®) were added. Digestion was carried out at 37 °C overnight and stopped with formic acid at 0.1% (v/v) final concentration until acidic pH (pH=2). The peptide mixtures were then desalted using OASIS cartridges (Waters) concentrated with a Centrivap Concentrator (Labconco, Kansas City, KS) and suspended in 20 µl of 0.1% (v/v) formic acid (FA). Samples were analyzed by SRM as described in 4.8 Material and method section.

4.11 Purification of MHC class I peptide from treated cell line.

MHC-bound peptide complexes are affinity purified from whole total cell lysate using Protein A Sepharose resin linked to MHC H2-K^Kmonocolonal antibody.

4.11.1 Preparation of Cross-Linked Immunoaffinity Column

Protein A coupled with Sepharose resin slurry (2ml) was packaged into 1 ml column (Econo-Column® Chromatography Columns, 1.5 × 10 cm coupled with flow adaptor) and washed with 10 column volumes (c.v.) of MS-grade H_2O and PBS respectively.

Monoclonal antibody of MHC H2-K^K (4 mg 0.5 mg/ml in PBS) was added to column and leave to rotate gently end-over-end at 4 °C for 1 h to allow the binding. After this time frame antibody solution was allowed to flow throw by gravity and antibody-bound resin was washed with 20 c.v. of 0.05 M borate buffer pH= 8.0 followed by 15 c.v. of freshly prepared 0.2 M triethanolamine (Millipore), pH 8.2 at room temperature (RT). Triethanolamine was used to ensure that there are no residual primary amines present that may interfere with the cross-linking reaction. At this point, 5 c.v. of freshly prepared Dimethyl pimelimidate (DMP-2HCl, Sigma) cross-linker solution (40 mM DMP-2HCl in 0.2 M triethanolamine pH 8.3) was added through the column at RT leaving a meniscus just over the protein A column bed and allowed to sit at RT for 1 h. Cross-linking reaction was terminate the by adding 10 c.v. of ice cold termination buffer (0.2 M Tris-HCl, pH 8.0).

The unbound antibody was remove by washing with 10 c.v of stripping buffer (0.1 M citrate pH 3.0) and 10 c.v. of PBS pH 7.4 was added to until pH of flow through was neutral.

4.11.2 Generation of cell lysate-C2C12 treated with VRPs/LNPs

C2C12 cells (5×10^8) were grown in 24 well plates and treated with VRPs/LNPs as previously described. Cell were washed in PBS, and harvested by centrifugation (2,000 × *g*, 10 min at 4 °C). Cell pellets (pellet derived from 5×10^7 per 1 ml of lysis buffer) were lysated in Lysis buffer constituted by 0.5 % (v/v) IGEPAL 630 (Sigma), 50 mM Tris-HCl pH 8.0 (from 1 M stock solution), 150 mM NaCl, and protease inhibitor cocktail (Roche).

Homogenation of cell suspension was done with 10 short bursts of 5 sec followed by intervals of 30 sec for cooling with amplitude 20% in an ultrasonic sonicator (Q-sonica) and rotated end-over-end at 4 °C for 1 h.

Lysate was then centrifuged for 10 min at 2000 × *g* at 4 °C and the obtained supernatant was spun for 75 min (100,000 × *g*) at 4 °C. After this step, often a lipid-containing layer is presented on the top of the tube. This layer was removed carefully and then the obtained lysate was filtered through a 0.8 μm and 0.45 μm filter.

4.11.3 Immunoaffinity purification of MHC class I peptide

Cell lysate was loaded onto a protein A Sepharose pre-column previously equilibrated in 10 c.v. of wash buffer 1. Pre-cleared lysate was collected and slowly load onto the cross-linked mAb MHC H2-K^K (Thermo Scientific) with a constant flow of 1 ml/min.

Column was washed with 20 c.v. of wash buffer in the following order: Wash buffer 1, wash buffer 2 (needed to remove detergent), wash buffer 3 (needed to remove no specifically bound material), wash buffer 4 (needed to remove salt to prevent crystal formation) and MHC complexes were eluted in 5 c.v. of elution buffer. Isotopically labeled peptides, required for precise quantification by targeted LC-SRM were added at this point. MHC bounded peptides were then separated from heavy chain, β2m and detergent by low protein binding spin filter. The obtained peptide mixtures were then desalted using OASIS cartridges (Waters), concentrated with a Centrivap Concentrator (Labconco, Kansas City, KS) and suspended in 20 μL of 98%

H2O, 2% CAN, 0.05% TFA. Samples were analyzed by SRM as previously described in 4.8 Material and methods section.

Solutions:

- Wash buffer 1: 0,005% IGEPAL 630, 50 mM Tris, pH 8.0, 150 mM NaCl, 5 mM EDTA in MS grade H_2O.
- Wash buffer 2: 50 mM Tris-HCl, pH 8.0, 150 mM NaCl in MS-grade H_2O.
- Wash buffer 3: 50 mM Tris-HCl, pH 8.0, 450 mM NaCl, in MS-grade H_2O.
- Wash buffer 4: 50 mM Tris-HCl, pH 8.0 in MS-grade H_2O.
- Elution buffer: 10% (v/v) acetic acid in MS-grade H_2O.

4.12 SISCAPA enrichment for low abundance protein quantitation

4.12.1 Rabbit immunization

Immunogens consisted of the target tryptic peptides (NP-PTPs) and MHC class I immunodominant peptide, (synthesized and quantified JPT Peptide Technologies GmbH according to amino acid composition analysis) that had been conjugated to keyhole lympet hemocyanin (KLH) and Bovine ovalbumin (BSA) via an N-terminal cysteine and succinimidyl trans-4-(maleimidylmethyl)cyclohexane-1-carboxylate (SMCC) (conjugation performed by JPT Peptide Technologies GmbH).

New Zeeland White female rabbit, 9-weeks old, 2 rabbits/group were immunized using a standard protocol of three immunizations on days 1, 21 and 35 and 2 bleeds for each rabbit. The subcutaneous injections were performed using the BSA-immunogens as follow:

- SALILR peptides conjugated to bovine serum albumin (BSA)
- GVFELSDEK peptides conjugated to bovine serum albumin (BSA)
- EGYSLVGIDPFR peptides conjugated to bovine serum albumin (BSA)
- SDYEGRLI peptides conjugated to bovine serum albumin (BSA)

All immunogens at the time of each injection was thawed and combined with 2 mg Alum Hydroxide ($AlOH_3$) adjuvant in 100 mM Histidine buffer, 2M Sodium Chloride and water for injection to 500 µl final volume. Formulates were then characterized for the pH, osmolality, formation of visible precipitates and for Alum adsorption by SDS-PAGE. Serum bleeds of 7.5 ml for each rabbit were obtained after the third immunizations (15 ml total). For each peptide target

group, the rabbit with the higher titer, as measured by peptide ELISA, was chosen for antibody purification as described below.

4.12.2 Antibody screening by peptide ELISA

Sera from each rabbit were tested for ELISA activity against the corresponding peptides group (see above). The peptide ELISAs were performed as reported [89]. Briefly, Maxisorp plates were coated overnight at 4 °C with 2 μg/ml of each peptide conjugated to KLH in PBS. The wells were washed once using 100 μl of Tris Buffer Saline (500 mM Tris, 60 mM KCl, 2.8 M NaCl) TBS plus 0.1% (v/v)Tween 20 (TBST) and blocked using 60 μl of TBST-0,1 % BSA (v/v) for 1 hour at RT. Serum samples and a standard serum were 2-fold serially diluted in PBS with 1% BSA and 0.05% (v/v) Tween-20, and transferred into coated and blocked plates. After 2 h at 37 °C, plates were incubated with alkaline phosphatase-conjugated goat anti-rabbit IgG (Sigma) for 90 min at 37°C to detect antigen-specific IgG antibodies. The plate was washed three times with 100 μl TBST and 50 μl of p-nitrophenyl phosphate, disodium salt (PNPP, Pierce) was added. Color was allowed to develop for 15 minutes at RT. Fifty microliters of 3 M NaOH was used to stop the reaction, and OD was measured at 405 nm.

4.12.3 Purification of Abs from rabbit serum

Purification of IgG was performed using Hi Trap Protein G HP columns 5 ml column (GE Healthcare Life Sciences) connected to AKTA purified. The column was first washed with 5 c.v. of distilled water and then equilibrate with 5 volume of binding buffer (300 mM NaCl, 50 mM sodium phosphate, pH 8.0) with a flow rate of 5 ml/min. Than 20 ml of higher ELISA titer sera for each target group were loaded. 10 c.v. of binding buffer were loaded at flow rate of 1 ml/min. The elution was performed using a one-step linear gradient with 10 c.v. of elution buffer (0.2 M glycine-HCl, pH 2.6). Immediately after the pH was neutralized using the neutralizing buffer (1 M Tris-HCl, pH 8).

To assess the integrity of the IgG purified a SDS-PAGE was performed. The purified fraction were dialyzed against dialysis buffer (PBS), using 10 kDa molecular weight cut-off (10K MWCO) "Slide-A-Lyzer" cassettes (Thermo Fisher®). Dialysis was carried out for 2 hours at

room temperature, then the dialysis buffer was changed and dialysis was allowed overnight. Dialyzed samples were again analyzed by SDS-PAGE and quantified by BCA assay.

4.13 In solution digestion and nano LC-MS/MS analysis

Samples contained commercially available form Influenza A H1N1 Nucleoprotein /NP protein (His tag) (Sino Biological Inc.) were denatured and reduced with Rapigest® (Waters) and 5 mm DTT at 100 °C, respectively, for 10 min. After a cool down at room temperature, 50 mM ammonium bicarbonate and 2 µg of Trypsin (Gold Mass Spectrometry Grade Promega®) were added. Digestion was carried out at 37 °C overnight. The digestion was stopped adding FA at 0.1% (v/v) final concentration until acid pH (pH=2).

The peptide mixtures were then desalted using OASIS cartridges (Waters) following the manufacturer's protocol. Desalted peptides were concentrated with a Centrivap Concentrator (Labconco, Kansas City, KS) and suspended in 50 µl of 0.1% (v/v) FA.

Peptides solution were analyzed by LC-MS/MS performed on a nanoAcquity UPLC system (Waters®) coupled a Waters SynaptG2 ESI mass spectrometer equipped with a nanospray source (Waters®). Samples were loaded onto a trap Symmetry C18 180 µm x 20 mm, 5µm (Waters®) using a full loop injection at a flow rate of 800 nl/min in a mobile phase A (0.1% FA). Peptide were than separated on a nano Acquity UPLC Peptide BEH C18 Column 75 µm x 100 mm (Waters®) using a 70 min gradient 3-98% mobile phase B (98% (v/v) ACN, 0.1% (v/v) FA) at a flow rate of 300 nl/min.

The eluted peptides were subjected to an automated data-dependent acquisition (DDA) using the MassLynx software (Waters®) where an MS survey scan was used to automatically select multi charged peptides over the *m/z* ratio range of 300–2,000 for further MS/MS fragmentation. Up to eight different peptides were individually subjected to MS/MS fragmentation following each MS survey scan. After data acquisition, individual MS/MS spectra were combined, smoothed, and centroided using ProteinLynx, (Waters®) to obtain the peak list file (pkl). Protein identification was carried from the generated peak list using the Mascot engine software (Matrix Science). Peptide identification was run on a database containing all Influenza virus protein sequences deduced from the sequenced Influenza virus H1N1 genomes, downloaded from NCBInr database. Search parameters as variable modifications were : methionine oxidation, glutamine

and asparagine deamidation, trypsin cleavage (cleaves the C-term side of KR unless next residue is P), peptide mass tolerance as 0.15 Da, peptide MS/MS tolerance as 0.15 Da, missed cleavage= 2, ion charge states: +2, +3, +4). Only significant hits were considered as defined by the Mascot scoring and probability system >25.

4.14 Selection of proteotypic peptide and in Solution Tryptic Digestion

In solution tryptic digestion and LC-MS/MS analysis were used to identify specific proteotypic peptides required for NP protein quantitation.

From this obtained Mascot list, NP specific peptides that not displayed amino acids with chemical modifications occurs during sample preparation (glutamine and asparagine deamidation, cysteine and methionine oxidation, N-terminal glutamic acid for cyclization), and present a specific length from 5 to 20 amino acids were selected. Moreover peptides with low MS intensity signal (low Mascot score) and characterized by KK, RK, RR, KR consecutive amino acids, cause of an incomplete tryptic digestion, were not selected. Furthermore each PTPs were investigated for the unique association to the targeted protein in the specific biological background. For this reason the sequence of the selected PTPs were inspected against a database containing sequences deduced from the C3H mouse model genome and no matches were found.

4.15 PTP dose-range linearity responses curve

The dose-range linearity response of all PTPs in a specific matrix was assessed. Each point of this curve was measured with a fixed amount of matrix (1 μg of C2C12 total cell lysate or 1 μg of total tissue lysate-immuno-affinity purified peptides) and heavy form of PTPs (^{13}C-^{15}N-labeled Arg, Lys or Ile) and scalar concentration of light PTPs (ranging from 0.2 to 810 fmol/μl or 0.2 to 51 fmol/μl in the case of MHC-I peptide). The protein mixture was digested with trypsin and the peptides were analyzed by LC-SRM as described in 4.8 Material and methods section**.** For each PTP, concentration was plotted against the peak area ratio obtained (light peak area/heavy peak area). From the dose-rang linearity curve the Lower Limit of Quantitation (LLOQ) for PTPs was identified and was set as the lowest concentration point on the fitted curve with an accuracy deviation ≤ 20%.

4.16 SRM analysis for the quantification of target protein/peptide in a complex biological background

All Peptides were analyzed by SRM assay in positive mode and the SRM method is reported below (RT means retention time in minutes).

	Light		Heavy				
	Q1	Q3	Q1	Q3	CE	RT	RT Range
	m/z		m/z		Voltz		
SALILR	336,724	401,29	341,73	411,295	12	18,01	17,01-->19,01
		514,37		524,329	14		
		585,41		595,416	16		
GVFELSDEK	512,253	591,3	516,26	599,312	20	22,25	21,25-->23,25
		720,34		728,355	18		
		867,41		875,423	16		
EGYSLVGIDPFR	676,846	704,37	681,85	714,382	23	31,96	30,91-->32,91
		803,44		813,499	23		
		1003,6		1013,55	23		
SDYEGRLI	476,74	458,31	480,24	465,324	23	22,2	20,99-->23,99
		587,35		594,367	23		
		750,41		757,432	23		

REFERENCES

1. Wrammert, J., et al., *Human immune memory to yellow fever and smallpox vaccination.* J Clin Immunol, 2009. **29**(2): p. 151-7.
2. Brazzoli, M., et al., *Induction of Broad-Based Immunity and Protective Efficacy by Self-amplifying mRNA Vaccines Encoding Influenza Virus Hemagglutinin.* J Virol, 2015. **90**(1): p. 332-44.
3. Gilbert, S.C., *Clinical development of Modified Vaccinia virus Ankara vaccines.* Vaccine, 2013. **31**(39): p. 4241-6.
4. Johnson, J.A., D.H. Barouch, and L.R. Baden, *Nonreplicating vectors in HIV vaccines.* Curr Opin HIV AIDS, 2013. **8**(5): p. 412-20.
5. Saxena, M., et al., *Pre-existing immunity against vaccine vectors--friend or foe?* Microbiology, 2013. **159**(Pt 1): p. 1-11.
6. Ulmer, J.B., et al., *Heterologous protection against influenza by injection of DNA encoding a viral protein.* Science, 1993. **259**(5102): p. 1745-9.
7. Geall, A.J., C.W. Mandl, and J.B. Ulmer, *RNA: the new revolution in nucleic acid vaccines.* Semin Immunol, 2013. **25**(2): p. 152-9.
8. Hekele, A., et al., *Rapidly produced SAM((R)) vaccine against H7N9 influenza is immunogenic in mice.* Emerg Microbes Infect, 2013. **2**(8): p. e52.
9. Ferraro, B., et al., *Clinical applications of DNA vaccines: current progress.* Clin Infect Dis, 2011. **53**(3): p. 296-302.
10. Liu, M.A., *Immunologic basis of vaccine vectors.* Immunity, 2010. **33**(4): p. 504-15.
11. Kutzler, M.A. and D.B. Weiner, *DNA vaccines: ready for prime time?* Nat Rev Genet, 2008. **9**(10): p. 776-88.
12. Petsch, B., et al., *Protective efficacy of in vitro synthesized, specific mRNA vaccines against influenza A virus infection.* Nat Biotechnol, 2012. **30**(12): p. 1210-6.
13. Martinon, F., et al., *Induction of virus-specific cytotoxic T lymphocytes in vivo by liposome-entrapped mRNA.* Eur J Immunol, 1993. **23**(7): p. 1719-22.
14. Magini, D., et al., *Self-Amplifying mRNA Vaccines Expressing Multiple Conserved Influenza Antigens Confer Protection against Homologous and Heterosubtypic Viral Challenge.* PLoS One, 2016. **11**(8): p. e0161193.
15. Deering, R.P., et al., *Nucleic acid vaccines: prospects for non-viral delivery of mRNA vaccines.* Expert Opin Drug Deliv, 2014. **11**(6): p. 885-99.
16. Johansson, D.X., et al., *Intradermal electroporation of naked replicon RNA elicits strong immune responses.* PLoS One, 2012. **7**(1): p. e29732.
17. Atkins, G.J., M.N. Fleeton, and B.J. Sheahan, *Therapeutic and prophylactic applications of alphavirus vectors.* Expert Rev Mol Med, 2008. **10**: p. e33.
18. Lundstrom, K., *Alphavirus vectors: applications for DNA vaccine production and gene expression.* Intervirology, 2000. **43**(4-6): p. 247-57.
19. Schlesinger, S., *Alphavirus vectors: development and potential therapeutic applications.* Expert Opin Biol Ther, 2001. **1**(2): p. 177-91.
20. Caskey, M., et al., *Synthetic double-stranded RNA induces innate immune responses similar to a live viral vaccine in humans.* J Exp Med, 2011. **208**(12): p. 2357-66.

21. Wang, Y., et al., *dsRNA sensors and plasmacytoid dendritic cells in host defense and autoimmunity.* Immunol Rev, 2011. **243**(1): p. 74-90.
22. Carroll, T.D., et al., *Alphavirus replicon-based adjuvants enhance the immunogenicity and effectiveness of Fluzone (R) in rhesus macaques.* Vaccine, 2011. **29**(5): p. 931-40.
23. Bernstein, D.I., et al., *Randomized, double-blind, Phase 1 trial of an alphavirus replicon vaccine for cytomegalovirus in CMV seronegative adult volunteers.* Vaccine, 2009. **28**(2): p. 484-93.
24. Brito, L.A., et al., *A cationic nanoemulsion for the delivery of next-generation RNA vaccines.* Mol Ther, 2014. **22**(12): p. 2118-29.
25. Brown, D.T. and R. Hernandez, *Infection of cells by alphaviruses.* Adv Exp Med Biol, 2012. **726**: p. 181-99.
26. Bredenbeek, P.J., et al., *Sindbis virus expression vectors: packaging of RNA replicons by using defective helper RNAs.* J Virol, 1993. **67**(11): p. 6439-46.
27. Rayner, J.O., S.A. Dryga, and K.I. Kamrud, *Alphavirus vectors and vaccination.* Rev Med Virol, 2002. **12**(5): p. 279-96.
28. Zimmer, G., *RNA replicons - a new approach for influenza virus immunoprophylaxis.* Viruses, 2010. **2**(2): p. 413-34.
29. Geall, A.J., et al., *Nonviral delivery of self-amplifying RNA vaccines.* Proc Natl Acad Sci U S A, 2012. **109**(36): p. 14604-9.
30. Semple, S.C., et al., *Rational design of cationic lipids for siRNA delivery.* Nat Biotechnol, 2010. **28**(2): p. 172-6.
31. Smerdou, C. and P. Liljestrom, *Non-viral amplification systems for gene transfer: vectors based on alphaviruses.* Curr Opin Mol Ther, 1999. **1**(2): p. 244-51.
32. Bogers, W.M., et al., *Potent Immune Responses in Rhesus Macaques Induced by Nonviral Delivery of a Self-amplifying RNA Vaccine Expressing HIV Type 1 Envelope With a Cationic Nanoemulsion.* J Infect Dis, 2014.
33. Ulmer, J.B., M.K. Mansoura, and A.J. Geall, *Vaccines 'on demand': science fiction or a future reality.* Expert Opin Drug Discov, 2015. **10**(2): p. 101-6.
34. Hoffmann, J. and S. Akira, *Innate immunity.* Curr Opin Immunol, 2013. **25**(1): p. 1-3.
35. Suri, A., S.B. Lovitch, and E.R. Unanue, *The wide diversity and complexity of peptides bound to class II MHC molecules.* Curr Opin Immunol, 2006. **18**(1): p. 70-7.
36. Viville, S., et al., *Mice lacking the MHC class II-associated invariant chain.* Cell, 1993. **72**(4): p. 635-48.
37. Bikoff, E.K., et al., *Defective major histocompatibility complex class II assembly, transport, peptide acquisition, and CD4+ T cell selection in mice lacking invariant chain expression.* J Exp Med, 1993. **177**(6): p. 1699-712.
38. Neefjes, J., et al., *Towards a systems understanding of MHC class I and MHC class II antigen presentation.* Nat Rev Immunol, 2011. **11**(12): p. 823-36.
39. Ghosh, P., et al., *The structure of an intermediate in class II MHC maturation: CLIP bound to HLA-DR3.* Nature, 1995. **378**(6556): p. 457-62.
40. Denzin, L.K. and P. Cresswell, *HLA-DM induces CLIP dissociation from MHC class II alpha beta dimers and facilitates peptide loading.* Cell, 1995. **82**(1): p. 155-65.
41. Pos, W., et al., *Crystal structure of the HLA-DM-HLA-DR1 complex defines mechanisms for rapid peptide selection.* Cell, 2012. **151**(7): p. 1557-68.
42. Wubbolts, R., et al., *Direct vesicular transport of MHC class II molecules from lysosomal structures to the cell surface.* J Cell Biol, 1996. **135**(3): p. 611-22.

43. Boes, M., et al., *T-cell engagement of dendritic cells rapidly rearranges MHC class II transport.* Nature, 2002. **418**(6901): p. 983-8.
44. Kleijmeer, M., et al., *Reorganization of multivesicular bodies regulates MHC class II antigen presentation by dendritic cells.* J Cell Biol, 2001. **155**(1): p. 53-63.
45. Canaday, D.H., *Production of CD4(+) and CD8(+) T cell hybridomas.* Methods Mol Biol, 2013. **960**: p. 297-307.
46. Velazquez, C., R. DiPaolo, and E.R. Unanue, *Quantitation of lysozyme peptides bound to class II MHC molecules indicates very large differences in levels of presentation.* J Immunol, 2001. **166**(9): p. 5488-94.
47. Ternette, N., et al., *Early Kinetics of the HLA Class I-Associated Peptidome of MVA.HIVconsv-Infected Cells.* J Virol, 2015. **89**(11): p. 5760-71.
48. Lippolis, J.D., et al., *Analysis of MHC class II antigen processing by quantitation of peptides that constitute nested sets.* J Immunol, 2002. **169**(9): p. 5089-97.
49. Gerber, S.A., et al., *Absolute quantification of proteins and phosphoproteins from cell lysates by tandem MS.* Proc Natl Acad Sci U S A, 2003. **100**(12): p. 6940-5.
50. Chahrour, O., D. Cobice, and J. Malone, *Stable isotope labelling methods in mass spectrometry-based quantitative proteomics.* J Pharm Biomed Anal, 2015. **113**: p. 2-20.
51. Croft, N.P., et al., *Kinetics of antigen expression and epitope presentation during virus infection.* PLoS Pathog, 2013. **9**(1): p. e1003129.
52. Dudek, N.L., et al., *A Systems Approach to Understand Antigen Presentation and the Immune Response.* Methods Mol Biol, 2016. **1394**: p. 189-209.
53. Tan, C.T., et al., *Direct quantitation of MHC-bound peptide epitopes by selected reaction monitoring.* Proteomics, 2011. **11**(11): p. 2336-40.
54. Bozzacco, L., et al., *Mass spectrometry analysis and quantitation of peptides presented on the MHC II molecules of mouse spleen dendritic cells.* J Proteome Res, 2011. **10**(11): p. 5016-30.
55. Mellman, I. and R.M. Steinman, *Dendritic cells: specialized and regulated antigen processing machines.* Cell, 2001. **106**(3): p. 255-8.
56. Palm, N.W. and R. Medzhitov, *Pattern recognition receptors and control of adaptive immunity.* Immunol Rev, 2009. **227**(1): p. 221-33.
57. Tarlinton, D.M., F. Batista, and K.G. Smith, *The B-cell response to protein antigens in immunity and transplantation.* Transplantation, 2008. **85**(12): p. 1698-704.
58. Callen, E., M.C. Nussenzweig, and A. Nussenzweig, *Breaking down cell cycle checkpoints and DNA repair during antigen receptor gene assembly.* Oncogene, 2007. **26**(56): p. 7759-64.
59. Jankovic, M., A. Nussenzweig, and M.C. Nussenzweig, *Antigen receptor diversification and chromosome translocations.* Nat Immunol, 2007. **8**(8): p. 801-8.
60. Kuhn, E., et al., *Quantification of C-reactive protein in the serum of patients with rheumatoid arthritis using multiple reaction monitoring mass spectrometry and 13C-labeled peptide standards.* Proteomics, 2004. **4**(4): p. 1175-86.
61. Picotti, P., et al., *Full dynamic range proteome analysis of S. cerevisiae by targeted proteomics.* Cell, 2009. **138**(4): p. 795-806.
62. Anderson, L. and C.L. Hunter, *Quantitative mass spectrometric multiple reaction monitoring assays for major plasma proteins.* Mol Cell Proteomics, 2006. **5**(4): p. 573-88.

63. Zweigenbaum, J. and J. Henion, *Bioanalytical high-throughput selected reaction monitoring-LC/MS determination of selected estrogen receptor modulators in human plasma: 2000 samples/day.* Anal Chem, 2000. **72**(11): p. 2446-54.
64. Yost, R.A. and C.G. Enke, *Triple quadrupole mass spectrometry for direct mixture analysis and structure elucidation.* Anal Chem, 1979. **51**(12): p. 1251-64.
65. Lange, V., et al., *Selected reaction monitoring for quantitative proteomics: a tutorial.* Mol Syst Biol, 2008. **4**: p. 222.
66. Kuster, B., et al., *Scoring proteomes with proteotypic peptide probes.* Nat Rev Mol Cell Biol, 2005. **6**(7): p. 577-83.
67. Mallick, P., et al., *Computational prediction of proteotypic peptides for quantitative proteomics.* Nat Biotechnol, 2007. **25**(1): p. 125-31.
68. Picotti, P. and R. Aebersold, *Selected reaction monitoring-based proteomics: workflows, potential, pitfalls and future directions.* Nat Methods, 2012. **9**(6): p. 555-66.
69. Peterson, A.C., et al., *Parallel reaction monitoring for high resolution and high mass accuracy quantitative, targeted proteomics.* Mol Cell Proteomics, 2012. **11**(11): p. 1475-88.
70. Gallien, S., et al., *Targeted proteomic quantification on quadrupole-orbitrap mass spectrometer.* Mol Cell Proteomics, 2012. **11**(12): p. 1709-23.
71. Schilling, B., et al., *Multiplexed, Scheduled, High-Resolution Parallel Reaction Monitoring on a Full Scan QqTOF Instrument with Integrated Data-Dependent and Targeted Mass Spectrometric Workflows.* Anal Chem, 2015. **87**(20): p. 10222-9.
72. Thomas, S.N., et al., *Multiplexed Targeted Mass Spectrometry-Based Assays for the Quantification of N-Linked Glycosite-Containing Peptides in Serum.* Anal Chem, 2015. **87**(21): p. 10830-8.
73. Ronsein, G.E., et al., *Parallel reaction monitoring (PRM) and selected reaction monitoring (SRM) exhibit comparable linearity, dynamic range and precision for targeted quantitative HDL proteomics.* J Proteomics, 2015. **113**: p. 388-99.
74. Domon, B. and S. Gallien, *Recent advances in targeted proteomics for clinical applications.* Proteomics Clin Appl, 2015. **9**(3-4): p. 423-31.
75. Rauniyar, N., *Parallel Reaction Monitoring: A Targeted Experiment Performed Using High Resolution and High Mass Accuracy Mass Spectrometry.* Int J Mol Sci, 2015. **16**(12): p. 28566-81.
76. Aebersold, R., A.L. Burlingame, and R.A. Bradshaw, *Western blots versus selected reaction monitoring assays: time to turn the tables?* Mol Cell Proteomics, 2013. **12**(9): p. 2381-2.
77. Towbin, H., T. Staehelin, and J. Gordon, *Electrophoretic transfer of proteins from polyacrylamide gels to nitrocellulose sheets: procedure and some applications.* Proc Natl Acad Sci U S A, 1979. **76**(9): p. 4350-4.
78. Towbin, H., T. Staehelin, and J. Gordon, *Electrophoretic transfer of proteins from polyacrylamide gels to nitrocellulose sheets: procedure and some applications. 1979.* Biotechnology, 1992. **24**: p. 145-9.
79. Bogers, W.M., et al., *Potent immune responses in rhesus macaques induced by nonviral delivery of a self-amplifying RNA vaccine expressing HIV type 1 envelope with a cationic nanoemulsion.* J Infect Dis, 2015. **211**(6): p. 947-55.

80. Lazzaro, S., et al., *CD8 T-cell priming upon mRNA vaccination is restricted to bone-marrow-derived antigen-presenting cells and may involve antigen transfer from myocytes.* Immunology, 2015. **146**(2): p. 312-26.
81. Wisniewski, J.R., et al., *Universal sample preparation method for proteome analysis.* Nat Methods, 2009. **6**(5): p. 359-62.
82. Gould, K.G., H. Scotney, and G.G. Brownlee, *Characterization of two distinct major histocompatibility complex class I Kk-restricted T-cell epitopes within the influenza A/PR/8/34 virus hemagglutinin.* J Virol, 1991. **65**(10): p. 5401-9.
83. Silva, J.C., et al., *Absolute quantification of proteins by LCMSE: a virtue of parallel MS acquisition.* Mol Cell Proteomics, 2006. **5**(1): p. 144-56.
84. Deshmukh, A.S., et al., *Deep proteomics of mouse skeletal muscle enables quantitation of protein isoforms, metabolic pathways, and transcription factors.* Mol Cell Proteomics, 2015. **14**(4): p. 841-53.
85. Perri, S., et al., *An alphavirus replicon particle chimera derived from venezuelan equine encephalitis and sindbis viruses is a potent gene-based vaccine delivery vector.* J Virol, 2003. **77**(19): p. 10394-403.
86. Jeffs, L.B., et al., *A scalable, extrusion-free method for efficient liposomal encapsulation of plasmid DNA.* Pharm Res, 2005. **22**(3): p. 362-72.
87. Heyes, J., et al., *Cationic lipid saturation influences intracellular delivery of encapsulated nucleic acids.* J Control Release, 2005. **107**(2): p. 276-87.
88. Lutz, M.B., et al., *An advanced culture method for generating large quantities of highly pure dendritic cells from mouse bone marrow.* J Immunol Methods, 1999. **223**(1): p. 77-92.
89. Razavi, M., et al., *MALDI immunoscreening (MiSCREEN): a method for selection of anti-peptide monoclonal antibodies for use in immunoproteomics.* J Immunol Methods, 2011. **364**(1-2): p. 50-64.